Dissertation

submitted to the

Combined Faculties for the Natural Sciences and for Mathematics

of the Ruperto-Carola University of Heidelberg, Germany

for the degree of

Doctor of Natural Sciences

presented by

Diplom-Biochemist Maria A. Ermolaeva

Born in Puschino, Moscow Region, Russia

Oral examination: _____

Analysis of the physiological function of TNF Receptor I Associated Death Domain Protein (TRADD) and Familial Cylindromatosis Protein (CYLD) by using conditional gene targeting in mice.

Referees: Dr. Walter Witke

Prof. Dr. Günter Hämmerling

Acknowledgments.

Analysis of the physiological function of TNF Receptor I Associated Death Domain Protein (TRADD) and Familial Cylindromatosis Protein (CYLD) by using conditional gene targeting in mice.

<u>Maria A. Ermolaeva.</u> EMBL-Mouse Biology Unit, Monterotondo, Italy; Department of Mouse Genetics and Inflammation, Institute for Genetics, University of Cologne, Cologne, Germany.

The aim of the project was to apply the conditional gene targeting approach based on the usage of Cre/LoxP system of site-specific DNA recombination to investigate physiological function of two putative mediators of inflammation – TNF Receptor 1 Associated Death Domain Protein (TRADD) and Familial Cylindromatosis Protein (CYLD), in a mouse model.

TRADD is an adaptor molecule postulated to be essential for signal transduction through TNF Receptor 1 (TNFR1). The *in vivo* physiological role of TRADD has not been determined so far. CYLD is a tumor suppressor that has been described as a negative regulator of TNFR1-mediated signaling and signaling by Toll like Receptors (TLRs). TLRs are essential components of mammalian innate immunity belonging to a group of sensors that directly recognize bacterial and viral products as well as markers of tissue stress. Upon activation TLRs induce intracellular signaling events leading to production of cytokines, chemokines and other mediators that promote protective responses. Tumor Necrosis Factor (TNF) is a pleiotropic cytokine produced by a variety of cells upon TLR stimulation. It plays a key role in the amplification of the initial immune response. The majority of effects that are induced by TNF are dependant on TNFR1. TLR signaling and TNF signaling through TNFR1 share common mechanism of negative regulation that is based on the the removal of K63-linked polyubiquitin chains from specific key components of receptor-associated complexes. Two de-ubiquitinating enzymes – A20 and CYLD are currently known to be responsible for this process. The physiological function of A20 is well characterized by gene knockout studies while the precise role of CYLD remains enigmatic.

We successfully generated mice carrying "floxed" (modified by the insertion of LoxP sites and extra DNA fragments at specific locations) alleles of TRADD and CYLD by using homologous recombination in embryonic stem cells. In case of TRADD the deletion of the LoxP-flanked sequence would generate a null TRADD allele; in case of CYLD the last exon of the gene would be replaced by a mutated copy resulting in the expression of C-terminally truncated form of CYLD that is lacking catalytic activity. We then generated TRADD knockout and CYLD complete mutant mice by crossing the homozygous "floxed" animals to a ubiquitous Cre-Deleter strain.

By analyzing TRADD knockout mice we could observe that TNFR1-mediated apoptosis was completely blocked in these mice while TNF-induced pro-inflammatory and anti-bacterial responses were dramatically reduced but still present. We obtained similar results by evaluating the response of TRADD deficient primary cells to TNF. To our surprise we discovered that TRADD knockout mice had impaired immediate responses to stimulation of Toll like receptors 3 and 4. Consistent with this observation TRADD deficient primary cells demonstrated reduced cytokine production as well as impaired activation of NF-κB and MAP kinases upon stimulation with poly(I:C) and LPS. On the basis of co-expression experiments performed in HEK293T cells we propose that TRADD is recruited to TLR adaptor TRIF via Receptor-Interacting Protein 1 (RIP1) and acts as a mediator of TRIF-dependant TLR signaling.

To our surprise CYLD homozygous mutant mice did not survive until the age of weaning. By carefully following the pups we observed that the mutants died within minutes after birth showing signs of cyanosis and respiratory distress. Mutant pups were smaller then control littermates and demonstrated altered morphology of the tail. We then produced mutant mouse embryonic fibroblasts (MEFs) and analyzed the response of these cells to cytokines. Consistent with the role of CYLD as a negative regulator of pro-inflammatory signaling, mutant cells showed elevated activation of NF-κB and JNK cascades upon stimulation with TNF and IL-1β.

Analyse der physiologischen Funktion des TNF Rezeptor I Associated Death Domain Proteins (TRADD) und des Familial Cylindromatosis Proteins (CYLD) durch konditionelles „Gene Targeting" in Mäusen.

Maria A. Ermolaeva. EMBL-Mouse Biology Unit, Monterotondo, Italy; Department of Mouse Genetics and Inflammation, Institut für Genetik, Universität zu Köln, Köln, Deutschland.

Das Ziel dieser Studie war die physiologische Funktion von zwei mutmaßlichen Inflammationsmediatoren – TNF Receptor 1 Associated Death Domain Protein (TRADD) und Familial Cylindromatosis Protein (CYLD) – in Mausmodelsystemen zu erforschen. Hierfür wurde die Methode des konditionellen „Gene Targetings" angewandt, welches auf der zielgerichteten Rekombination der DNA durch das Cre/LoxP Systemberuht.

Von dem Adapter Molekül TRADD wird angenommen, dass es für die Signaltransduktion durch TNF Rezeptor 1 (TNFR1) essentiell ist. Die physiologische Rolle von TRADD wurde *in vivo* bisher noch nicht bestimmt. CYLD ist ein Tumorsuppressor, der TNFR1- und Toll like Receptor (TLR) vermittelte Signale inhibiert. TLRs sind essentielle Sensoren des unspezifischen Immunsystems, die sowohl bakterielle und virale Produkte als auch Stressmarker erkennen. Werden TLRs aktiviert, so führt dies zu einer intrazellulären Signaltransduktionskaskade, die die Produktion von Zytokinen, Chemokinen und anderen Mediatoren als Schutzantwort bewirkt. Tumor Nekrose Faktor (TNF) ist ein vielseitiges Zytokin, das von verschiedenen Zelltypen zur Antwort auf TLR-Stimulation hergestellt wird. TNF spielt eine Schlüsselrolle in der Verstärkung der initialen Immunantwort. Der Großteil der TNF vermittelten Effekte ist von TNFR1 abhängig. Die von TLR- und TNFR1- vermittelten Signalkaskaden haben einen negativen Regulationsmechanismus gemeinsam. Dieser beruht auf der Abspaltung K63 verbundener Polyubiquitinketten von rezeptorassoziierten Schlüsselkomponenten. Bisher sind zwei deubiquitinierende Enzyme – A20 und CYLD – bekannt, die für diesen Prozess verantwortlich sind. Während die physiologische Funktion von A20 durch Inaktivierung des Gens gut charakterisiert wurde, ist die genaue Rolle von CYLD noch rätselhaft.

Uns ist es durch homologe Rekombination in embryonalen Stammzellen gelungen, Mäuse zu generieren, die „gefloxte" (modifiziert durch die Insertion von LoxP Sequenzen und zusätzlicher DNA Fragmente an spezifischen Positionen) Allele von TRADD und CYLD tragen. Im Falle von TRADD ergibt die Deletion der LoxP flankierten Sequenz ein TRADD Nullallel; im Fall von CYLD wird das letzte Exon durch eine Variante ersetzt, die zur Expression einer C-terminal verkürzten Form von CYLD führt, die keine katalytische Aktivität mehr besitzt. Die Kreuzung homozygot „gefloxter" Tiere mit einem generellen CRE-Deleter Stamm ergab dann Nachkommen, denen entweder TRADD vollständig fehlte, oder in denen das Wildtyp CYLD durch das mutierte CYLD ersetzt war.

Die Analyse der TRADD knockout Mäuse ergab, dass die TNFR1-vermittelte Apoptose in diesen Tieren vollständig blockiert war, wohingegen die TNF-induzierte proinflammatorische und antibakterielle Antwort zwar dramatisch reduziert, aber prinzipiell vorhanden war. TNF-Behandlung von TRADD defizienten Zellkulturen zeigte ähnliche Ergebnisse. Überraschenderweise war die frühe Immunantwort nach Stimulation von TLR3 und TLR4 in TRADD knockout Mäusen eingeschränkt. Übereinstimmend mit dieser Beobachtung war die verminderte Zytokinproduktion und eingeschränkte Aktivität von NF-κB und MAP Kinase nach poly(I:C) Stimulation in TRADD defizienten Zellen. Basierend auf den Ergebnissen von Koexpressionsexperimenten in Hek293T Zellen nehmen wir an, dass TRADD via RIP zum TLR Adapter TRIF rekrutiert wird und als Vermittler in der TRIF-abhängigen TLR Signalübertragung agiert.

Mäuse, die homozygote Träger des mutierten CYLD Allels waren, starben überraschenderweise innerhalb von Minuten nach der Geburt mit Zyanose- und Atemnotsymptomen, wobei die Tiere mit mutiertem CYLD Gen kleiner als Wildtypmäuse waren und eine veränderte Schwanzmorphologie aufwiesen. Deshalb analysierten wir die Reaktion auf Zytokinstimulation in mutierten embryonalen Mausfibroblasten. In den Zellen mit mutiertem CYLD war erhöhte NFkB und JNK Aktivität nach TNF und IL-1b Stimulation feststellbar, was mit einer Funktion von CYLD als negativer Regulator der proinflammatorischen Signalvermittlung im Einklang steht.

Table of contents.

Table of contents

1. Abbreviations

AIF – Apoptosis inducing factor

ALT – Alanine aminotransferase

AOM – Azoxymethan

Apaf - Apoptotic protease-activating factor

ARE – AU-rich element

BAC – Bacterial artificial chromosome

Bcl - B-cell lymphoma gene

BSA – Bovine serum albumin

BSS – Brook-Spiegler syndrome

CHX – Cyclohexamide

CNS – Central nervous system

CR – Complement receptor

CRD – Cysteine-rich domain

Cre – Cyclization Recombination

CTAR – C-terminal activator region

CYLD – Familial cylindromatosis protein

DAMP – Danger associated molecular pattern

DD – Death domain

DED – Death effector domain

DIF – Differentiation inducing factor

DMBA - 7,12-dimethyl-benz[a]anthracene

DMEM - Dulbecco's minimal essential medium

DNA - Deoxyribonucleic acid

DSS – Dextran sulfate sodium

DTT – Dithiothreitol

EDTA - Ethylene diamine tetraacetate

EGFP – Enhanced green fluorescent protein

EGTA - Ethyleneglycol-bis[β-aminoethyl ether]-N, N, N', N'-tetraacetate

ELISA - Enzyme-linked immune sorbent assay

ERK - Extracellular-signal-regulated kinase

ES cell – Embryonic stem cell

Etk – Endothelial/Epithelial tyrosine kinase

FACS - Fluorescence activated cell sorting

FADD – Fas associated death domain protein

FAN – Factor associated with neutral sphingomyelinase

FasL – Fas ligand

FCS - Fetal calf serum

FDC – Follicular dendritic cells

FF – Floxed fragment

FLIP – FLICE-like inhibitory protein

FloxM – Mutated floxed fragment

Gal-N – Galactosamine

GC – Germinal center

Abbreviations

HEK – Human embryonic kidney cells

HEPES - N-2-Hydroxyethylpiperazine-N'-2-ethane sulfonic acid

HSV – Herpes simplex virus

IAP – Inhibitor of apoptosis protein

ICAM – Intracellular cell adhesion molecule

IFN – Interferon

IκB – Inhibitor of κB

IKK – IκB kinase

IL – Interleukin

i.p. – Intraperitoneal

IRAK - IL-1R associated kinase

IRF – IFN regulatory factor

i.v. – Intravenous

JNK - C-Jun N-terminal kinase

kDa – Kilodalton

K63 – Lysine 63

K48 - Lysine 48

LA – Left arm of homology

Lck – Leukocyte specific kinase

LIF – Leukemia inhibitory factor

LMP – Latent membrane protein

LoxP – Locus of X-over P1

LPS – Lipopolysaccharide

MAPK – Mitogen activated protein kinase

Mal - MyD88-adaptor like

MCMV – Mouse cytomegalovirus

MCSF - Macrophage colony stimulating factor

MEF – Mouse embryonic fibroblast

MHC - Major histocompatibility complex

MKP – MAP kinase phosphatase

MnSOD – Manganous superoxide dismutase

MS – Multiple sclerosis

MTT - (3-(4,5-dimethyl thiazol-2-yl-) 2,5-diphenyl tetrazolium bromide

Myd88 – Myeloid differentiation marker 88

NEMO – NF-κB essential modifier

NES – Nuclear export signal

NF-κB – Nuclear factor kappa B

NK – Natural killer cell

NLS – Nuclear localization signal

NSD – Natural sphingomyelinase activation domain

PBS - Phosphate buffered saline

PCR – Polymerase chain reaction

PML - Promyelocytic leukemia protein

PNA - Peanut agglutinin

Poly(I:C) - Polyinosinic:polycytidylic acid

PRR – Pattern recognition receptor

RA – Right arm of homology

RBC – Red blood cells

RHIM – RIP homotipic interaction motif

RIP – Receptor interacting protein

RNA - Ribonucleic acid

ROS – Reactive oxygen species

SA – Splice acceptor

SDS - Sodium dodecyl sulfate

Smac- Second mitochondrial activator of caspases

SMase – Sphingomyelinase

SODD – Silencer of death domains

SRBC – Sheep red blood cells

STAT - Signal transducer and activator of transcription

TAB - TAK1 binding protein

TACE – TNF-alfa converting enzyme

TAK - TGF-beta activated-kinase

TBK – TANK binding kinase

TCR – T-cell receptor

TIR – Toll/Interleukin-1 receptor homologous domain

TIRAP - TIR domain-containing adaptor protein

TLR – Toll like receptor

TNF – Tumor necrosis factor

TNFR – TNF receptor

TPA - 12-*O*-tetradecanoylphorbol-13 acetate

TRADD – TNF receptor associated death domain protein

TRAF – TNF receptor associated factor

TRAM - TRIF-related adaptor molecule

TRIF – TIR-related adaptor protein inducing interferon

UCH – Ubiquitin C-terminal hydrolase

UTR – Untranslated region

VCAM – Vascular cell adhesion molecule

VEGF – Vascular endothelial growth factor

VSV - vesicular stomatitis virus

2. Introduction.

2.1 Tumor Necrosis Factor (TNF). TNF receptors – TNF receptor 1 (TNFR1, p55) and TNF receptor 2 (TNFR2, p75).

Tumor Necrosis Factor (TNF) was discovered in 1975 as a mediator of endotoxin induced tumor necrosis. *Carswell et al*. isolated TNF from the serum of mice exposed to endotoxin, and characterized it as a novel glycoprotein with the property of killing tumor cells both *in vitro* and *in vivo* [1]. Independently, TNF was described as a factor mediating differentiation of hematopoetic cells into monocyte/macrophage linage (DIF − Differentiation Inducing Factor) [2] and as cachectin - a hormone produced by activated macrophages, responsible for hypertriglyceridemia and wasting of adipose tissue in cancer patients and patients suffering from infections [3, 4].

TNF is currently known to perform multiple physiological functions. Most of these functions are related to the immune response and inflammation. The cytokine has been shown to play an important role in leukocyte migration, tissue resorption, the acute-phase response, and fever response [5]. At the same time the excessive production of TNF has been implicated in the development of uncontrolled and chronic inflammation, autoimmune diseases and insulin resistance [6-8].

The main sources of TNF in the body are activated macrophages, lymphocytes and Natural Killer cells, although other, non-immune cell types can produce low levels of the cytokine [9]. Due to the potent physiological effects of TNF, its expression must be and is tightly controlled at multiple levels. The transcription of the respective gene is regulated by various signaling cascades mainly through members of the NF-κB family of transcription factors [10], although in certain cell types other transcription factors may also play a role [11]. An additional step of *TNF* gene expression control is executed at the level of mRNA stability and translation efficiency. The 3' untranslated region (UTR) of the TNF mRNA contains the AU-rich element (ARE) that serves as a binding site for a number of protein factors which

regulate mRNA stability and translation. Various cascades, involved in TNF biosynthesis, in turn regulate the action of these protein factors [151, 152].

TNF is initially synthesized as a 26-kDa precursor that is expressed on the cell surface as a type II transmembrane protein [12]. The 17-kDa soluble form of TNF is generated via cleavage of the precursor by the specific membrane associated metalloproteinase named TACE (for TNF-alpha converting enzyme) [13, 14]. *In vitro* and *in vivo* studies have suggested that the membrane-associated form is more important for local TNF-dependant responses while the soluble form has more impact at the systemic level [15-17].

TNF mediates its activities via interacting with two distinct receptors, TNF receptor type 1 (p55 or p60) and TNF receptor type 2 (p75 or p80) [18-20]. The two receptors share homology in the extracellular region that is responsible for the ligand binding, but have completely different intracellular parts [21]. The cytoplasmic part of the p55 TNF receptor (TNFR1) contains a ~ 80 amino acid Death Domain that is shared by a number of cell death inducing receptors [22]. The Death Domain creates a binding platform for downstream mediators of TNFR1 signaling such as TNFR1 Associated Death Domain protein (TRADD), Fas Associated Death Domain protein (FADD), Receptor Interacting Protein 1 (RIP1), TNF Receptor Associated Factor 2 (TRAF2) and other factors [23-25]. It has been demonstrated that a p55 TNF receptor with mutated Death Domain was unable to perform most of its functions [22]. The C-terminal (intracellular) part of the p75 TNF receptor (TNFR2) contains a unique region of 78 amino acids that is indispensable for signal transduction through the receptor [26]. This region is responsible for the recruitment of TNFR2 signaling mediators to the cytoplasmic part of the receptor upon ligand binding. The list of such mediators includes TNF Receptor Associated Factors 1 and 2 (TRAF1 and TRAF2), cIAP1 (cellular IAP 1, for homology with the Inhibitor of Apoptosis Protein originally identified in baculoviruses), cIAP2 and other factors [26, 27].

Despite differences in intracellular domains and cytoplasmic binding partners both TNF receptors were shown to mediate similar downstream effects such as activation of NF-κB,

activation of MAP kinases and cytotoxicity. TNFR1 was demonstrated to induce cell death via the TRADD-FADD-caspase-8 signaling axis, while NF-κB activation as well as activation of MAP kinases (JNK, p38, ERK) was induced through cooperation between TRADD, TRAF2 and RIP1 [23-25, 28, 29]. TNFR2 activates NF-κB and JNK (but not p38 and ERK) via a TRAF2-dependant cascade [27, 30]. In addition to adaptors shared with TNFR1, TNFR2 may also recruit specific mediators such as Etk (for Endothelial/Epithelial Tyrosine Kinase) – a kinase implicated in endothelial cell migration and formation of blood vessels [31]. Based on results from a number of *in vitro* and *in vivo* studies the TNFR2 was suggested to have a specific function in TNF-mediated toxicity [30, 32-35]. Still the mechanism of TNFR2-mediated toxicity remains unclear. One way for TNFR2 to induce cell death or enhance the proapoptotic effect of TNFR1 could be through mediating ubiquititnation and subsequent degradation of pro-survival messenger TRAF2 [36]. On the other hand TNFR2 induces sustained JNK activation (unlike TNFR1 that only induces transient phosphorylation of JNK) [30] that may also contribute to triggering cell death [37]. See Figure 1 for a schematic of the signaling pathways mediated by the two TNF receptors.

Gene knockout studies in mice provided essential information about the distinct physiological functions of the two TNF receptors. TNFR1 but not TNFR2 deficient mice were resistant to endotoxic shock induced by LPS or lethal amounts of *S. aureus* but showed increased susceptibility to infection with *Listeria monocytogenes* [34, 38]. These data suggested that signal transduction through TNFR1 was more important for TNF-mediated systemic toxicity and induction of immune response against pathogens. Although the analysis of TNFR2 deficient mice overall did not reveal such an important physiological function for this receptor, some specific functions could still be identified. For instance animals lacking TNFR2 showed less necrosis of the surrounding tissue upon subcutaneous injection of TNF, indicating the putative involvement of the receptor in local TNF cytotoxic effects.
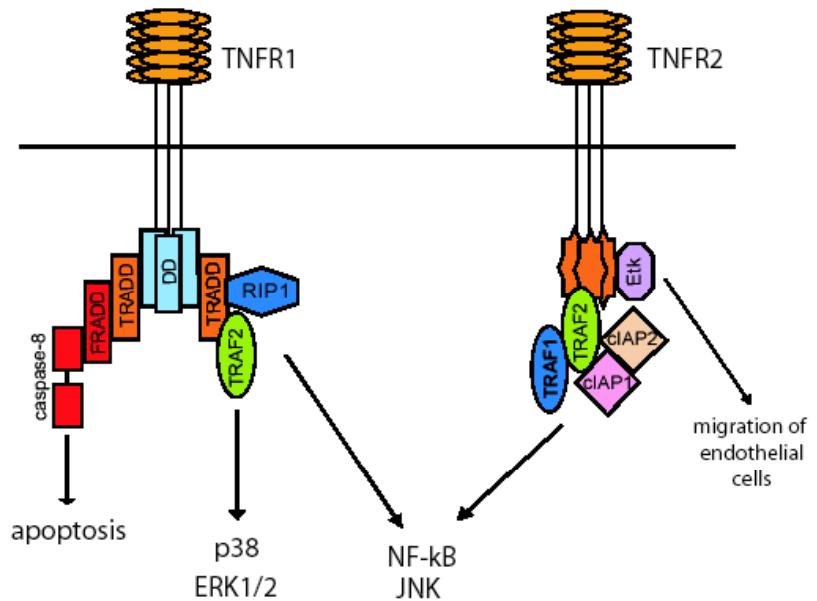
Figure 1. Key molecules involved in signal transduction through TNFR1 and TNFR2. See text for further details.

In addition to differences in respective signaling cascades, non-redundant physiological roles of the two TNF receptors are believed to arise also from their distinct expression patterns and ligand specificity. TNFR1 is ubiquitously expressed while high levels of TNFR2 are present only in a limited number of cell types such as immune cells and endothelial cells. Moreover, the expression of the p55 receptor is controlled by a non-inducible house-keeping promoter while the promoter that drives expression of the p75 receptor can be induced by stimuli like cytokines and mitogens [40]. It was demonstrated that TNFR1 has higher affinity for the 17 kDa soluble TNF while TNFR2 is much more efficiently triggered by the 26 kDa membrane-associated form of the cytokine [41]. Overall it seems that due to limited expression levels, TNFR2 can mediate detectable and physiologically significant responses mainly when cells expressing sufficient levels of the cell-associated ligand are present in the local environment. At the same time the TNFR1-soluble TNF signaling pair appears to be implicated in a broad range of effects in multiple tissues.

2.2 The role of TNF and TNF receptors in physiological and pathological processes.

2.2.1 The role of TNF in mammalian development.

Gene knock out studies in mice demonstrated that TNF-, TNFR1- and TNFR2-deficient animals were viable, fertile and did not exhibit significant developmental defects in most tissues with the exception of secondary lymphoid organs. The formation of B cell follicles and follicular dendritic cell networks in spleen, lymph nodes and Peyer's patches was impaired in mice knock out for TNF or TNFR1 genes [42, 43]. This effect was accompanied by impaired germinal center formation and T-cell-dependant antibody responses. At the same time mutant mice did not show alterations in the development or overall localization of lymphocytes and dendritic cells, suggesting that the TNF-TNFR1 signaling pair controlled cell-to-cell interactions responsible for the establishment of the correct architecture of secondary lymphoid organs rather then general development of their cellular components.

2.2.2 TNF in inflammation and immunity.

TNF plays a critical role in the induction and the regulation of inflammation and of immune responses. It is among molecules that get produced by cells of the innate immune system (such as macrophages and mast cells, high levels) and non-immune cells (relatively low levels) as part of the immediate response to the presence of a pathogen. The secretion of TNF by these cell types is initiated via signal transduction through cytosolic and cell surface pattern recognition receptors that are directly activated by pathogen-derived products [5, 44, 45]. Subsequently TNF serves as a signal of potential danger. It acts to amplify the original response and to inform the rest of the immune system about the presence and the location of a putatively harmful entity. TNF enhances the production of pro-inflammatory cytokines by surrounding cells. At the same time it triggers local vascular endothelial cells to express adhesion molecules (such as E-selectin, intracellular adhesion molecule-1, ICAM-1 and vascular cell adhesion molecule-1, VCAM-1) as well as molecules that are involved in chemotaxis and transmigration (such as IL-8) [46, 47]. Thereby TNF mediates trafficking of circulating leukocytes (neutrophils, monocytes and lymphocytes) to the site of infection or tissue damage. Simultaneously, TNF provides an additional maturation signal to dendritic

cells that have captured bacterial or viral antigen at the site of infection. Mature dendritic cells migrate to lymphoid organs where they present respective antigens to T-cells and shape the T-cell response toward T helper type 1 (Th1) or T helper type 2 (Th2) via producing co-stimulatory cytokines such as IL-12 or IL-10 respectively [48].

Consistent with the importance of TNF for mammalian host defense, TNF- and TNFR1-deficient mice are unable to counteract the infection with a variety of bacterial pathogens such as *Listeria monocytogenes*, *Mycobacterium tuberculosis*, *M. avium*, *Salmonella typhimurium*, intracellular parasites such as *Leishmania major* and *Triponasoma cruzi* or viruses such as herpes simplex virus (HSV-1), mouse cytomegalovirus (MCMV) and lymphocytic choriomeningitis virus (LCMV) [49]. Among other immune impairments, mice knock out for either TNF or TNFR1 fail to form functional granulomas upon infection with *Mycobacterium* [50, 51]. Granulomas are protective structures that get assembled around a potential source of infection (the infected cell, the egg of the worm or the spore of bacteria) in order to isolate the pathogen from the rest of the body. These structures contain T-cells and activated macrophages and are most relevant for the host defense against parasites or bacteria. Upon clearance of the pathogen, granulomas are substituted by scar tissue. The formation of granulomas is defective in TNF-deficient mice although knock out T-cells and macrophages have no impairment in neither development nor activation. TNFR1-deficient animals do form granulomas initially but fail to maintain them functional due to excessive recruitment and proliferation of T-cells. Such granulomas undergo acute disintegration and develop into granulomatous lesions causing inflammatory damage of tissues and death of mice. It was demonstrated that the lethality of mice knock out for TNFR1 upon infection with *Mycobacterium* could be rescued ether by depletion of T-cells or by anti-IL-12 treatment. These data suggested that the detrimental effect was caused by the absence of appropriate regulation of immune response rather then general lack of it. Later it was demonstrated that TNF could directly inhibit the production of IL-12 and IL-23 by macrophages and dendritic cells [52]. Thereby, in addition to its role in the onset of inflammation, TNF became implicated in controlling the strength, the duration and the resolution of immune response.

2.2.3   TNF in autoimmune diseases and chronic inflammation.

Deregulated production and action of TNF often leads to the development of pathological conditions. For example the cytokine is implicated in the pathogenesis of diseases like rheumatoid arthritis (inflammatory disorder of the joints) and Crohn's disease (inflammatory disorder of the intestine). The successful usage of anti-TNF drugs for the treatment of both arthritis and Crohn's disease indicated its importance for the pathogenesis of these disorders [53-57]. Along the same line, it was demonstrated that impaired on/off regulation of TNF biosynthesis could cause spontaneous joint and gut-associated immunopathologies in mice [58]. At the same time TNF-deficient mice still developed arthritis in an antibody-induced model with lower incidence but same severity [59], suggesting that TNF was most probably involved in the onset but dispensable for the progression of the disease.

It has been demonstrated that the short-term effect of TNF on the immune system is pro-inflammatory, while chronic exposure to the cytokine suppresses effector functions of immune cells including T-cells (through inhibition of TCR signaling) and NK cells [60, 61]. The lack of such suppression may contribute to the development of autoimmune disease, like it happens in case of systemic lupus erythematosus [62, 63] or cause stronger relapses of pre-existing disorder, like it happens in multiple sclerosis (MS) - a chronic inflammatory demyelinating disease of the central nervous system (CNS). The example of MS is particularly important. Initial studies performed in mouse models strongly pointed toward a pro-inflammatory role of TNF in multiple sclerosis. The cytokine was implicated in mediating primary demyelination and dysfunction of neurons along with promoting the infiltration of immune cells into the CNS [64, 65]. Based on such evidence, TNF was selected as a drug target and anti-TNF therapy was applied to human MS patients in a number of clinical trials. Strikingly, patients that received the therapy demonstrated more frequent and stronger relapses of the disease upon initial clinical improvement [66]. Subsequently, it was confirmed in an inducible mouse model that the pro-inflammatory action of TNF at early stages of MS is followed by a clear immunosuppressive effect at later stages [67].

2.2.4 *Non-immune functions of TNF*.

The effects of TNF are not entirely restricted to inflammation and immunity. TNF plays a role in the homeostasis of the bone via inducing bone resorption and promoting differentiation of osteoclast progenitors into osteoclasts [68]. The cytokine is important for the formation of blood vessels due to its ability to mediate the expression of pro-angiogenic factors such as VEGF (vascular endothelial growth factor) [69, 70]. TNF produced by glial cells of the CNS has an impact on homeostatic synaptic scaling and activity-dependant wiring of the mammalian brain [71, 72]. In addition, the cytokine is involved in controlling body weight and glucose metabolism [73-75]. TNF is expressed by the fat tissue and acts on adipocytes in an autocrine manner reducing their ability to store and produce lipids. Due to the negative effect of the cytokine on insulin receptor signaling, high serum levels of fat-derived TNF often cause insulin resistance and diabetes in obese individuals.

2.3 Tumor Necrosis Factor Receptor 1 (TNFR1).

TNFR1 (CD120a, p55/60) is responsible for the majority of effects mediated by TNF. TNFR1 is a type I transmembrane glycoprotein that is ubiquitously expressed. The extracellular part of the receptor contains a repetitive amino acid sequence pattern of four cysteine-rich domains (CRDs) that is used for ligand binding [76]. The intracellular part contains two motifs involved in protein-protein interactions: the N-terminal Neutral Sphingomyelinase activation Domain (NSD) and the C-terminal Death Domain (DD).

The NSD stimulates the sphingomyelinase (SMase) that is active at neutral pH via recruiting the adaptor protein FAN (for Factor Associated with Neutral SMase activation). The activated N-SMase performs hydrolysis of the membrane phospholipid sphingomyelin (SM) producing ceramide (Cer). Ceramide in turn activates pro-inflammatory responses through the c–Raf-1 signaling cascade [77].

The DD binds to the adaptor protein TRADD (TNF Receptor Associated Death Domain) as discussed previously. TRADD is suggested to recruit signaling mediators such as FADD,

RIP1 and TRAF2 in order to induce ether cell death or activation of pro-survival and pro-inflammatory gene expression [23-25].

In the absence of the ligand TNF receptor 1 is expressed on the cell surface as a monomer and its intracellular part is associated with a protein called SODD (for Silencer of Death Domains). The putative function of SODD is to prevent spontaneous aggregation of death domain containing receptors in the absence of stimulation and the dissociation of SODD from the receptor is the first event that happens upon ligand binding [78].

The trimeric TNF induces receptor oligomerization via ligating to three monomers of TNFR1. The trimerization of the intracellular domain triggers the recruitment of adaptor proteins and formation of the receptor proximal signaling complex. Recent studies suggest that two kinds of such complex can be formed at the cytoplasmic part of TNFR1 [79, 80]. The initial complex (Complex 1) is formed within minutes after TNF stimulation. Complex 1 is associated with the plasma membrane. It contains FAN, TRADD, c-IAP1, TRAF2 and RIP1 but not FADD and caspase-8 [79]. Assembly of Complex 1 results in the activation of N-SMase via the mechanism described previously. At the same time c-IAP1, TRAF2 and RIP1 collaborate in inducing posttranslational modifications (phosphorylation and ubiquitination) of the upstream MAP kinases and the members of the IKK (for IκB Kinase) complex.

It was demonstrated that RIP1 undergoes poly-ubiquitination mediated by TRAF2 in a TNF-dependant manner [81, 82]. The ubiquitinated RIP1 binds to the IKK complex through its regulatory subunit NEMO (for NF-κB Essential Modifier) and recruits the complex containing a potent kinase TAK1 [82] that in turn mediates phosphorylation of IKK members and upstream MAP kinases [83]. In addition c-IAP1 participates in IKK activation by ubiquitinating NEMO [84].
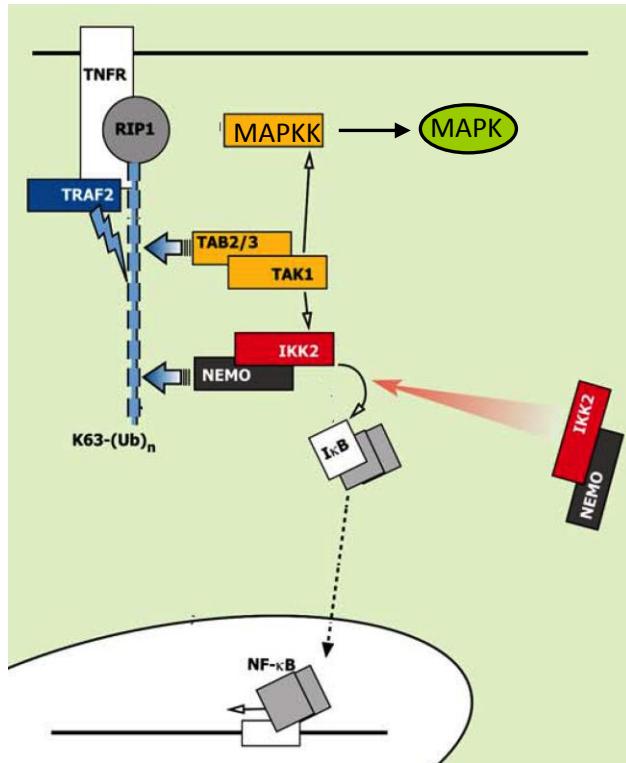
<u>Figure 2.</u>   Activation of NF-κB and MAP kinases by Complex 1. Modified from *Kovalenko and Wallach, 2006*

The NF-κB transcription factors are kept inactive in the cytoplasm in the absence of stimulation through binding to inhibitor of κB (IκB) proteins. The activated IKK complex targets IκB for the degradation in the proteosome thereby allowing the transcription factor to go into the nucleus and mediate expression of respective responsive genes [85] (see <u>Figure 2</u> for the summary).

Some data indicates that upon formation of Complex 1, TNFR1 undergoes internalization, regulated by the specific domain that is located in the cytoplasmic part of the receptor in close proximity to the transmembrane domain [80].
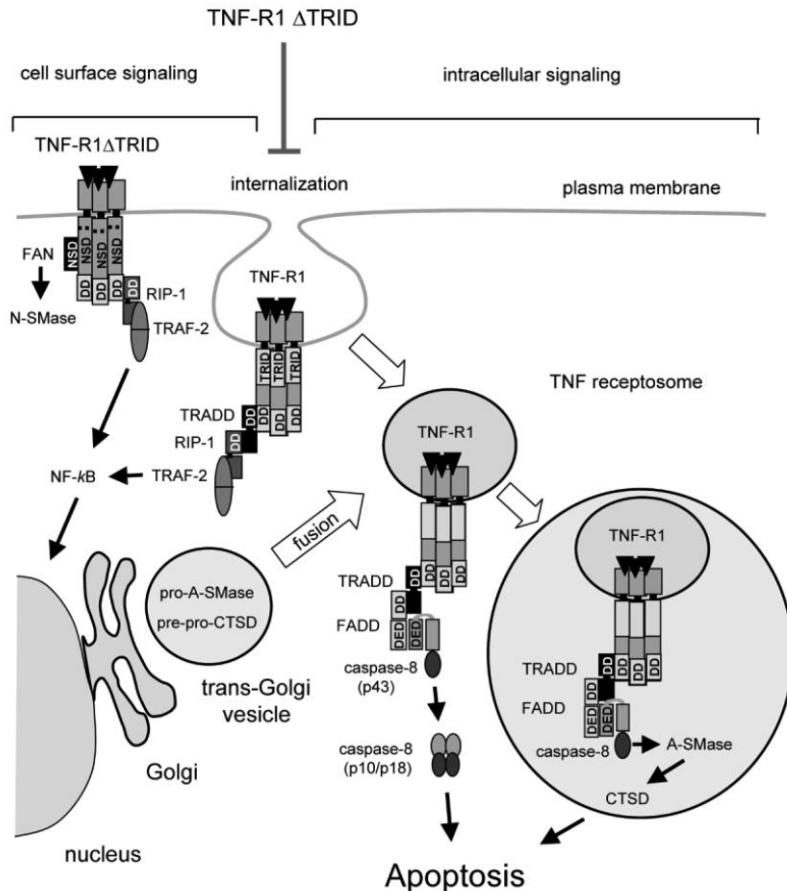
Figure 3. The formation of TNFR1-proximal signaling complex: timing, composition and sub-cellular localization. Adapted from *Schneider-Brachert et al, 2004*

TNFR1 becomes localized in the membrane of intracellular vesicles. Such vesicles move within the cell, mature toward becoming endosomes and fuse with the Trans-Golgi compartment (see Figure 3). Along the way the composition of the receptor proximal signaling complex changes: RIP1 and TRAF2 dissociate from the complex and get substituted by FADD and caspase-8 [79]. The complex containing FADD and caspase-8 (Complex 2) is responsible for the induction of apoptosis. In healthy cells and tissues the pro-apoptotic function of Complex 2 is blocked by the protective response that was induced earlier through Complex 1.

Such protective response includes production of a number of anti-apoptotic proteins. One of such proteins is c-FLIP (for FLICE-like inhibitory protein). c-FLIP binds to Death Effector Domains (DEDs) of FADD and caspase-8 and interferes with the recruitment of caspase-8 to

the cytoplasmic part of TNFR1 (and other death domain containing receptors) [86]. The levels of c-FLIP in the cytoplasm are determined by the expression of the respective gene and by the half-life of the protein. Complex 1 induces the expression of c-FLIP through the NF-κB family of transcription factors. At the same time the assembly of Complex 1 leads to the activation of JNK, which phosphorylates and activates a protein called Itch (from "itching" – the mice deficient for the *itch* gene develop chronic inflammation accompanied by constant itching of the skin [87]). Itch is an ubiquitin ligase that modifies c-FLIP and targets it for degradation by the proteosome, reducing the levels of c-FLIP in the cytoplasm and favoring the induction of apoptosis by Complex 2. As mentioned previously, NF-κB restores cytoplasmic levels of c-FLIP by inducing the expression of the respective gene. At the same time NF-κB induces expression of proteins involved in removal of reactive oxygen species (ROS) from the cell, such as MnSOD (for Manganous Superoxide Dismutase). Reactive oxygen species are known to inhibit MAP kinase phosphotases (MKPs) – the phosphotases that specifically inactivate MAP kinases including JNK [88]. The removal of ROS from the cytoplasm activates MKPs and thereby negatively regulates the JNK-mediated signaling (summarized on Figure 4) [89].

In addition to inhibiting apoptosis at the level of TNFR1 proximal signaling complex, NF-κB is known to inhibit cell death at the level of the mitochondria by inducing the expression of genes like Bcl2 and BclXL. Bcl2 and BclXL participate in maintaining the integrity of the mitochondrial outer membrane, preventing the release of pro-apoptotic mediators such as cytochrome-c, Smac/DIABLO (for Second Mitochondria-derived Activator of Caspase, a c-IAP binding protein) and AIF (Apoptosis Inducing Factor) from the inter-membrane space of the organelle [90].
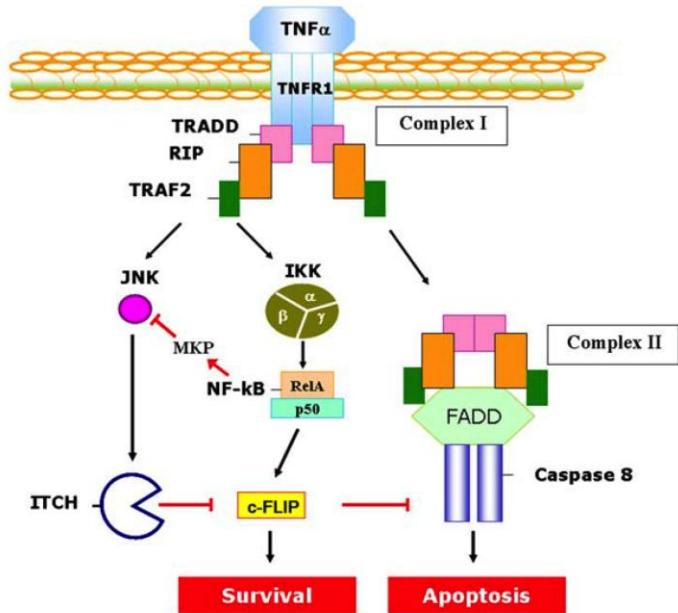
<u>Figure 4.</u> Complex 1 inhibits apoptosis induced by Complex 2: the role of JNK, NF-κB and c-FLIP. Adapted from *Chang et al, 2006*

The inhibition of cell death mediated by the mitochondria is important for the final outcome of signaling through TNFR1. It was demonstrated that caspase-8 could directly cleave the pro-apoptotic bcl2 family member Bid. The cleaved form of Bid inserts into the mitochondrial outer membrane and disrupts the integrity of the membrane. Subsequently cytochrome-c is released into the cytoplasm where it cooperates with the adaptor protein Apaf-1 to activate caspase-9 and further induce apoptosis [91]. The amplification of pro-apoptotic signaling through mitochondria is essential for the induction of death in certain cell types. Another link between TNF-mediated death and mitochondria is established through intra-vesicular Complex 2. Upon entry into the trans-Golgi network, Complex 2 is put in contact with the inactive form of acidic sphingomyelinase - A-SMase and the inactive form of cathepsin D - CTCD (both proteins are present in the vesicles of the trans-Golgi; see <u>Figure 3</u>) [80].
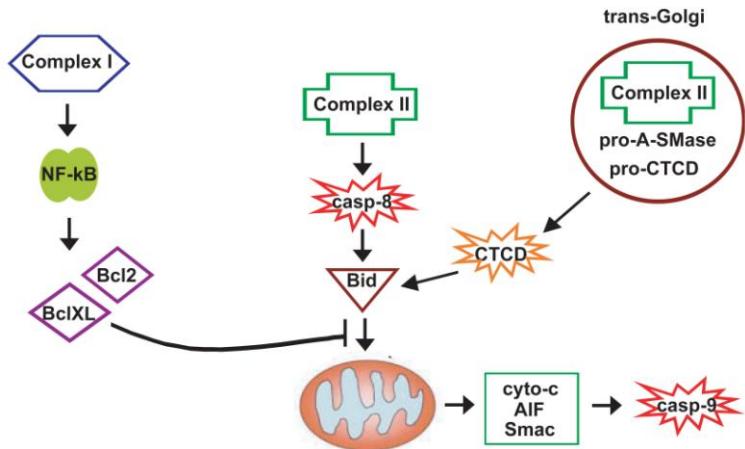
Figure 5. Links between TNFR1 mediated signaling and the mitochondria.

A-SMase gets activated in a FADD/caspase-8 dependant manner and produces ceramide. Ceramide in turn induces auto-activation of the CTCD. The active form of Catepsin D is transported into the cytoplasm where it performs the cleavage of Bid followed by the previously mentioned pro-apoptotic events [92] (see Figure 5).

The model of TNF-signaling that supports intracellular translocation of TNFR1 via vesicular transport [80] is in conflict with the earlier work by Micheau and Tschopp [79] who introduced Complex 1 and Complex 2 for the first time. The authors isolated Complex 2 from cell lysates through immunoprecipitation with an antibody specific for caspase-8. They could detect RIP1, TRADD, FADD and caspase-8 but not TNFR1 as members of Complex 2. At the same time the complex was present in the cytosolyc rather then in the membrane fraction of the cell. Based on this evidence the authors suggested that, upon formation of the membrane proximal Complex 1, the TRADD-RIP1 portion of the complex dissociates from the cytoplasmic part of TNFR1 (see Figure 6). In the cytosol the death domains of both RIP1 and TRADD become available for interaction with FADD and caspase-8, allowing the formation of death inducing Complex 2.
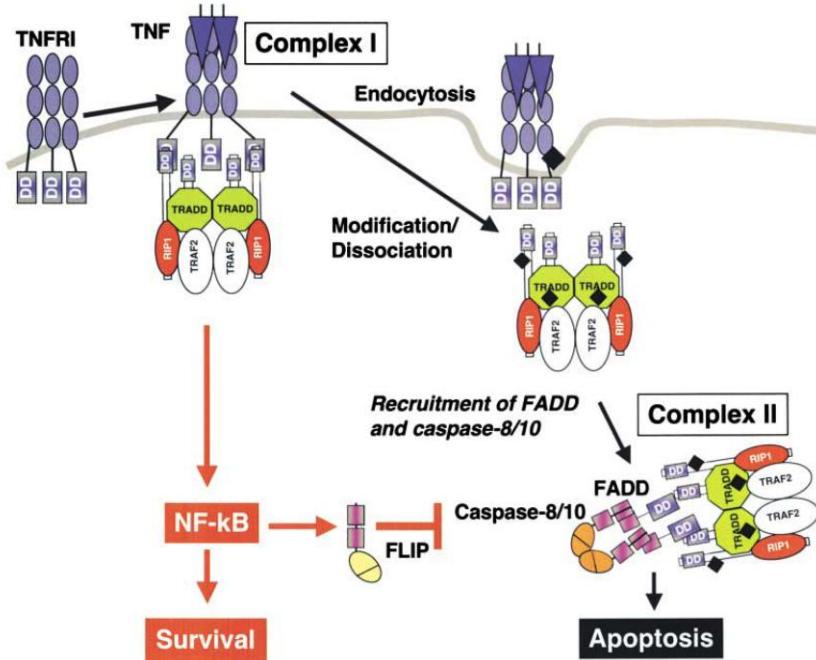
Figure 6. Formation of Complexes I and II according to *Micheau and Tschopp, 2003*

In case of the "vesicular transport" model, Schneider-Brachert and colleagues purified various complexes through their association with magnetically labeled TNF [80]. This implies that TNFR1 must have been present in all isolated complexes. At various times upon TNF stimulation the authors observed differences in the composition of the TNFR1 proximal complex. At the same time the complex gradually associated with markers of distinct vesicle compartments such as early endosome, trans-Golgi and lysosome. The authors could demonstrate that cells expressing a TNFR1 mutant that lacked the internalization domain did not show any Complex 2 related activities upon stimulation with TNF, while Complex 1 related activities were present. Consistent with this observation RIP1 and TRAF-2 were still recruited to mutant TNFR1, while FADD and caspese-8 could no longer be detected within the complex.

2.4   TRADD – TNFR1 Associated Death Domain Protein.

TNFR1 Associated Death Domain Protein (TRADD) was isolated from a two-hybrid screen for proteins interacting with the Death Domain of TNFR1 in 1995 by the group of David Goedell [23]. A year later the same group demonstrated that TRADD played a role in both

TNF-induced apoptosis and TNF-induced NF-κB activation via recruiting FADD and RIP1/TRAF2 respectively to the cytoplasmic part of the TNFR1 in a TNF dependant manner [24, 25].
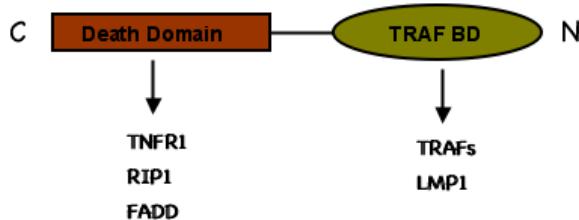
Figure 7. The scheme of the TRADD molecule.

It was shown by deletion mutagenesis that the C-terminal Death Domain of TRADD was essential for the interaction with RIP1, FADD and TNFR1 while the N-terminal part of the molecule interacted with TRAF2 (see Figure 7). Based on the listed evidence TRADD was proposed to be a unique adaptor molecule linking TNFR1 to both the induction of cell death and the activation of pro-inflammatory and pro-survival gene expression. As TRADD deficient mice were not available, the mentioned theory could not be clearly proven or denied. Recently two different groups of researchers employed a strategy of gene expression knockdown by specific small interfering RNA in order to further investigate the role of TRADD in TNFR1 mediated signaling [99, 100]. It was demonstrated that downregulation of TRADD expression had a negative effect on the recruitment of TRAF2 to the receptor upon TNF stimulation, while the recruitment of RIP-1 seemed to be enhanced. Moreover, higher amounts of TRADD associated with activated TNFR1 in cells with knockdown for RIP-1, leading researchers to conclude that RIP-1 and TRADD competed for the binding with TNFR1 upon TNF stimulation. Surprisingly, TNF induced NF-κB activation was only partially impaired in TRADD knockdown cells while c-Jun phosphorylation was significantly affected. At the same time the sensitivity of such cells to TNF induced apoptosis was similar to that of wild type cells, as demonstrated by one of the groups [99]. The evidence obtained by the second group on the contrary suggested that TRADD was essential for TNF mediated programmed cell death. At the same time TNF-induced necrosis did not depend on TRADD but required the presence of RIP-1 [100]. Overall the data presented by the two groups

appeared confusing and to a large extent contradictory, although both studies were based on the same experimental approach using siRNA mediated knockdown. Therefore further investigations must be conducted in order to uncover the exact role of TRADD in signal transduction via TNFR1.

It had been shown that TNFR1 could associate with tyrosine kinases JAK1 and 2 (for Janus Tyrosine Kinases) upon ligand binding. This association led to the activation of JAKs and phosphorylation of their downstream targets including the transcription factor STAT-1α [101]. Surprisingly STAT-1α DNA binding could not be detected upon such phosphorylation, suggesting that the factor was putatively involved in some alternative signaling cascade. Later it was shown that, instead of translocating into the nucleus, STAT-1α was recruited to the cytoplasmic part of TNFR1 via direct interaction with TRADD [102]. The binding of STAT-1α to TRADD had a negative effect on interactions of TRADD with TRAF2 and RIP1 and subsequently suppressed NF-κB activation.

To follow up on the role of the TRADD-STAT-1α complex in TNF mediated signaling Wesemann and colleagues investigated whether the complex could influence pathways that use STAT-1α as a primary signal transducer [103]. Surprisingly, they discovered that TRADD played a role in IFN-γ signaling. TRADD co-immunoprecipitated with phosphorylated STAT-1α upon stimulation of cells with IFN-γ. Moreover IFN-γ induced translocation of TRADD into the nucleus where TRADD co-localized with STAT-1α. The nuclear translocation of TRADD seemed transient. It seemed to peak at 0.5 hour upon IFN-γ stimulation curiously at the time when STAT-1α activation was peaking as well. Most of the TRADD - associated STAT-1α was phosphorylated. Co-immunoprecipitation experiments had shown that the interaction between TRADD and STAT-1α occurred in the nucleus. When an inhibitor of the STAT-1α phosphorylation was added, TRADD could still translocate into the nucleus upon stimulation with IFN-γ, but did not interact with STAT-1α. The activation of STAT-1α induced by IFN-γ is regulated via nuclear-cytoplasmic shuttling (phosphorylation – nuclear translocation – induction of gene expression – extraction from the nucleus – dephosphorylation). Based on the obtained evidence, the authors suggested that

TRADD binds to phosphorylated STAT-1α in the nucleus and subsequently mediates the translocation of the transcription factor from the nucleus to the cytoplasm. Thereby TRADD acts as a negative regulator of IFN-γ induced gene expression. The model was tested in cells where the expression of TRADD was knocked down by specific siRNA. It was demonstrated that in TRADD knock-down cells phosphorylated STAT-1α remained in the nucleus 12 hours after stimulation with IFN-γ compared to a maximum of 1-3 hours in stimulated wild type cells. Moreover, the expression of genes responsive to STAT-1α was enhanced and prolonged by the knock down of TRADD.

Focusing on the sub cellular localization of TRADD and related effects, it was demonstrated in 2002 by Morgan and colleagues that TRADD could translocate into the nucleus and be exported back into the cytoplasm [104]. The functional nuclear localization signal (NLS) and nuclear export signal (NES) were found within the TRADD molecule. Despite the presence of the NLS TRADD could only be detected in the cytoplasm unless the nuclear-cytoplasmic transport was blocked suggesting that rapid export of TRADD from the nucleus occurred under normal physiological conditions. To investigate whether nuclear TRADD had a specific function, the authors generated fusion proteins that localized exclusively in the nucleus and contained either full length TRADD or the death domain of TRADD. The expression of such proteins resulted in apoptotic death of transfected cells. The induction of death by nuclear TRADD required promyelocytic leukemia protein (PML) and p53 and was blocked by the expression of BclXL. In order to dissect mechanisms of cell death induced by nuclear TRADD and cytoplasmic TRADD, the same group used modified TRADD molecules that could reside exclusively in the cytoplasm or in the nucleus. It was demonstrated that death induced by the nuclear TRADD didn't require FADD or caspase-8 while both molecules were involved in the induction of apoptosis by cytoplasmic TRADD [105]. The accumulation of TRADD in the nucleus resulted in the activation of caspase-9. Caspase-9 is activated by a complex of the cytoplasmic protein Apaf-1 with cytochrom-c. The latter has to be released from the intermembrane space of the mitochondria in response to pro-apoptotic stimuli. The death induced by the nuclear TRADD was partially inhibited in Apaf-1 deficient cells. Interestingly, the apoptosis mediated by p53 also depends on mitochondria, cytochrome-c and caspase-9. Given the results of the previous work by the same authors, it seemed probable that nuclear TRADD acted by inducing p53-dependant cell

death via interaction with components of PML bodies. Curiously the pan-caspase inhibitor zVADfmk was not sufficient to block death induced by the nuclear TRADD providing only partial inhibition. The complete block was achieved by combining caspase inhibitors with the broad spectrum serine protease inhibitor AEBSF suggesting that non-caspase serine proteases (such as cathepsins, calpains or granzymes [106]) could play a role in this process.

It was demonstrated in 2000 that keratin 8 (K8) and keratin 18 (K18) protected epithelial cells from death mediated by TNF. The two keratins bound to the cytoplasmic part of TNFR2 and modulated receptor-induced activation of JNK and NF-κB [107]. One year later keratin 18 was identified in a two-hybrid screen as a protein interacting with TRADD [108]. This interaction was further confirmed by an *in vitro* co-sedimentation assay and by the fact that myc-tagged TRADD co-localized with K8/K18 filaments in various epithelial cell lines. Endogenous TRADD co-immunoprecipitated with endogenous K18 under physiological conditions. The association was disrupted by the stimulation of cells with high doses of TNF. The dissociation of TRADD from K8/K18 filaments paralleled with the induction of the apoptotic cell death suggesting that keratin 18 may play an inhibitory role in apoptosis mediated by TNFR1. Overexpression of the full length K18 or the N-terminal portion of K18 that contained a TRADD binding motif decreased the sensitivity of cells to TNF-induced apoptosis.

Recently it was demonstrated that another keratin – keratin 17 (K17) could also interact with TRADD [109]. Keratin 17 deficient keratinocytes shown increased susceptibility to TNF-induced apoptosis. Curiously TNF-induced NF-κB activation was also increased in K17 null cells suggesting that the association between K17 and TRADD may have a general inhibitory effect on TNFR1 mediated signal transduction.
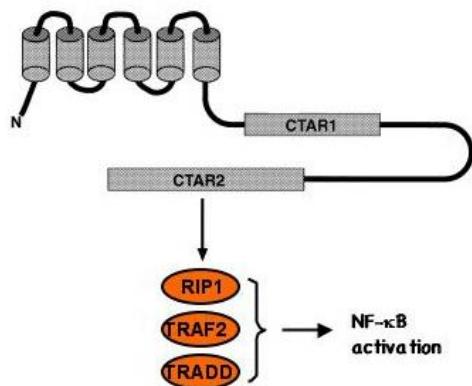
Signal transduction through LMP1. Modified from *Kieser et al, 1999*

In addition to its role in homeostatic signaling events, TRADD participates in NF-κB activation and B-cell transformation induced by the Epstein-Barr Virus oncogene Latent Membrane Protein 1 (LMP1)[110]. LMP1 is an integral membrane protein that has 6 transmembrane-spanning domains a short intracellular N-terminal domain and a long C-terminal domain also projected into the cytoplasm (see Figure 8). LMP1 acts as a constitutively active receptor that doesn't require ligand binding. The transmembrane domain mediates the oligomerization of LMP1 molecules in the plasma membrane thereby promoting signal transduction. The C-terminus of LMP1 contains two regions involved in protein-protein interactions − C-terminal Activator Regions 1 and 2 (CTAR1 and 2). Both regions are involved in the NF-κB activation: CTAR1 - via interaction with TRAFs and CTAR2 - via recruiting TRADD, TRAF2 and RIP1 [111, 112].

2.5 Toll like receptors (TLRs). Signal transduction through TLR3 and TLR4.

Toll like receptors belong to a large family of Pattern Recognition Receptors (PRRs) that are essential components of innate immunity. Although pattern recognition receptors are widely expressed, particularly high amounts can be found on the surface of macrophages, natural killer cells, mast cells and antigen presenting dendritic cells. PRRs recognize DAMPs (for Danger Associated Molecular Patterns) - invariant molecular structures present in pathogens

(like lipopolysaccharides and unmethylated CpG DNA) or released upon tissue damage (like heat shock protein hsp-70). Binding of the respective ligand to a given pattern recognition receptor activates effector functions and mediates expression of co-stimulatory molecules [113, 114].

Mammalian Toll like receptors share structural and functional homology with the product of the Toll gene from *Drosophila.* Originally discovered as a transmembrane protein responsible for the dorsal-ventral polarity of the developing embryo [115] Toll mediates nuclear translocation of the *Drosophila* NF-κB family member Dorsal in response to the soluble ligand Spatzle [116]. One of the genes induced by NF-κB in a Toll-dependant manner encodes the antifungal peptide Drosomycin [117].

TABLE 1 Toll-like receptors and their ligands

TLR family	Ligands (origin)
TLR1	Tri-acyl lipopeptides (bacteria, mycobacteria)
	Soluble factors (Neisseria meningitides)
TLR2	Lipoprotein/lipopeptides (a variety of pathogens)
	Peptidoglycan (Gram-positive bacteria)
	Lipoteichoic acid (Gram-positive bacteria)
	Lipoarabinomannan (mycobacteria)
	A phenol-soluble modulin (Staphylococcus epidermidis)
	Glycoinositolphospholipids (Trypanosoma Cruzi)
	Glycolipids (Treponema maltophilum)
	Porins (Neisseria)
	Zymosan (fungi)
	Atypical LPS (Leptospira interrogans)
	Atypical LPS (Porphyromonas gingivalis)
	HSP70 (host)
TLR3	Double-stranded RNA (virus)
TLR4	LPS (Gram-negative bacteria)
	Taxol (plant)
	Fusion protein (RSV)
	Envelope proteins (MMTV)
	HSP60 (Chlamydia pneumoniae)
	HSP60 (host)
	HSP70 (host)
	Type III repeat extra domain A of fibronectin (host)
	Oligosaccharides of hyaluronic acid (host)
	Polysaccharide fragments of heparan sulfate (host)
	Fibrinogen (host)
TLR5	Flagellin (bacteria)
TLR6	Di-acyl lipopeptides (mycoplasma)
TLR7	Imidazoquinoline (synthetic compounds)
	Loxoribine (synthetic compounds)
	Bropirimine (synthetic compounds)
TLR8	?
TLR9	CpG DNA (bacteria)
TLR10	?

Adapted from *Takeda et al, 2003*

Therefore Toll plays a role in the defense of the fly against pathogens. Ten different human and twelve different murine homologues of Toll have been identified till now all sharing the same structural features: leucine-rich repeats (LRR) in the extra cellular part and the TIR (for Toll/IL-1 Receptor homologous) domain projected into the cytosol [118]. Despite similar structure, different TLRs are activated by different pathogen- and stress-related ligands (see Table 1).

Toll like receptors are activated via ligand-induced conformational changes [161]. Some TLRs (TLR3, 4, 5, 9 and 11) act as homodimers; TLR2 forms heterodimers with either TLR1 or TLR6 (the ligand specificity is determined by the composition of the dimer), TLR7 functions as a heterodimer with TLR8. Toll like receptors also require adaptor proteins in order to transmit the signal into the cell. Such adaptor proteins can be subdivided into signaling adaptors and sorting adaptors. Signaling adaptors communicate with downstream effectors while sorting adaptors mediate the recruitment of a certain signaling adaptor to the receptor that resides in a particular cellular microenvironment [119].

The signaling adaptor Myd88 (for Myeloid Differentiation marker 88) participates in signal transduction through IL-1 receptor and all Toll like receptors but TLR3 [120]. Human Myd88 was discovered in 1998 [121] and subsequently mice deficient for the murine homolog were generated [122]. Myd88 knock out animals demonstrated impaired responses to IL-1β, LPS (Gram-negative bacteria, TLR4), peptidoglycan (Gram-positive bacteria, TLR2) and CpG DNA (bacteria, TLR9) [123-125] confirming the importance of Myd88 for TLR signaling.

Myd88 is recruited to the TIR domain of Toll like receptors via its own TIR domain upon ligand-induced dimerization of the receptor (see Figure 9 for an overview). After binding to the TIR domain of the receptor, Myd88 utilizes its second protein-protein interaction motif – the death domain – to recruit a death domain containing kinase IRAK-4 [126, 127]. IRAK-4 is a member of a family of kinases called IRAKs for IL-1β Receptor Associated Kinases. All mammalian IRAKs share sequence homology with Pelle – a kinase that participates in the Toll signaling cascade in *Drosophila*. IRAK-4 is the only mammalian family member that requires kinase activity to perform its function. Activated IRAK-4 phosphorylates downstream IRAKs – IRAK-1 [128] and IRAK-2 [129]. IRAK-1 is ubiquitously expressed

while the expression of IRAK-2 is restricted to certain cell types. Both IRAK-1 and IRAK-2 contain death domains and are presumably recruited to the cytoplasmic part of TLRs via the death domain of Myd88. Downstream IRAKs recruit TRAF6. TRAF6 is a RING finger domain protein that functions together with ubiquitin conjugating enzymes Ubc13 and Uev1A to catalyze the synthesis of polyubiquitin chains linked through lysine-63 (K63) of ubiquitin [130].
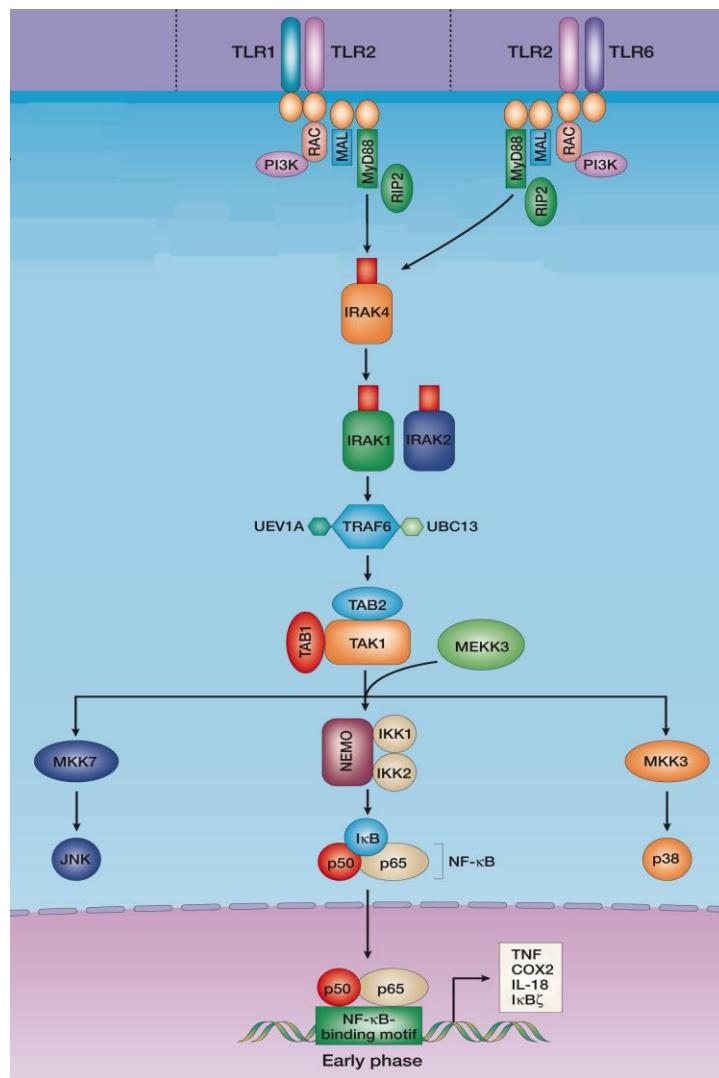
Figure 9. Schematic representation of classical Myd88 dependant TLR signaling. Modified from *O'Neill, 2004*

Upon recruitment to the complex associated with the Toll like receptor TRAF6 acquires the capacity of ubiquitinating itself. Ubiquitinated TRAF6 acts a platform for the recruitment of

the TAB1/TAB2/TAK1 complex that mediates NF-κB and MAPK activation through phosphorylation of IKK members and upstream MAP kinases [83, 131]. Another important signaling mediator that can be recruited to TLRs via Myd88 is TRAF3 [132]. The mechanism of such recruitment is not well understood. TRAF3 forms a complex with TANK-binding kinase 1(TBK1) and IKK-ε. This complex acts as a kinase specific for IFN regulatory factor 7 (IRF 7). IRF7 is a transcription factor that mediates expression of a number of pro-inflammatory genes including type I interferons. Signal transduction via Myd88/TRAF3 is utilized by TLR9 and TLR7/8 – Toll like receptors that participate in anti-viral response. Signal transduction through TLR5, TLR7/8, TLR9, TLR 11, TLR2/1 and TLR2/6 relies solely on Myd88.

Toll like receptor 3 (see Figure 10) is the only known TLR that does not utilize Myd88. TLR3 signals through a different adaptor called TRIF (for TIR-related adaptor protein inducing interferon) or TICAM-1 (for TIR-containing adaptor molecule -1) [133, 134].

Unlike Myd88, TRIF does not contain a death domain but it contains other motifs involved in protein-protein interactions. TRIF uses its N-terminal TRAF-binding domain to directly recruit TRAF6 and TRAF3 to the cytoplasmic part of the TLR3 [135, 136]. TRAF6 mediates the activation of NF-κB and MAP kinases presumably through the same mechanism that it utilizes within Myd88 dependant signaling. TRAF3 forms a complex with TBK1 and IKK-ε. This complex acts as a kinase specific for IFN regulatory factor 3 (IRF3) – another transcription factor that mediates expression of type I interferons.

In was demonstrated that TRIF could recruit RIP1 to the cytoplasmic part of the TLR3 via the C-terminal RIP homotipic interaction motif (RHIM) [137]. RIP1 deficient mouse embryonic fibroblasts failed to induce NF-κB activation upon stimulation with the synthetic ligand for Toll like receptor 3 (polyI:C). It was shown later that RIP1 was K63 polyubiquitinated in response to polyI:C [138]. The ubiquitination of RIP1 correlated with the enhanced association between TLR3 and TAK1. However the corresponding ubiquitin ligase was never identified. Further molecular details of this branch of TLR3 signaling are currently not known.
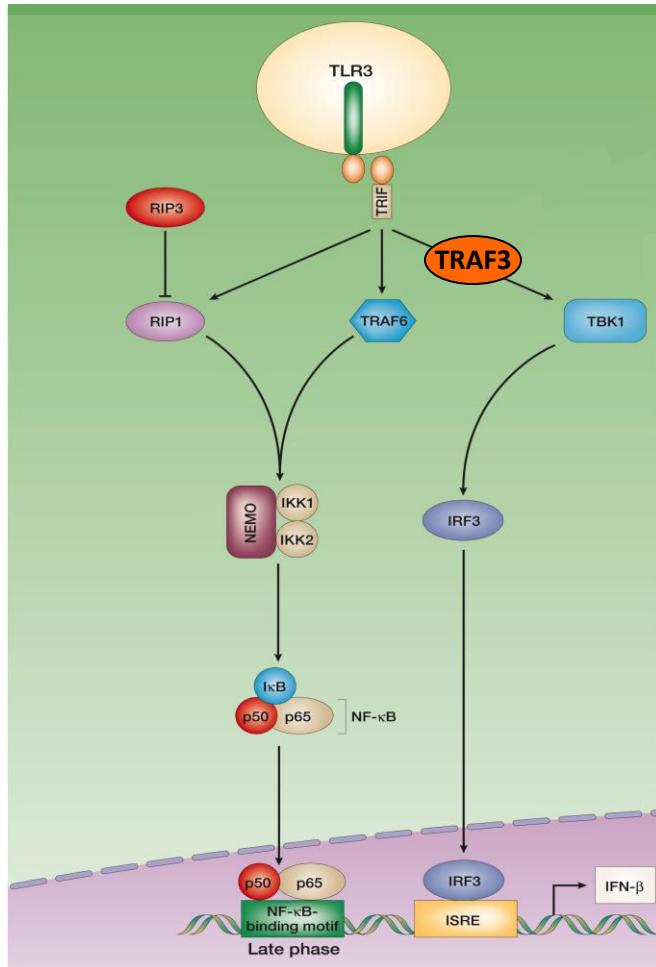
Figure 10. Schematic representation of TLR3 signaling. Modified from *O'Neill, 2004*

Unlike other known Toll like receptors that signal through ether TRIF or Myd88, Toll like receptor 4 (see Figure 11) is capable of utilizing both adaptor proteins [139]. The response of cells to the TLR4 ligand LPS could only be ablated by double deficiency for both TRIF and Myd88. Recent work by Medzhitov and Kagan had demonstrated that the choice to use one signaling adaptor or the other is most probably determined by the subcellular localization of the receptor [119]. The authors discovered that TIRAP/Mal (the adaptor that is essential for the Myd88-dependant branch of TLR4 signaling) contains a phosphatidylinositol 4,5-bisphosphate (PIP2) binding domain. This domain targets TIRAP to the plasma membrane. The authors hypothesized that TLR4 molecules that are located in the plasma membrane would signal via TIRAP/Myd88 while molecules located in a different membrane compartment would utilize the TRAM/TRIF cascade. TRAM is an adaptor molecule that is

essential for the TRIF-dependant branch of TLR4 signaling. Kagan and Medzhitov define TIRAP and TRAM as sorting adaptors that do not transmit the signal but determine the way the signal goes.

The usage of adaptors and downstream effectors by Toll like receptors may also depend on the cell type. For example the loss of TRAF6 has a stronger effect on TLR signaling in mouse embryonic fibroblasts then in macrophages [140]. Moreover it has been suggested that in different cell types the same receptor may reside in a different subcellular compartment and face different physiological ligands. These factors taken together increase the overall complexity of TLR signaling and may in part explain non-coherent results that are often obtained by using the same TLR ligand on different cells.
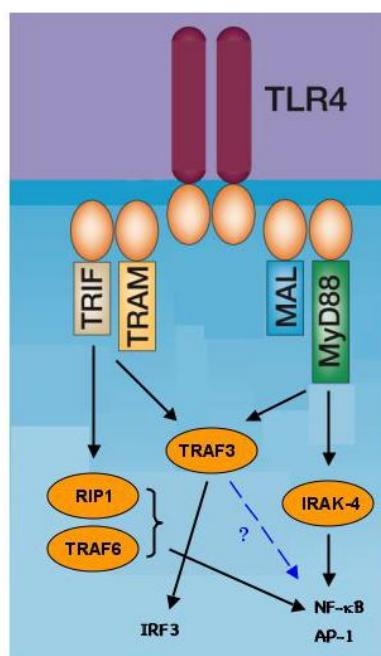
Figure 11. Schematic representation of TLR4 signaling. Modified from *O'Neill, 2004*

2.6 Negative regulation of TNF Receptor I and Toll like receptor signaling.

As discussed previously Toll like receptors and TNFR1 are essential for the defense of the organism against bacterial and viral infections. The activation of pro-inflammatory cascades by these receptors leads to rapid induction of cytokine expression contributing to the efficient systemic response to pathogens. However the pro-inflammatory signaling downstream of TLRs and TNFR1 has to be kept under control in order to prevent cytokine-induced shock

and the development of chronic inflammation. For this reason both groups of receptors evolved to self-control their own activity in a negative feedback loop fashion.

Among the genes that are induced by TLR ligands and TNF through the NF-κB family of transcription factors two – A20 [93] and CYLD [94] - encode K63 de-ubiquitinating enzymes. It was demonstrated that both CYLD and A20 could be recruited to receptor associated complexes and remove K63-linked poly-ubiquitin chains from molecules like RIP1, TRAF2, TRAF6 and NEMO [95, 96]. The removal of ubiquitin chains results in downregulation of associated enzymatic activities (like IKK kinase activity in case of NEMO) or in loss of interaction with downstream mediators (like recruitment of TAK1 and NEMO in case of RIP1).
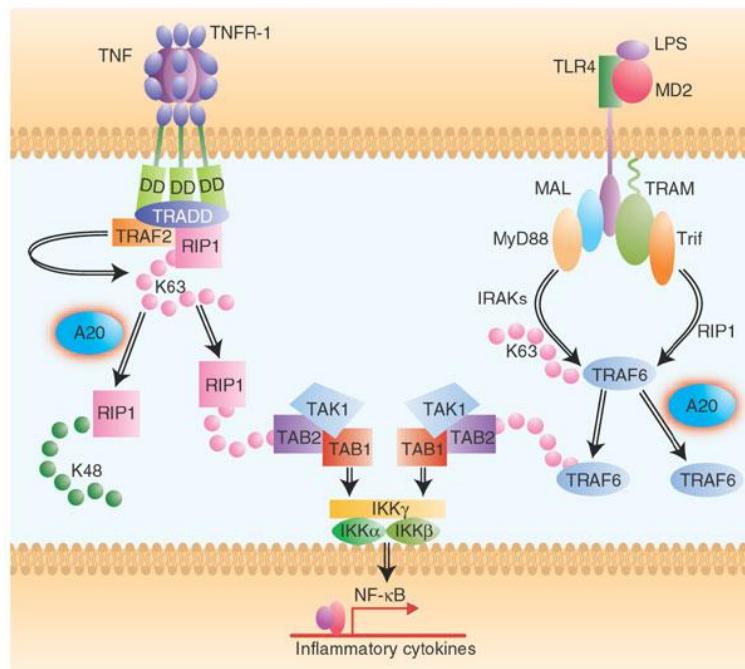
Figure 12. The role of A20 in TNFR1 and TLR signaling. Adapted from *Silverman and Fitzgerald, 2004*

Moreover A20 was shown to posses a K48 ubiquitin ligase activity (C-terminal) in addition to the de-ubiquitinating function (N-terminal). It was demonstrated that upon removal of K63-linked polyubiquitin chains from RIP1, A20 subsequently ubiquitinates the same substrate with K48-linked chains thereby targeting RIP1 for proteosomal degradation [97]

(see Figure 12 for summary). Both A20 and CYLD inhibit TNF- and TLR-mediated NF-κB and MAPK activation [95, 96, 98].

Gene knockout studies in mice confirmed the essential role of A20 in the control of inflammatory responses. A20 deficient animals appeared hypersensitive to TNF [153] and died prematurely demonstrating severe multiple organ inflammation and cachexia. The lethality could be rescued by crossing A20 -/- mice to Myd88 -/- mice [154] unveiling the causative role of TLR signaling in the development of the original phenotype. Unlike A20 the precise physiological function of CYLD is yet to be determined.

2.7   CYLD – a product of the gene mutated in Brook-Spiegler syndrome.

The Brook-Spiegler syndrome (BSS) is an autosomal dominant disorder characterized by the development of multiple benign tumors originating from skin appendages (hair follicles and sweat glands; see Figure 13 for the schematic of the structure of human skin).
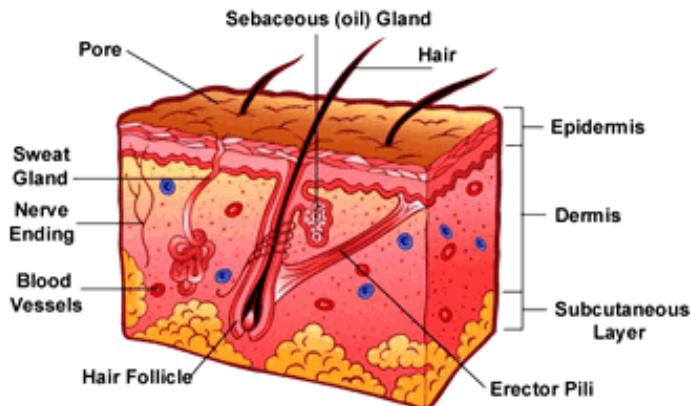
Figure 13. The schematic of the human skin.

The manifestations of BSS include three morphologically different types of lesions – cylindroma, trichoepithelioma and spiroadenoma [155, 156]. All three types of lesions are caused by biallelic mutations in the cylindromatosis (*CYLD)* gene [157, 158] named after one of BSS manifestations. The gene residing on chromosome 16q12-q13 was identified in 2000 by detecting germline mutations in 21 families suffering from cylindromatosis [141].

Based on the sequence of the gene CYLD was predicted to be a protein of 956 amino acids. According to the prediction the N-terminal part of CYLD contained five putative protein-protein interaction motifs – three regions homologous to the CAP-Gly domain (for cytoskeleton-associated protein-glycine conserved domain) [142] and two proline rich regions; while the C-terminal part shared homology with the catalytic domain of the ubiquitin C-terminal hydrolase 2 (UCH2, a de-ubiquitinating enzyme) [143]. The majority of naturally occurring mutations analyzed by the authors were predicted to produce C-terminal truncations of CYLD that varied in size.

2.8 The familial cylindromatosis protein (CYLD) acts as a de-ubiquitinating enzyme specific for various targets.

In 2003 two independent groups of researchers isolated CYLD from yeast two-hybrid screens, where the regulatory subunit of the IKK complex, NEMO was used as the bait [95, 144]. They searched for other candidate proteins that could interact with CYLD and identified TRAF2 and TRAF6 as CYLD binding partners. It was demonstrated by deletion mutagenesis that specific motifs within the N-terminal part of CYLD were involved in recruitment of TRAF2, TRAF6 and NEMO.

Both groups of authors noticed that the C-terminus of the CYLD molecule contained motifs similar to the cysteine and histidine boxes found in the UBP ubiquitin-specific protease subfamily. They also noticed that mutations isolated from human familial cylindromatosis mostly affected the C-terminus of the molecule. Based on these observations both groups did a number of experiments and discovered that CYLD acted as an enzyme with deubiquitinase activity specific for K63-linked poliubiquitin chains.

NEMO, TRAF2 and TRAF6 were identified as targets for deubiquitination mediated by CYLD. The ability of CYLD to directly bind to its targets was shown to be essential for performing the enzymatic activity on them. Some CYLD mutants, isolated from

cylindromatosis patients (including the CYLD Δ932 mutant that is lacking last 20 C-terminal amino acids of the protein) were tested for the ability to function as deubiquitinating enzymes and were shown to be catalitically inactive.

Both TRAF2 and TRAF6 were known to trigger signal transduction (including NF-κB activation downstream of a number of receptors) by acting as E3 ubiquitin ligases and ubiquitinating themselves and other targets through K63-Ub conjugation. Consistent with its role as a deubiquitinating enzyme specific for TRAF2 and TRAF6, CYLD inhibited NF-κB activation induced by TNF, IL-1β and CD40. Knock down of CYLD by specific siRNA or expression of catalytically inactive mutants led to an increase in NF-κB activation induced by over-expression of CD40 and TRAF2 or stimulation of cells with TNF.

At the same time another group isolated CYLD from a high-throughput RNA interference screen in mammalian cells that was done to identify novel regulators of NF-κB among proteins containing a conserved catalytic domain of de-ubiquitinating enzymes [145]. Just as in previously described work the authors demonstrated that CYLD interacted with TRAF2 and NEMO and antagonized NF-κB activation induced by TNF.

A year later it was demonstrated that the expression of CYLD could be induced in response to stimuli like TNF and IL-1β through NF-κB family of transcription factors [94]. This finding suggested that CYLD and NF-κB activation could be linked by a negative feed-back loop. Later the putative physiological role of CYLD was extended from inhibition of NF-κB activation to influencing the activation of MAP kinases, induced by stimuli like TNF [98]. Another link between CYLD and the cascade implicated in NF-κB activation was suggested by a study that reported TNF-induced phosphorylation of CYLD by the IκB kinase complex. The phosphorylation had an inhibitory effect on the enzymatic function of CYLD [146]. In the same study it was demonstrated that the expression of CYLD could be induced upon TLR2 activation.

The first paper describing a phenotype of a CYLD deficient mouse was published in April of 2006 [147]. The knock out was generated by knocking a gene encoding the resistance to neomycin (neo^R) into the first exon of the *cyld* gene. The lack of CYLD expression was confirmed by Western blot analysis. CYLD knock out mice didn't exhibit gross defects, which was surprising given the previously suggested physiological role of the molecule. Moreover, TNF-induced activation of NF-κB and MAP kinases in bone marrow derived macrophages was not influenced by the CYLD deficiency in contrast to the previously published data. It was demonstrated that CYLD null animals had less T-lymphocytes in peripheral organs compared to control animals. The authors discovered that mutant T-cells died at the point of transition from the double positive stage to the single positive stage of thymocyte development due to a T-cell intrinsic defect, most likely some alteration in signal transduction through the T-cell receptor (TCR). During normal TCR signaling the recognition of a complex of the MHC molecule with the antigen brings together the TCR and its co-receptor (CD4 or CD8 depending on a type of T-cell) that is associated with a cytoplasmic tyrosine kinase called Lck (for leukocyte specific kinase). Lck phosphotylates the CD3ζ subunit of the T cell receptor and thereby mediates the recruitment of another tyrosine kinase called Zap70 (for zeta-chain-associated protein 70 kD) to the complex associated with the TCR. Zap70 becomes active upon phosphorylation that is also mediated by Lck. The recruitment and the activation of Zap70 is a central event in T cell receptor signaling. The authors demonstrated that the activating phosphorylation of Lck was unaltered in anti-CD3 stimulated CYLD deficient thymocytes, instead the phosphorylation of Zap70 could no longer be detected, suggesting that the catalytic activity of Lck must have been influenced by the lack of CYLD. It had been demonstrated previously that the activity of Lck was inhibited by K63- ubiquitination. Considering the function of CYLD as a K63-deubiquitinating enzyme, the authors suggested that CYLD counteracted the inhibition of Lck and provided experimental prove for this hypothesis.

Another paper describing a different CYLD deficient mouse was published in May 2006 [148]. The mouse was generated by inserting a LacZ reporter gene into the ATG-encoding exon four of the murine *cyld* gene. The lack of CYLD mRNA and protein was confirmed by

RT-PCR and Western blot analysis respectively. CYLD deficient mice generated in a described way didn't show any evident spontaneous phenotype (just like previously reported CYLD null animals) but were more susceptible to the development of skin tumors upon combined DMBA/TPA treatment. Increased expression levels of cyclin D1 were detected in TPA-stimulated CYLD deficient keratinocytes along with enhanced proliferation. Curiously the UV irradiation – a putative triggering factor of human BSS, had a similar effect on mutant keratinocytes as did TPA. The authors demonstrated that TPA induced the expression of cyclin D1 through transcription factors belonging to the NF-κB family – p50 and p52. These transcription factors lack the transactivation domain and therefore they must rely on such domain that belongs to their binding partner – an IκB family member Bcl-3. It was demonstrated that Bcl-3 served as a substrate for the de-ubiquitination performed by CYLD. The de-ubiquitination stopped Bcl-3 from translocating into the nucleus and binding to the NF-κB transcription factors. In TPA (or UV) stimulated CYLD deficient cells or cells reconstituted with the catalitically inactive CYLD mutant, Bcl-3 remained ubiquitinated and almost all of it located in the nucleus, while in control cells stimulated in parallel Bcl-3 remained in the cytoplasm.

CYLD deficient mice were also sensitized to DSS-induced colitis and DSS/AOM-induced colon cancer, as demonstrated by Zhang and colleagues [149]. AOM (azoxymethan) is a DNA-alkylating agent that provokes somatic mutagenesis in colonic epithelium; DSS (dextran sulfate sodium) is a chemical that is capable of inducing inflammation in the colon. The chronic inflammation that can be caused by the repetitive administration of DSS in drinking water is known to increase the incidence of AOM-induced tumors. The inflammatory damage of the colon as well as the weight loss upon treatment with DSS was greater in CYLD-/- animals compared to control animals. CYLD-/- mice that were treated with DSS/AOM developed tumors earlier then wild type mice. They also had more and bigger tumors. CYLD deficient mice of interest were generated by replacing exons 2 and 3 of the murine *cyld* gene with the *LacZ* reporter. These mice demonstrated lymphoid hyperplasia and lymphoid inflammatory infiltrates into many tissues at the age of 10 month. Such phenotype may indicate the inability of CYLD deficient mice to properly control and block inflammation. In fact the DNA-binding of NF-κB that was induced by stimulation with anti-

IgM and anti-CD3 was elevated in CYLD-/- B and T lymphocytes respectively. This result correlated with the enhanced K63 ubiquitination of NEMO that was found in anti-CD3 stimulated CYLD deficient T-cells. NF-κB activation was also increased in knock out macrophages that were treated with several microbial components that activate Toll like receptors. Surprisingly the absence of CYLD had no effect on NF-κB activation that was induced by giving TNF to bone marrow derived macrophages. It was demonstrated that K63 ubiquitination of RIP1 upon TNF stimulation (which is proposed to play the key role in TNF-induced NF-κB activation) was not affected by CYLD deficiency in this cell type. On the contrary, TNF-induced JNK activation was increased in knock out macrophages. This result correlated with elevated K63 ubiquitination of TRAF2 upon TNF stimulation that was found in CYLD-/- cells. Overall CYLD deficient cells seemed to overreact to pro-inflammatory stimuli. The inability to control inflammation at the systemic level could be the cause of the lymphoid phenotype of aged CYLD knockout mice. It could also explain elevated sensitivity of these mice to AOM/DSS-induced tumorogenesis, as the model is known to depend on inflammation.

A recent study demonstrated B-cell hyperplasia and abnormalities of peripheral lymphoid organs in CYLD deficient mice [150]. Consistent with the phenotype of the mouse, mutant B-cells showed activation in the absence of stimulation and hyper-responsiveness to a number of ligands. IκBα was constantly phosphorylated and degraded in CYLD-/- lymphocytes. Mutant cells demonstrated increased basal activity of NF-κB and elevated activation of it in response to ligands such as LPS and anti-IgM. Therefore the authors concluded that the loss of CYLD causes constitutive activation of canonical NF-κB members in B-cells.

Other most recent studies implicated CYLD in processes unrelated to its role in the immune system function such as regulation of timely entry into mitosis and regulation of spermatogenesis [159, 160].

3. Conditional targeting of TNFR1 associated Death Domain protein (TRADD) and Familial Cylindromatosis protein (CYLD). Aim of the study.

Tumor Necrosis Factor (TNF) is a pleiotropic cytokine involved in a wide variety of responses at the systemic and at the local, tissue specific level. Among all, TNF is one of the key regulators of inflammation and immunity. Correctly timed TNF biosynthesis and unaltered signal transduction through respective receptors are essential for appropriate immune response against pathogens. At the same time uncontrolled or excessive production of TNF as well as impaired TNFR signaling may lead to acute inflammatory conditions such as septic shock or chronic inflammatory disorders such as rheumatoid arthritis.

Toll like receptors (TLRs) are essential components of mammalian innate immunity. They belong to a group of sensors that directly recognize bacterial and viral products as well as markers of tissue stress. The role of these sensors is to initiate the protective systemic response against tissue damage or infection. Upon activation TLRs induce intracellular signaling events leading to production of cytokines, chemokines, cell adhesion molecules and other mediators that promote the protective response. These activities however have to be tightly regulated in order to avoid cytokine induced shock or chronic inflammation.

In summary, TNF- and TLR-mediated signaling cascades play a key role in host defense against pathogens and response to tissue damage. Optimal strengths of signaling is critical for the outcome of the activation of these cascades. Therefore it is challenging and relevant from the clinical point of view to develop tools for the cell-specific modulation of TNF and TLR signaling in the desired direction.

3.1 Part A: Conditional targeting of TRADD.

The 55 kDa TNF receptor (TNFR1) is the main mediator of TNF signaling. The binding of TNF to TNFR1 ether results in the induction of apoptosis or leads to the activation of pro-

survival and pro-inflammatory gene expression. It has been postulated that the adaptor named TNFR1 Associated Death Domain Protein (TRADD) is needed for both responses. Upon binding to TNFR1 TRADD is thought to recruit both molecules that mediate the induction of gene expression (such as RIP1 and TRAF2) and molecules that mediate cell death (such as FADD and caspase-8). The recruitment of the two signaling modules putatively takes place at different times upon the activation of the receptor and at different subcellular compartments.

The primary aim of this part of the project was to investigate the physiological role of TRADD and to evaluate the existing model of signal transduction through TNFR1 by generating mice deficient for the TRADD gene. By using these mice we also planed to investigate whether TRADD could be involved in any other signaling cascade related to inflammation and immunity.

We chose to generate TRADD deficient mice by using a conditional targeting approach based on Cre/LoxP system of site-specific DNA recombination. In addition to obtaining the complete knock out mouse, such approach also allows to knock-out TRADD in a cell type specific and/or inducible manner.

3.2 Part B: Conditional targeting of CYLD.

Toll like receptors and TNFR1 share a common mechanism of signal termination that is based on the disruption of receptor-associated protein complexes due to the removal of K63-linked polyubiquitin chains from specific key components of these complexes. Two de-ubiquitinating enzymes – A20 and CYLD are currently known to be responsible for this process. It was demonstrated that both enzymes could inhibit TNFR1- and TLR-induced activation of NF-κB and MAP kinases by acting on targets such as RIP1, TRAF2, TRAF6 and NEMO.

Consistent with the key role of the K63-linked chain specific deubiquitination in the restriction of pro-inflammatory responses, mice knockout for A20 died prematurely developing a chronic inflammatory condition. Unlike A20, the precise physiological role of

CYLD remains enigmatic. Therefore it is challenging and important for the field to develop a mouse model lacking CYLD catalytic activity in the whole body or in specific cell types.

The aim of this part of the project was to investigate the physiological function of CYLD by generating mice that express a mutated catalytically inactive CYLD protein. We chose to use a conditional targeting approach based on Cre/LoxP system of site-specific DNA recombination to introduce the catalytically inactive CYLD mutant in the mouse. As it was mentioned previously this approach allows us to generate various tissue specific and/or inducible mutants in addition to the complete mutant mouse.

4. **Materials and Methods.**

4.1 Generation of mutant mice.

4.1.1 *Generation of TRADD deficient mice.*

4.1.1.1 Construction of the targeting vector.

Most DNA fragments that were used for the construction of the targeting vector were obtained via polymerase chain reaction (PCR). All fragments were amplified using a mixture of high fidelity Pfu polymerase (Invitrogen) with the Taq polymerase (Invitrogen); the ratio of Pfu to Taq was 1 to 25 units. All primers were purchased from the Metabion GmbH (Martinsried, Germany). Following composition of reagents was used for the PCR (values are given for 1 reaction; reaction volume is 30µl):

10x Pfu-specific reaction buffer (Invitrogen) - 3µl

25mM MgCl - 1.8µl

2mM dNTPs (2mM dATP + 2mM dGTP + 2mM dCTP + 2mM dTTP) - 3µl

Primers - 25 pmol of each

Taq polymerase - 2.5 units = 0.5µl

Pfu polymerase - 0.1 unit = 0.05µl

DNA template - 2 ng

H_2O - up to 30µl depending on the volume of the template

The following PCR program was used for the amplification of the "floxed" fragment and the arms of homology:

Step 1: 94^0C – 3 minutes

Step 2: 94^0C – 30 seconds

Step 3: 60^0C – 30 seconds

Step 4: 72^0C – 5 minutes

Steps 2-4 repeated 30 times

Step 5: 72^0C – 4 minutes

BAC clone (BACPAC) containing *tradd* genomic DNA served as a template for obtaining arms of homology and the "floxed" fragment. The "floxed" fragment (to be inserted between loxP sites) was 3.4 kb in size; it contained exons 2-5 of the *tradd* gene and polyadenylation sequence of the gene. The 2.4 kb fragment of the first intron of the *tradd* gene was used as the left arm of homology. The 3.5 kb fragment that was positioned downstream of the polyadenylation sequence of the *tradd* gene was chosen as the right arm of homology. Recognition sequences for specific restriction enzymes were placed at 5′ ends of PCR primers, to be used for further insertion of respective fragments into the backbone vector or for the ES cell screening. For the amplification of the "floxed" fragment following primers were used:

> ***Sense primer*** *(recognition sequence for Sal I restriction enzyme was added; underlined and indicated with a bold italic font):*
>
> 5′ GCA***GTCGAC***CAAGTTTTGACTGGCTCCTGA 3′
>
> ***Anti-sense primer*** *(recognition sequences for Sal I, EcoR I and Sca I were added; underlined or indicated with a different font size; listed in 5′ to 3′ order):*
>
> 5′ AAT***GTCGAC***GAATTC***AGTACT***CCTCAGGGCCTTGGTTATATC 3′

For the amplification of the left arm of homology following primers were used:

> ***Sense primer*** *(recognition sequence for Not I was added; underlined):*
>
> 5′ GCAT***GCGGCCGC***CTTCTTAGACGTCCTTGCTTG 3′
>
> ***Anti-sense primer*** *(recognition sequence for Not I was added; underlined):*
>
> 5′ GCAT***GCGGCCGC***GATATTGGCTCAAACTGGACT 3′

For the amplification of the right arm of homology following primers were used:

Sense primer *(recognition sequence for Asc I was added; underlined):*

5′ GC*GGCGCGCC*AAAGGTCTACCACTGAGCTAC 3′

Anti-sense primer *(recognition sequence for Asc I was added; underlined):*

5′ GC*GGCGCGCC*CACAGACTTGACAGCGATGAG 3′

The pSAβgeo plasmid was used as the template for the amplification of the adenoviral splice acceptor sequence. This plasmid was obtained by cloning the splice acceptor-linked fusion between the cDNA encoding β-galactosidase and the cDNA encoding the resistance to neomycin into the pBluescript KS(-) vector (Stratagene). Following primers and PCR program were used:

Sense primer *(recognition sequences for EcoR I and BssH II were added; underlined or indicated with a different font size; listed in 5′ to 3′ order):*

5′ A*GAATTC*GCGCGCTAGGGCGCAGTAGTCCAG 3′

Anti-sense primer *(recognition sequence for Bam HI was added; underlined):*

5′ CG*GGATCC*AGTACTGGAAAGACCGCG 3′

The PCR program:

Step 1: 94^0C – 3 minutes

Step 2: 94^0C – 30 seconds

Step 3: 60^0C – 30 seconds

Step 4: 72^0C – 1 minute

Steps 2-4 repeated 30 times

Step 5: 72^0C – 4 minutes

PCR fragments were purified using QIAEX II gel extraction kit (Qiagen) according to manufacturer instructions and sub-cloned into TOPO vectors (Invitrogen). For further cloning steps, fragments were obtained by digestion of a fragment-containing TOPO plasmid with

respective restriction enzyme or enzymes. All enzymes, respective reaction buffers and supplements were purchased from New England Biolabs. Digestions were performed for 2-3 hours or overnight depending on the efficiency of the enzyme at temperatures suggested by the manufacturer. Small reaction aliquots were analyzed via agarose gel electrophoresis to insure complete digestion. Upon digestion, the backbone vector was always treated with shrimp alkaline phosphatase to avoid self-ligation. The vector was then purified using the QIAEX II protocol for desalting and concentrating DNA solutions (Qiagen). Fragments to be inserted into the backbone vector were purified via the same protocol directly after digestion (no SAP treatment). Ligation reactions were performed using T4 DNA ligase and respective reaction buffer from New England Biolabs. Inserts were added in excess compared to the amount of the backbone vector. Small reaction aliquots were analyzed via agarose gel electrophoresis to insure efficient ligation. Remaining reaction volumes (typically 8 µl) were electroporated into electo-competent E. Coli using the Gene Pulser machine (BioRad Laboratories). Bacterial clones, putatively positive for the desired ligation product were identified based on their resistance to Ampicillin (encoded by the pEASY-Flrt backbone vsector). Plasmid DNA was obtained using QIAprep Spin Miniprep Kit (Qiagen) according to manufacturer instructions. The presence and the direction of the appropriate insert were in each case confirmed by specific restriction analysis. Large amounts of plasmid DNA were obtained using QIAfilter Plasmid Midi or Maxi Kit (Qiagen) according to manufacturer instructions. The final targeting vector was generated via the following sequence of steps:

Step 1: The adenoviral splice acceptor sequence was excised from the TOPO+SA (SA= splice acceptor) plasmid by double digestion with EcoR I/BamH I and cloned into the p31HR123-EGFP II vector that was previously linearized by using the same combination of restriction enzymes. The p31HR123-EGFP II vector contains the cDNA sequence encoding the enhanced green fluorescent protein (eGFP). The splice acceptor was placed directly upstream of this cDNA sequence.

Step 2: The pEASY-Flrt plasmid (the backbone plasmid for the generation of the targeting vector) was linearized by digestion with the Not I restriction enzyme. The left arm of homology was obtained by digesting the TOPO+LA (LA = left arm) plasmid with the same

enzyme. Subsequently the left arm and the pEASY-Flrt were ligated. Left arm of homology had to be cloned into the backbone vector before the insertion of the "floxed" fragment because the letter contains the recognition sequence for Not I.
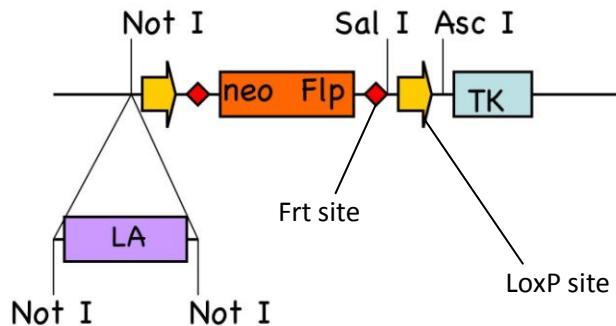
Step 3: The "floxed" fragment was obtained by digesting the TOPO+FF (FF = "floxed" fragment) plasmid with the Sal I restriction enzyme. The pEASY-Flrt+LA vector was linearized via digestion with the same enzyme. Subsequently the vector and the "floxed" fragment were ligated. The "floxed" fragment had to be cloned into the vector before inserting the right arm of homology as the letter contains the recognition sequence for SalI.
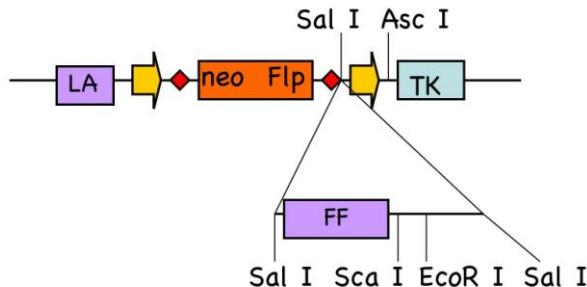
Step 4: The splice acceptor-eGFP fragment was excised from the p31HR123-EGFP II+SA vector by digestion with Asc I / BssH II. As part of the recognition sequence for the Asc I restriction enzyme matches the recognition sequence for the BssH II restriction enzyme, the vector was first digested with the Asc I, purified and further digested with the BssH II. This was done in order to generate a fragment with Asc I cohesive end on one side and the BssH II cohesive end on the other side. The pEASY-Flrt+LA+FF vector was opened by digestion with Asc I restriction enzyme and ligated to the previously generated splice acceptor-eGFP fragment. As recognition sequences for Asc I and BssH II restriction enzymes are partially

matching, the respective cohesive ends can be ligated, resulting in the loss of the Asc I recognition sequence upon ligation. Therefore only one Asc I recognition sequence remained in the pEASY-Flrt+LA+FF+SA-eGFP vector.
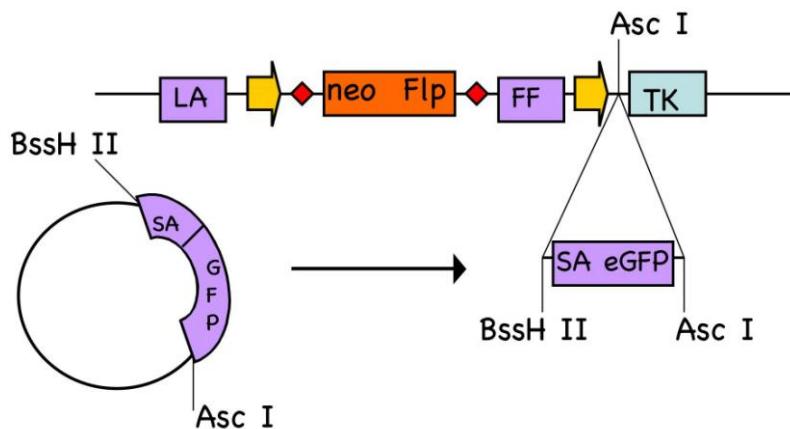
Step 5: The pEASY-Flrt+LA+FF+SA-eGFP vector was linearized via digestion with the Asc I restriction enzyme. The right arm of homology was excised from the TOPO+RA plasmid via digestion with the same restriction enzyme and subsequently ligated with the vector.
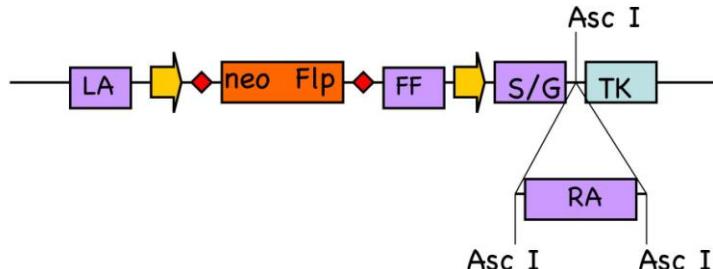
The final targeting vector was linearized via digestion with the Cla I restriction enzyme. The highly concentrated stock of Cla I (50 units/µl, New England biolabs) was used. The reaction was carried out in a large volume (300 µl), 100 µg of plasmid DNA and 300 units of Cla I were added to the reaction mixture. Small reaction aliquots were analyzed hourly by agarose gel electrophoresis to insure complete digestion. The reaction was stopped after 3 hours. The digestion product was purified via subsequent phenol/chloroform - chloroform extraction,

followed by DNA precipitation with 0.3 M NaAc/100% Ethanol. The pallet was washed 2 times with 70% Ethanol and further stored at -20^0C in 70% Ethanol.

4.1.1.2 Targeting of the locus of interest in ES cells.

*All protocols related to ES cell work were created by Dr. Manolis Pasparakis.

Electroporation of the targeting vector into murine embryonic stem cells (ES cells), further culturing of cells and selection of ES clones, positive for the insertion of the genetically manipulated fragment into appropriate genomic locus were performed as follows:

Mitomycin treated, neo resistant mouse embryonic fibroblasts (feeder cells) were plated at 100% confluence on 10 cm tissue culture dishes (Falcon®, Becton Dickinson) that were pre-coated with gelatin (Sigma-Aldrich). Bruce-4 embryonic stem cells derived from C57Bl/6 mice were plated on top of the feeder layer and grown to sub-confluence. On the day of transfection the tube containing the linearized targeting vector was transferred into the cell culture hood, the ethanol was removed, the DNA pallet was air-dried and subsequently dissolved in PBS at a concentration of 0.5 μg/ml. ES cells were fed with the fresh medium 3 hours prior to harvesting. Shortly before transfection cells were lifted from plates via incubation with Trypsin-EDTA (Gibco ®, Invitrogen) +2% chicken serum (37^0C, 3-5 minutes). Trypsinization was terminated by adding double volume of the ES medium. A near single cell suspension was obtained by vigorous pipetting. Cells were centrifuged (250x g, 5 minutes) and re-suspended in PBS at a concentration of 1.5 x 10^7 cells/ml. 0.7 ml of such cell suspension was incubated with 30μg (60μl) of the targeting vector for 5 minutes at room temperature, subsequently transferred into the electroporation cuvette and given a single pulse at 230 V, 500 μF. Upon electroporation, cells were briefly mixed, incubated at room temperature for 5 more minutes and plated on 10 cm dishes, containing confluent feeder cells, freshly fed with ES medium (3-5 plates for each cuvette).

For the first 24 hours after transfection cells were cultured in normal ES medium. After that the positive selection (ES medium + G418, the antibiotic that blocks polypeptide synthesis by inhibiting the elongation step) was applied for 4 days. Clones that did not contain the targeting vector and therefore did not have the neo gene (encodes aminoglycoside 3′-phosphotransferase, the enzyme that conferres resistance to G418) died between day 3 and day 5 post-transfection. On post-transfectional day 5 additional negative selection ($2x10^{-6}$ M Ganciclovir) was applied to the cell culture. Clones that had the targeting vector randomly integrated into the genome, maintained the cDNA encoding the herpesvirus thymidine kinase (TK, see the scheme of the targeting vector). Such clones could metabolyze Ganciclovir and insert it into the replicating DNA instead of the pGTP, causing termination of the DNA synthesis followed by cell death. Negative selection was applied to the culture for 2 days.

ES clones that survived both the positive and the negative selection were sterile picked on post-transfectional days 8-10 (depending on the clone size) and plated on 96 well plates containing confluent feeder cells, freshly fed with ES medium: 10 cm dishes that contained survived clones were washed and re-filled with PBS. Clones were identified using stereomicroscope, picked in a small volume of PBS and placed into individual wells of a U-shaped 96 well plate (Costar®, Corning Incorporated) containing Trypsin-EDTA+2% chicken serum. The plate was kept on ice until it was filled with ES clones. After that the plate was placed at 37^{0}C for 3-5 minutes. Trypsinization was terminated by adding ES medium (4 times the volume of trypsin) to each well. A near single cell suspension was obtained for each clone by vigorous pipetting with a multi-channel pipette. In the end the contents of each well were transferred into respective wells of the feeder containing plate. Upon picking ES cells were cultured on 96 well plates until most wells of a given plate reached sub-confluence. At this point contents of each well were lifted via trypsinization and split between respective wells of three other 96 well plates containing confluent feeder cells.

One of the three replica plates was frozen 24-48 hours later, when the fastest growing clones were approaching confluence; the second plate was frozen one day after the first: 2-4 hours prior to freezing cells were fed with the fresh medium. Cells were tripsinized for 3-5 minutes, after that equal volume of the 2x freezing medium was added to each well. A near single cell

suspension was obtained by quick and vigorous pipetting. The content of every well was covered by sterile mineral oil (Sigma-Aldrich). The plate was quickly sealed and placed at the -80^0C. The contents of each well of the third replica plate were split between respective wells of three 96 well plates that were pre-coated with gelatin. This was done on the same day when the second replica plate was frozen. The three resulting plates were kept until every well reached absolute confluence. The medium was then removed; the cells were washed with PBS, dried by aspiration and placed at the -80^0C. These plates were then used for the DNA preparation.

4.1.1.3   Analysis of ES clones that were obtained as a result of targeting for the insertion of the modified allele into the appropriate genomic location.

For the DNA preparation each well of the 96 well plate was washed with PBS. After that 50 μl of lysis buffer (10 mM NaCl, 10 mM Tris-Hcl pH 7.5, 10 mM EDTA, 0.5% Sarcosyl, 0.4-1 mg/ml freshly added proteinase K) were added to each well. The plate was transferred into a pre-warmed box containing wet paper towels (the towels are used to create humidified atmosphere). The box was incubated at 56^0C overnight. After that the box was kept at room temperature for 1 hour in order to allow the contents to cool down. 100 μl of 100% ethanol were added to each well. The plate was incubated at room temperature for another 2 hours. During this time the filamentous DNA precipitate was formed and became visible. After that the plate was carefully inverted in order to discard the liquid content. The DNA remained attached to the walls and the bottom of the wells. The wells were then washed 3 times with 100 μl of 70% ethanol. The ethanol was carefully discarded each time by carefully inverting the plate. After the last wash the DNA containing plate was drained with paper towels. The DNA was air dried at room temperature for 10-15 minutes. The drying time had to be carefully respected, as completely dry DNA is difficult to dissolve. 35 μl of the restriction digestion mix (1x restriction buffer, 1 mM spermidine, 1mM DTT, 100 μg/ml BSA, 50 μg/ml RNAse A and 50 U of restriction enzyme per reaction) was added to each well. The enzyme of choice in case of the TRADD targeting was EcoR1(see Results for the detailed description of the screening strategy). Highly concentrated batch of the enzyme was used. The plate was the incubated overnight at 37^0C in a humidified chamber. The next day the digested DNA was loaded on an agarose gel and prepared for Southern blot analysis that was performed by using two external probes – probe A and probe B (see Results for the placement of probes).

Probe A was obtained via polymerase chain reaction with following primers and conditions:

Sense primer:

5′ TTC CTA AGG GGA CAG TGA GAA 3′

Anti-sense primer:

5′ TAG CTC GTG ATT CAT GAA ACA 3′

The PCR conditions:

Step 1: 94^0C – 3 minutes

Step 2: 94^0C – 30 seconds

Step 3: 60^0C – 30 seconds

Step 4: 72^0C – 1 minute

Steps 2-4 repeated 30 times

Step 5: 72^0C – 4 minutes

For the preparation of probe B the BAC that contained *tradd* genomic DNA and the surrounding genomic region was digested with EcoR1. The digested DNA was loaded on the agarose gel. The area corresponding to fragment sizes of 7 to 8 kb (the fragment of interest was 7.5 kb long) was excised from the gel and purified by using QIAEX II gel extraction kit. The mixture of fragments was ligated with the EcoR1 digested Bluescript vector. The clone containing the correct fragment was identified via specific restriction analysis. The 500 bp EcoRI-BamHI fragment of the resulting plasmid was used as probe B.

4.1.1.4 Preparation of ES cells for blastocyst injections.

Frozen cells from correctly targeted clones that were identified in the previous step were thawed and grown on 6 well plates (Costar®, Corning Incorporated) that contained confluent feeders to produce more ES cells of a given kind. Most of the cells were then frozen in 1x

freezing media and some were used for the DNA preparation. DNA was subjected to the analysis by Southern blot with the same probes that were used previously in order to confirm that the clones were correctly isolated from the respective 96 well plate. The additional analysis by using the Flp probe (see Results for details) was also performed. The 750 bp HindIII-EcoRI fragment of plasmid 136 from Manolis Pasparakis DNA archive was used as a Flp probe.

ES cells were thawed several days before injection and plated on one well of the 6 well plate containing confluent feeders. When cells reached sub confluence they were lifted by trypsinization and split into 2 wells of the feeder containing 6 well plate. 1 or 2 days before injection (depending on the confluence that should not exceed 80%) ES cells were lifted again and split into 3 wells of the feeder containing 6 well plates. Different dilutions of ES cells were used for each well – 1:3, 1:6 and 1:9. These different dilutions were made in order to generate at least one well that will have optimal confluence of cells on a day of the injection. On a day of injection cells should not be to confluent or too few. The confluence of cells in culture affects cell metabolism, therefore it determines the ability of ES cells to survive within the embryo and to remain pluripotent. These two parameters are critical for the potential of ES cells to mediate germ line transmission of the genetically modified allele.

ES cells were fed with fresh medium 2-4 hours before processing them. Cells were lifted by trypsiniztion as described previously. A single cell suspension was obtained by vigorous pipetting. Cells were centrifuged and re-suspended in ES medium. They were plated on a gelatinized 10 cm tissue culture dish and placed into the incubator for 20-30 minutes. During this time feeder cells would strongly attach to the dish while ES cells would be loosely attached or float in the supernatant. The plate was removed from the incubator at the appropriate time; the supernatant containing non-adhering cells was placed into a sterile tube (tube 1). Similar volume of ES media was added to the plate and loosely adhering cells were lifted by vigorous pipetting. The obtained cell suspension was placed into a sterile tube (tube 2). The tube 2 should contain good quality ES cells while some cells in the tube 1 could be dead or dyeing.

Cells from both tubes were centrifuged, re-suspended in the injection medium and given for injection

4.1.1.5 Solutions and media for ES work.

Media for feeder cells:

500 ml of DMEM (Gibco®, Invitrogen)

50 ml (10%) of heat inactivated fetal calf serum (Gibco®, Invitrogen)

5 ml of 100x Penicillin/Streptomycin concentrate (Gibco®, Invitrogen)

5 ml of 100mM L-Glutamine (Gibco®, Invitrogen)

ES cell media:

500 ml Ko-DMEM (Gibco®, Invitrogen)

90 ml (15% of the final volume) of heat inactivated ES-FCS (tested for ES cells)

6 ml of 100mM L-Glutamine (Gibco®, Invitrogen)

6 ml of 100x Non-essential amino acids (Gibco®, Invitrogen)

0.6 ml of 100mM β-mercaptoethanol

6 ml of 100x Penicillin/Streptomycin concentrate (Gibco®, Invitrogen)

600 μl of 10^6 units/ml LIF

Freezing media:

2x - ES-FCS + 20% DMSO

1x – ES-FCS + 10% DMSO

100mM β-mercaptoethanol:

50 μl of β-mercaptoethanol (Sigma) were diluted in 7 ml of sterile PBS (Gibco®, Invitrogen). The solution was kept at 4^0C for no longer then 7 days.

Injection media:

Was provided by EMBL-Monterotondo Transgenic Core Facility.

4.1.2 Generation of CYLDΔ932 mice.

4.1.2.1 Construction of the targeting vector.

DNA fragments that were used for the generation of the targeting vector were obtained via polymerase chain reaction (PCR). The BAC clone containing *cyld* genomic DNA was used as a template for all reactions. All fragments were amplified by using high fidelity Pfu polymerase and the Pfu-specific reaction buffer (both were purchased from Invitrogen). All primers were purchased form Metabion GmbH (Martinsried, Germany); all DNA fragments were manipulated as described previously. The 2.6 kb floxed fragment included exon 17 of the *cyld* gene. The 4.2 kb left arm of homology included exons 14-16 of the gene; the 3 kb region downstream of exon 17 was used as the right arm of homology. Following PCR primers and reaction conditions were used:

For the left arm of homology

Recognition sequences for Asc I restriction enzyme were inserted into both the sense and the antisense primer; recognition sequence for the Spe I restriction enzyme was introduced into the antisense primer. Restriction sites are underlined or indicated with different font size.

Sense primer:

5′ GA*GGCGCGCC*TGTGGGCATGCTACTATTCTA 3′

Anti-sense primer:

5′ A*GGCGCGCC***ACTAGT**CATGCGCTGTTTATGCACTGA 3′

The PCR program:

Step 1: 94^0C – 3 minutes

Step 2: 94^0C – 30 seconds

Step 3: 65^0C – 30 seconds

Step 4: 72^0C – 5 minutes

Steps 2-4 repeated 30 times

Step 5: 72^0C – 4 minutes

For the floxed fragment

Two sets of primers were designed; recognition sequences for Pac I restriction enzyme were inserted into both primers of one set, recognition sequences for the BamH I restriction enzyme were inserted into both primers of the second set. Homologous parts of primers were identical between the two sets, restriction sites are highlighted.

Set 1

Sense primer:

5′ AC***TTAATTAA***TAGAGGTGTGCAAGTATGTCC 3′

Anti-sense primer:

5′ CT***TTAATTAA***AGAACACAGTGCAATTTCGAG 3′

Set 2

Sense primer:

5′ CAG***GGATCC***TAGAGGTGTGCAAGTATGTCC 3′

Anti-sense primer:

5′ TAC***GGATCC***AGAACACAGTGCAATTTCGAG 3′

PCR program for set 1:

Step 1: 94^0C – 3 minutes

Step 2: 94^0C – 30 seconds

Step 3: 60^0C – 30 seconds

Step 4: 72^0C – 5 minutes

Steps 2-4 repeated 30 times

Step 5: 72^0C – 4 minutes

PCR program for set 2:

Step 1: 94^0C – 3 minutes

Step 2: 94^0C – 30 seconds

Step 3: 68^0C – 30 seconds

Step 4: 72^0C – 5 minutes

Steps 2-4 repeated 30 times

Step 5: 72^0C – 4 minutes

For the right arm of homology:

Recognition sequence for the Sfi I restriction enzyme was introduced into both the sense and the anti-sense primers.

Sense primer:

5′ AAT*GGCC*GCTAT*GGCC*TTAGCAGTAGTGGCTGGGTAG 3′

Anti-sense primer:

5′ CAG*GGCC*ATAGC*GGCC*TAATGACTAGATCCCGAAAC 3′

The PCR program:

Step 1: 94^0C – 3 minutes

Step 2: 94^0C – 30 seconds

Step 3: 68^0C – 30 seconds

Step 4: 72^0C – 5 minutes

Steps 2-4 repeated 30 times

Step 5: 72^0C – 4 minutes

Amplified fragments were gel purified as described previously and sub-cloned into TOPO vectors. The excision of fragments from TOPO vectors, their purification, placement into the targeting vector and identification of correct ligation products were performed as described previously.

The targeting vector was generated via the following sequence of steps:

Step1: The exon 17 within TOPO+FF-BamHI (TOPO vector containing the floxed fragment amplified by using primers that contain the recognition sequence for BamH I) plasmid was mutated via Dpn I-mediated site directed mutagenesis. Following PCR primers were used for the initial amplification step. The defined mutation at the specific position (see Results for details) was introduced into both primers; the rest of the primer sequence was homologous to the genomic area of interest. The sequence of the sense primer is shown in comparison with the endogenous sequence of the area.

Sense primer:

5′ TCAAGGCTGT***TGA***CGCAGACTTC 3′ - mutated

5′ TCAAGGCTGT***GCG***CGCAGACTTC 3′ - endogenous

The mutation not only introduced a stop codon into the area but also removed the recognition site for the BssH II restriction enzyme (highlighted with green) providing a convenient tool for the future identification of the mutated allele in the mouse.

Anti-sense primer:

5′ GAAGTCTGCGTCAACAGCCTTGA 3′

Amplification was performed by using high fidelity Pfu DNA polymerase and the respective reaction buffer. TOPO+FF-BamH I plasmid served as a template.

The PCR program:

> **Step 1:** 94^0C – 3 minutes
>
> **Step 2:** 94^0C – 30 seconds
>
> **Step 3:** 55^0C – 1minute
>
> **Step 4:** 72^0C – 2 minutes/kb of plasmid length
>
> **Steps 2-4 repeated 30 times**
>
> **Step 5:** 72^0C – 4 minutes

After the amplification was completed, the PCR reaction was cooled down. 10 units of Dpn I were added to the reaction. The resulting mixture was incubated for 1 hour at 37^0C. Dpn I specifically digests methylated DNA, therefore it would remove the parental template DNA from the reaction mixture. 2 µl of the digested PCR reaction were transformed into bacteria. Several clones were picked and analyzed for the presence of the mutation by BssH II digestion and sequencing. Later we refer to the resulting plasmid as TOPO-FloxM-BamH I.

The following backbone plasmid was used for the generation of the targeting vector: p24 from the Geert van Loo DNA archive, the pEASY-Flrt plasmid modified by the insertion of the stop cassette.
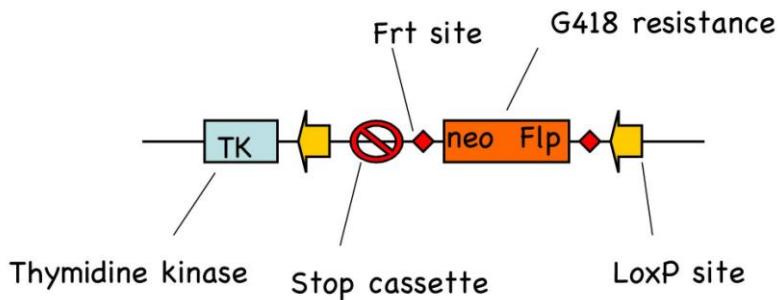
Step 2: The p24 was linearized by digestion with the Sfi I restriction enzyme. The right arm of homology was obtained by digesting the TOPO+RA (RA = right arm) plasmid with the same enzyme. Subsequently the right arm and the p24 were ligated.
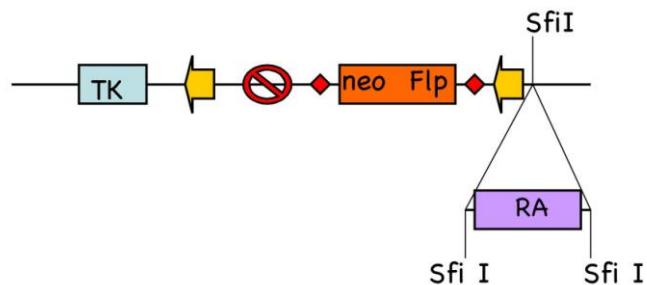
Step 3: The wild type "floxed" fragment was obtained by digesting the TOPO+FF-Pac I (TOPO vector containing the floxed fragment amplified by using primers that contain the recognition sequence for Pac I) plasmid with the Pac I restriction enzyme. The p24+RA vector was linearized via digestion with the same enzyme. Subsequently the vector and the "floxed" fragment were ligated.
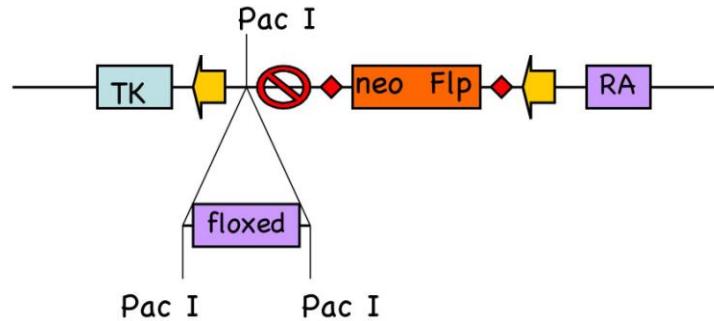
Step 4: The p24+RA+FF vector was linearized via digestion with the Asc I restriction enzyme. The left arm of homology was excised from the TOPO+LA (LA=left arm) plasmid via digestion with the same restriction enzyme and subsequently ligated with the vector.
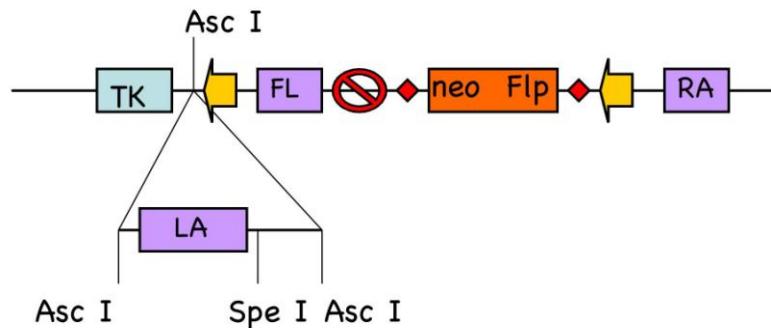
Step 5: The mutated "floxed" fragment (FloxM) was obtained by digesting the TOPO+FloxM-BamH I plasmid with the BamH I restriction enzyme. The p24+RA+FF+LA vector was linearized via digestion with the same enzyme. Subsequently the vector and the "FloxM" fragment were ligated.

71
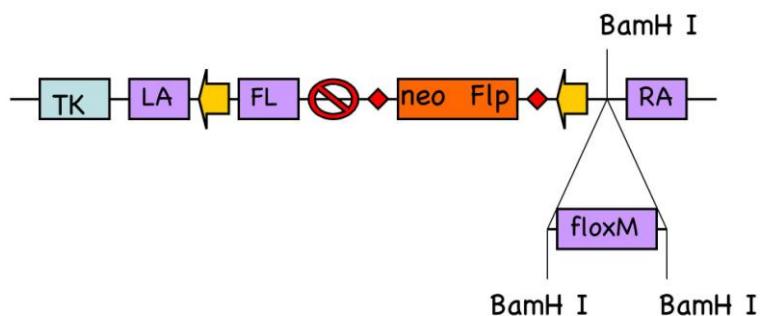
Materials and Methods

4.1.2.2 Targeting of the cyld gene in ES cells.

The targeting vector was linearized, purified and electroporated into mouse embryonic stem cells as described previously. Upon electroporation ES clones underwent two rounds of selection, as it was described for the TRADD targeting. The surviving clones were isolated and treated as described previously. The correct insertion of the modified allele into the appropriate genomic location was determined by Southern blot using external probes A and B (see Results for the description of the screening strategy). Probes A and B were obtained via PCR amplification. The BAC clone containing *cyld* genomic DNA was used as a template. Following primers and reaction conditions were used:

Probe A

Sense primer:

5′ CACCTGCGCTTCTAGTTGAAC 3′

Anti-sense primer:

5′ GAAAGGGTGGCAGCTAAGGGA 3′

Probe B

Sense primer:

5′ TCATGGCCAGCAGTCTCGAAG 3′

Anti-sense primer:

5′ TTTCTGTGGGCCTACATACGG 3′

The PCR program:

Step 1: 94^0C – 3 minutes

Step 2: 94^0C – 30 seconds

Step 3: 65^0C – 30 seconds

Step 4: 72^0C – 1 minute

Steps 2-4 repeated 30 times

Step 5: 72^0C – 4 minutes

4.1.3   Genotyping of TADD deficient and CYLD Δ932 mice.

4.1.3.1 TRADD

Three different primers were used in one PCR reaction in order to determine the presence of TRADD deleted (Del), TRADD floxed and TRADD wild type (wt) alleles in the genome of mice or cells:
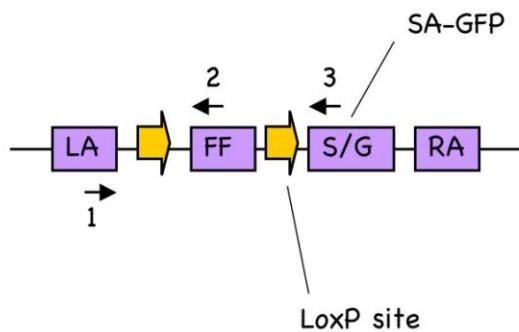
The primers:

Primer 1

5′ GGC CAG ACA TCT CCA CCG TAG 3′

Primer 2

5′ TTT GCC TTC AGC CTA AGT TCC 3′

Primer 3

5′ GTT GTG GCG GAT CTT GAA GTT 3′

Expected bands:

Wt = 400 bp

Floxed = 440 bp

Del = 900 bp

The PCR program:

Step 1: 94^0C – 3 minutes

Step 2: 94^0C – 30 seconds

Step 3: 57^0C – 30 seconds

Step 4: 72^0C – 1 minute 30 seconds

Steps 2-4 repeated 35 times

Step 5: 72^0C – 4 minutes

Reaction conditions: conditions for the amplification of fragments by using Taq DNA polymerase were as described previously.

4.1.3.2 CYLDΔ932

Two separate PCR reactions and two different combinations of primers were used in order to detect the presence of the CYLDΔ932 (Mut), CYLD floxed and CYLD wild type (wt) alleles in the genome of mice or cells:
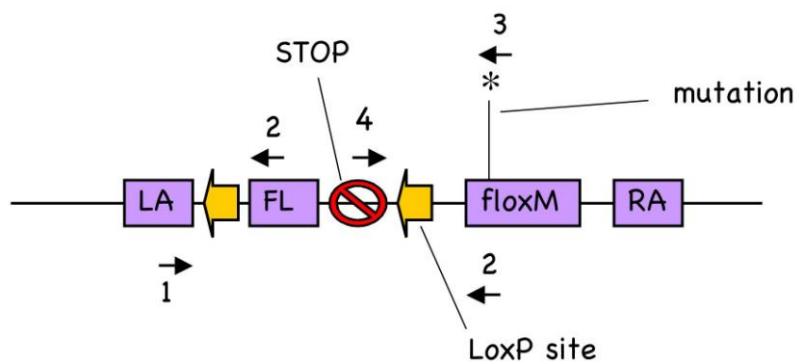
1+2 = Mod (floxed or Mut) and wt

1+3+4 = Mut and floxed

PCR 1

Primer 1

5′ CCA AGC TCT AGG CCC TAA GGT 3′

Primer 2

5′ ATG TCT AAG TCC TTC TGG CAT 3′

This combination of primers allows distinguishing between the wild type and the modified (floxed or mutated) alleles of CYLD.

Expected bands:

Wt = 729 bp

Mod (floxed or mutated) = 760 bp

PCR 2

Primer 1

5′ CCA AGC TCT AGG CCC TAA GGT 3′

Primer 3 (specifically binds to the mutated sequence)

5′ ATC GCA AAG AAG TCT GCG TCA 3′

Primer 4

5′ GCC GTT CTG GTG GTA GAT GGA T 3′

This combination of primers allows distinguishing between the floxed and the mutated alleles of CYLD.

Expected bands:

Floxed = 680 bp

Mutated = 959 bp

The PCR program (is the same for both PCR1 and 2)

Step 1: 94^0C – 3 minutes

Step 2: 94^0C – 30 seconds

Step 3: 56^0C – 30 seconds

Step 4: 72^0C – 1 minute

Steps 2-4 repeated 35 times

Step 5: 72^0C – 4 minutes

Reaction conditions: conditions for the amplification of fragments by using Taq DNA polymerase were as described previously.

4.1.4   Other mutant mice.

TNFR1 deficient mice were provided by K. Pfeffer. TNF deficient mice are described in Pasparakis *et al*. J Exp.Med (1996) 184, 1397-1411. Myd88 deficient mice were provided by S. Akira.

4.2   In vivo experiments.

4.2.1   In vivo infection of mice with Listeria monocytogenes.

Mice were infected intraperitoneally with 500 cfu of *Listeria monocytogenes* and followed for 10 days in order to determine survival rates.

4.2.2   SRBC immunization.

8 to 10 week old mice were injected i.p. with 2.5 x 10^8 sheep red blood cells (SRBC) in 0.9% saline. Serum and tissue samples were collected 15 days after immunization.

4.2.3 *Mouse models of acute liver failure.*

For TNF/β-GalN induced model wild type and TRADD -/- mice were injected intraperitoneally with a single dose of β-GalN (20 mg/mouse) followed by intravenous injection of TNF (0,4μg/20g of body weight). Mortality rate was recorded for up to 24 h after treatment. Serum samples were obtained prior to treatment and 8 h after treatment. Liver samples were collected at 8 h post injection. For FasL-Fc mediated liver failure wild type, TRADD -/- and FADD[HEPko] mice were challenged by intravenous injection of the ligand (10 μg/mouse). Mortality rate was recorded for up to 8 h after treatment.

4.2.4 *In vivo treatment of mice with TLR ligands.*

In order to measure the steady state expression of cytokines in the serum of mice blood was collected from the tail vein 4-5 days prior to stimulation. Following quantities of TLR ligands were used: 5 μg/20 g of body weight poly(I:C); 5 μg/10 g or 50 ng/g of body weight LPS; 50 μg/mouse CpG DNA. CpG DNA and poly(I:C) were injected intravenously via the tail vein; LPS was injected intraperitoneally. Blood was collected at 1h of stimulation and analyzed for the expression of TNF by ELISA.

4.2.5 *Preparation of serum from blood.*

Whole blood was directly drawn into centrifuge tubes that did not contain anti-coagulant. The blood was then kept at room temperature for 30 minutes in order to let it clot. The clotted blood was centrifuged at 4^0C, 2000-3000x g for 15 minutes. The upper transparent phase − the serum, was transferred into new individual tubes and snap frozen by placement into liquid nitrogen.

4.3 In vitro cell culture experiments.

4.3.1 *Preparation of mouse embryonic fibroblasts (MEFs).*

The pregnant female was sacrificed at day 13.5 p. c. by cervical dislocation. Uterine horns were dissected out under semi-sterile conditions, placed into a tube containing sterile PBS

(Gibco®, Invitrogen) and transferred into the cell culture hood. Under the hood the uterus was transferred to a Petri dish containing the sterile PBS and individual embryos were isolated. The inner organs of the embryos (particularly the "red organs") were removed. Each embryo was placed in individual 35 mm cell culture dish (Falcon®, Becton Dickinson) with 4 ml 0.125% Trypsin-EDTA. The embryos were finely minced and placed into the 37^0C incubator for 30 minutes. After that 5 ml of MEF medium was added to each dish. The contents were transferred into individual 15 ml tubes (Falcon®, Becton Dickinson). Embryos were dissociated by vigorous pipetting and left at room temperature for 5 minutes in order to allow big fragments to settle in the bottom of the tube. The top 5-7 ml containing the single cell suspension were plated into 175 cm flasks and cultured further.

4.3.2   Preparation of cell suspension from spleen.

Freshly removed spleen was transferred into a 50 ml tube containing sterile PBS and placed on ice until the preparation started. The 70 µm cell strainer (Falcon®, Becton Dickinson) was placed on top of the fresh 50 ml tube and pre-flushed with 1 ml of D-MEM supplemented with 10% FCS, antibiotics and glutamine. The spleen was cut into 3-4 pieces, transferred into the cell strainer and pressed against it with moderate force. After the pieces were dissociated the strainer was flushed with 4 ml of the media. The contents of the tube were centrifuged for 5 minutes at 1000x and re-suspended in 4 ml of RBC lysis buffer. The mixture was incubated for 4-5 minutes at room temperature. The reaction was stopped by adding 8 ml of the medium. The resulting cell suspension was centrifuged as described previously. The remaining cells were washed with 5 ml of sterile PBS and counted. For the FACS analysis 10^6 cells were directly used. For the stimulation with TLR ligands cells were re-suspended in serum free medium at a concentration of 10^6 cells/ml and left for 2 hours in the cell culture incubator (37^0C). Free floating cells were then collected, centrifuged, re-suspended again in the same quantity of serum free medium containing the stimulus and placed back into the same wells. After the stimulation culture supernatants were collected, centrifuged in order to remove remaining cells and snap frozen by placing into the liquid nitrogen.

4.3.3 Preparation of bone marrow cells.

The mice were sacrificed by cervical dislocation. Tibia and femur were isolated, carefully cleaned without breaking the bones and placed into the 50 ml tube (Falcon®, Becton Dickinson) containing sterile PBS. The tube was placed on ice until the preparation of cells started. The bones were washed for two minutes in 70% ethanol and transferred into a clean Petri dish. The tips of bones were cut off with sharp scissors. The bone marrow was flushed from the inside of the bones into a 35 mm tissue culture dish by using 1 ml syringe filled with the culture medium (different for macrophages and dendritic cells; will be described below). The 25G needles were used. The bone marrow was dissociated on a dish by vigorous pipetting. The cell suspension was transferred into a 50 ml tube (Falcon®, Becton Dickinson) and centrifuged for 5 minutes at 1000x g. The pallet was re-suspended in 3 ml of Red Blood Cell (RBC) lysis buffer (8.3g NH4C, l1.0g KHCO3, 1.8ml of 5% EDTA in 1000 ml of water) and incubated for 4 minutes at room temperature. The reaction was stopped by adding 8 ml of the culture medium. The resulting suspension was centrifuged for 5 minutes at 1000x g. Remaining cells were re-suspended in the culture medium and plated on bacterial plates. In order to produce macrophages bone marrow cells were cultured for 7 days in the medium that was supplemented with MCSF. The medium was not replaced during this time. Only the cells that differentiated into macrophages could attach to bacterial plates that were not treated for use in tissue culture.

4.3.4 Cell culture conditions.

Mouse embryonic fibroblasts (MEFs), splenocytes and human embryonic kidney (HEK) 293T cells were grown in DMEM (Gibco®, Invitrogen) supplemented with 10% heat-inactivated FCS, glutamine and antibiotics. Bone marrow derived macrophages were cultured in the same medium supplemented with 20% supernatant obtained from confluent L929 cells. Embryonic stem cells (ES cells) were grown on a layer of neomycin-resistant feeder cells (mouse embryonic fibroblasts) in Knock Out D-MEM (Gibco®, Invitrogen) supplemented with 15% ES FCS, 2 mM L-glutamine, 0.1 mM nonessential amino acids, 0.1 mM β-mercaptoethanol, 100 u/ml penicillin/streptomucin mixture and 1000U/ml of leukemia inhibitory factor (LIF).

4.3.5   Stimulation of cells with various ligands.

Cells were starved prior to stimulation by replacing the regular culture medium with the medium that doesn't contain serum. This was done in order to remove (or reduce) the background activation of various signaling cascades by the components of the serum. Different cell types were starved for different periods of time: mouse embryonic fibroblasts – for 30 minutes or 1 hour; splenocytes and macrophages – for 1 or 2 hours. After that the medium was aspirated. Equal volumes of serum free medium that contained appropriate concentration of the ligand of interest were provided to the cells. Non-stimulated controls received fresh serum free medium. The stimulation was terminated at appropriate times by aspirating the ligand-containing medium and washing the cells with ice cold PBS. In cases when secretion of certain molecules by cells had to be measured, culture supernatants were collected and frozen by placement into liquid nitrogen. For the preparation of protein extracts, plates were placed on ice immediately after the wash with ice cold PBS. Cells were then collected mechanically in small volume of PBS and treated, as it will be described below.

4.3.6   Induction of apotosis and cytotoxicity assay.

Mouse embryonic fibroblasts were incubated with murine TNF and cyclohexamide in serum free D-MEM at 37^0C. Quantification of cell survival was carried out by 3-(4,5-dimethylthiazol-2-yl)-2,5-diphenyl tetrazolium bromide (MTT) assay. Briefly: 20μl of MTT solution (1.25mg/ml) were added to each well (for the assay cells were typically cultured in 96 well plates). After 2 hr incubation, 60μl of medium were removed from each well, and cells were lysed by adding 140μl of isopropyl-HCl solution (600μl of HCl/ 250ml isopropyl alcohol) and mix by pipetting for 15mn. The absorbance at 570nm was determined for each well.

4.4   Biochemical experiments.

4.4.1   Preparation of DNA from mouse tissues.

Mouse tissues were placed into the 1,5 ml centrifuge tube (Eppendorf) containing 500μl of

the lysis buffer for Proteinase K (100 mM Tris-HCl pH 8.5; 5 mM EDTA; 200 mM NaCl and 0.2% SDS). 20 µl of the 10 mg/ml stock of the Proteinase K were added. The mixture was incubated overnight at 56^0C and after that centrifuged for 5 minutes at maximum speed to pallet the non-digested debris. The supernatant was transferred into a fresh tube and mixed with 500µl of 2-propanol. The tube was closed and carefully inverted several times. In case of low amount of DNA (the DNA precipitate couldn't be seen by eye as a defined jelly-like mass) the mixture was incubated for 10 minutes at room temperature and then centrifuged for 10-15 minutes at maximum speed. If DNA precipitate was substantial and visible, it could be isolated without centrifuging by fishing the DNA out with the pipette tip. The DNA was washed with 70% ethanol, dried and re-suspended in TE or water. If the resulting solution was non-transparent due to contamination with lipids or proteins (which is characteristic for certain tissues, like liver) an additional phenol/chloroform extraction was performed.

4.4.2   *Preparation of protein lysates from mouse tissues and primary cells.*

Dissected mouse organs were placed in lysis buffer (20 mM HEPES pH7.9, 350 mM NaCl, 20% ultra pure Glycerol, 1 mM MgCl2, 0.5 mM EDTA pH 8.0, 0.1 mM EGTA), and dounced until the tissue was completely dissociated. The lysate was incubated on ice for 30 minutes and then centrifuged for 20 minutes at 14000xg at 4^0C. The supernatant was transferred to fresh tubes and protein concentration determined using the Bradford assay. The same procedure was used for the lysis of primary cells, if not mentioned otherwise.

4.4.3   *Western blot analysis.*

For SDS Polyacrylamide Gel Electrophoresis (10% SDS-PAGE), proteins were diluted in 2X Sample buffer (100mM Tris-HCl pH 6.8, 4% SDS, 0.2% Bromphenolblue, 20% Glycerol, 5% β-Mercaptoethanol) boiled for 5 min at 96°C and subjected to discontinuous gel electrophoresis in 1X Running buffer (1g SDS, 3.03g Tris, 14.47g glycine in 1 liter H_2O). For Western blot, proteins were transferred onto a plyvinylidone difluoride (PVDF) membrane (Immobilon-P, Millipore), using a semi-dry blotting apparatus (Trans-Blot SD, BioRad), by applying 20V for 1hr. The PVDF-membrane was made hydrophilic by brief incubation in methanol. Gel and membrane were equilibrated in 1X Tranfer buffer (3.63g Tris, 17.3g

glycine, 240ml methanol in 1 liter H_2O) before the transfer. After the transfer, the membrane was incubated in blocking solution (5% non-fat milk powder dissolved in t-TBS buffer (150mM NaCl, 10mM Tris-HCl pH 7.4, 0.1% Tween-20)) at room temperature (RT) for 2hr. Primary antibodies were diluted in blocking solution or in BSA buffer (5% BSA powder dissolved in t-TBS buffer) depending on manufacturer instructions. The incubation with primary antibodies was carried out at 4°C overnight or at RT for 2 hours. Secondary antibodies were diluted in blocking solution and applied to the membrane for 1 hour at RT. Between the antibody incubations, the membranes were washed three times in t-TBS buffer. For detection, horseradish peroxidase (HRP) conjugated secondary antibodies were used at dilutions recommended by the manufacturer. The enhanced chemiluminescence system (Amersham Pharmacia) was used for revealing the bands, followed by exposure to x-ray film (Biomax MR, Eastman Kodak Co.).

4.4.4   Southern blot analysis.

Genomic DNA was digested overnight with the respective restriction enzyme. The DNA fragments were then separated on a 0.8% agarose gel, and transferred overnight by capillary flow onto a surface of a charged nylon membrane. The following day the membrane was baked at 80^0C for 1 hour and pre-incubated in hybridization buffer (1M NaCl; 50 mM Tris, pH 7.5; 10% dextrane sulfate; 1% SDS; 250 μg/ml sonicated salmon sperm DNA) at 65^0C for 2 hours. Specific DNA probes labeled by random priming with ^{32}Pα-GTP were then added to the hybridization buffer and allowed to hybridize with the membrane overnight at 65^0C. The next day the membrane was washed for 20 minutes with 2x SSC/1% SDS at 65^0C, followed by another 20-minute wash with 1x SSC/0.5% SDS. It was then exposed to a Phosphorimager screen for 1-2 hours or overnight.

4.4.5   ELISA for SRBC-specific serum antibodies.

96-well flat-bottomed Immuno-Maxisorp plates (Nunc, NUNCBRAND) were coated by adding 100 μl/well of a solubilised extract from SRBC (5 μg/ml in carbonate buffer, pH 9.6) and incubated at 4^oC overnight. Plates were washed and serum samples were diluted in phosphate buffered saline containing 0.05% Tween 20 (SIGMA), 1% BSA (SIGMA), added

in duplicate wells (100μl/well) and incubated for 3 hours at 37°C. Bound antibodies were detected with horse radish peroxidase conjugated goat anti-mouse IgG (Southern Biotech) for 1hour at room temperature. OD values were converted to arbitrary units (A.U.) by comparison to a pool of sera, which was obtained after immunization of 10 wild-type mice with SRBC.

4.4.6   TNF ELISA.

TNF ELISA was purchased from R&D Systems and used according to the manufacturer instructions.

4.4.7   Luciferase assay

Luciferase gene expression was measured using a commercial kit (Promega, France). Upon stimulation the medium was removed and the cells were washed with PBS three times. After that the 1x lysis reagent was added and the plate was incubated at RT for 30 minutes. The lysates were collected and centrifuged at 14,000 g for 5 minutes. 20μl of cell lysate were mixed with 100μl of Luciferase Assay Reagent. The luminescence (RLU) was monitored with a luminometer (Berthold, France). Results were normalized according to the concentration of proteins in the lysate that was measured by using BIO-RAD protein assay.

4.5   Analysis of complex formation.

4.5.1   Expression vectors.

pCR3-Rip1-VSV, pCR3-Rip3-VSV and pCR3-Trif-Flag have been described previously (Meylan et al, Nat Immunol, 2004). pCR3-Tradd-myc was obtained by restriction of the pRK5-Tradd (provided by D.V. Goeddel, Tularik, South San Francisco, California) and subsequently cloned into a derivative of pCR3 (Invitrogen), in frame with an N-terminal myc tag. The Rip1 delta death domain (ΔDD) construct (amino acids 1-568) was obtained by restriction of the pCR3-Rip1-VSV. Rip1ΔDD was subsequently cloned into a derivative of pCR3 (Invitrogen), in frame with an N-terminal VSV tag.

4.5.2   Preparation and transfection of siRNA.

siRNA oligonucleotides against Rip1 (GGCGAAGATGATGAACAGA) were obtained from Ambion and HEK293T cells were transfected using the calcium-phosphate precipitation technique.

4.5.3   TNF-R1 complex analysis by immunoprecipitation.

TNF-R1 complex analysis was performed as previously described (Micheau and Tschopp, Cell, 2003). Briefly, MEFs were stimulated for the indicated times with 1 µg/ml of Flag-tagged TNF-α (Apotech) and lysed in lysis buffer (20 mM Tris-Hcl pH7.4, 250 mM NaCl, 1% Nonidet P40, 10% glycerol and complete protease inhibitor cocktail) for 15 min on ice. Lysates were immunoprecipitated overnight with M2-Flag beads (Sigma) at 4°C on a rotating wheel. Beads were recovered and washed five times with lysis buffer before analysis by SDS-PAGE and Western blotting.

4.5.4   Coimmunoprecipitation experiments.

Transient transfection of HEK293T cells was performed as previously described (Thome et al, Curr Biol, 1998). For coimmunoprecipitation experiments, transfected HEK293T cells were resuspended in lysis buffer (50mM Tris pH7.8, 150 mM NaCl, 0.1% Nonidet P-40, 5 mM EDTA and complete protease inhibitor cocktail) for 15 min on ice, and lysed by three freeze/thaw cycles. Lysates were immunoprecipitated overnight at 4°C on a rotating wheel with M2-Flag beads (Sigma) or anti-myc (upstate) bound to protein G. Beads were recovered and washed five times with lysis buffer before analysis by SDS-PAGE and Western blotting.

4.6   Bone vs cartilage staining and immunohistochemistry.

4.6.1   Preparation and staining of skeletons.

Cadavers of newborn mice were skinned, eviscerated, and fixed in ethanol for 4 days and in acetone for 3 days. After rinsing with water, the specimens were incubated for 5 days in the

staining solution: 0.0075% alizarin red/0.003% alcian blue/5% acetic acid/82.5% ethanol (vol/vol). Skeletons were rinsed with water and transferred into 20% (vol/vol) glycerol/1% potassium hydroxide at 37°C until the tissue cleared, and then gradually into 100% ethanol for storage.

4.6.2 Immunohistochemical analysis.

Spleens from immunized mice were frozen in OCT compound (BDH) and 6 μm cryostat sections were placed on gelatinized slides. For detection of germinal centers, sections were fixed for 10 minutes in acetone containing 0.5% H_2O_2 (FLUKA) to block endogenous peroxidase activity, blocked with phosphate buffered saline containing 5% FBS (BIOCHROM) and finally 25μg ml^{-1} peanut agglutinin-horse radish peroxidase antibody (SIGMA) were applied as described previously. Bound peroxidase activity was detected with diaminobenzidine (SIGMA). For detection of follicular dendritic cells, sections were fixed on acetone, blocked as above and incubated with 5μg ml^{-1} rat anti-CD35 (CR1; clone 8C12, Pharmigen BD). Conjugation to alkaline phosphatase was perfomed using VECTASTAIN ABC-AP kit (Vector Laboratories) according to the manufacturer's specifications. Alkaline phosphatase activity was visualized with made in house NBT-BCIP. Stainings were envisioned in a E-800 Eclipse (Nikon) microscope.

4.7 Antibodies and reagents.

Antibodies used for immunoblot analysis were anti-RIP1 (Transduction Labs), anti-TRAF2 (Santa Cruz), anti-TRADD (Transduction labs), anti-phospho IκB (Cell Signaling), anti-TRIF (Apotech), anti-myc (Upstate), anti-Flag and anti-VSV (Sigma). Anti-IkB (Santa Cruz), anti-JNK (Santa-Cruz), anti-phospho JNK, anti-ERK, anti-phospho ERK, anti-p38 and anti-phospho p38 (Cell Signaling), anti-TRADD and anti-actin (Santa Cruz), anti-Caspase-8 (Alexis), anti-Caspase-3 (Cell Signaling), ant-CYLD (Santa Cruz). 3-(4,5-dimethylthiazol-2-yl)-2,5-diphenyl tetrazolium bromide (MTT) was purchased from Sigma, untagged murine TNF (if not mentioned specifically) was obtained from R&D systems. We used PolyI:C from

Amersham. LPS, β-GalN and cyclohexamide were purchased from Sigma. CpG DNA was purchased from HyCult biotechnology.

5. Results

5.1 Conditional targeting of TRADD.

5.1.1 Generation of TRADD deficient mice.

The mouse *tradd* gene is located on chromosome 8. Exons 2-5 of the gene contain the region that is coding for the TRADD protein. Exon 1 that is located in close proximity to the promoter of the gene is non-coding. To achieve a complete knockout of TRADD we decided to delete exons 2-5 by flanking them with recognition sequences for the Cre recombinase (LoxP sites).

The Cre (for Cyclization Recombination)/LoxP (locus of X-over P1) system is a system of site-specific recombination from Bacteriophage P1. The system consists of an enzyme (Cre) that catalyses recombination of DNA between specific sites (LoxP sites). The LoxP site is 34 base pair long. It consists of an asymmetric 8 base pair sequence that is flanked by 13 base pair palindromic sequences on both sides. The palindromic sequences are binding sites for the Cre recombinase. The asymmetric sequence is the area where the recombination occurs. When Cre is expressed in cells that contain LoxP sites in their genome, a reciprocal recombination event may take place between two LoxP sites. The asymmetric sequence gives directionality to the LoxP site. The outcome of the recombination depends on the spatial orientation of two LoxP sites one against the other. When two sites are placed on the same arm of the chromosome and have the same direction, the recombination will result in deletion of the DNA region that was located between LoxP sites. This effect is commonly used in genetics in order to introduce mutations or delete gene regions in a controlled and inducible manner. The loxP sites are placed at the desired location of the genome by homologous recombination. The presence of the mutation or deletion is regulated via transducing Cre into cells or via expressing Cre under the control of an inducible or tissue specific promoter.

We placed a cDNA encoding for the enhanced green fluorescent protein (eGFP) fused to a splice acceptor site (SA) downstream of the second LoxP site, see Figure 1.
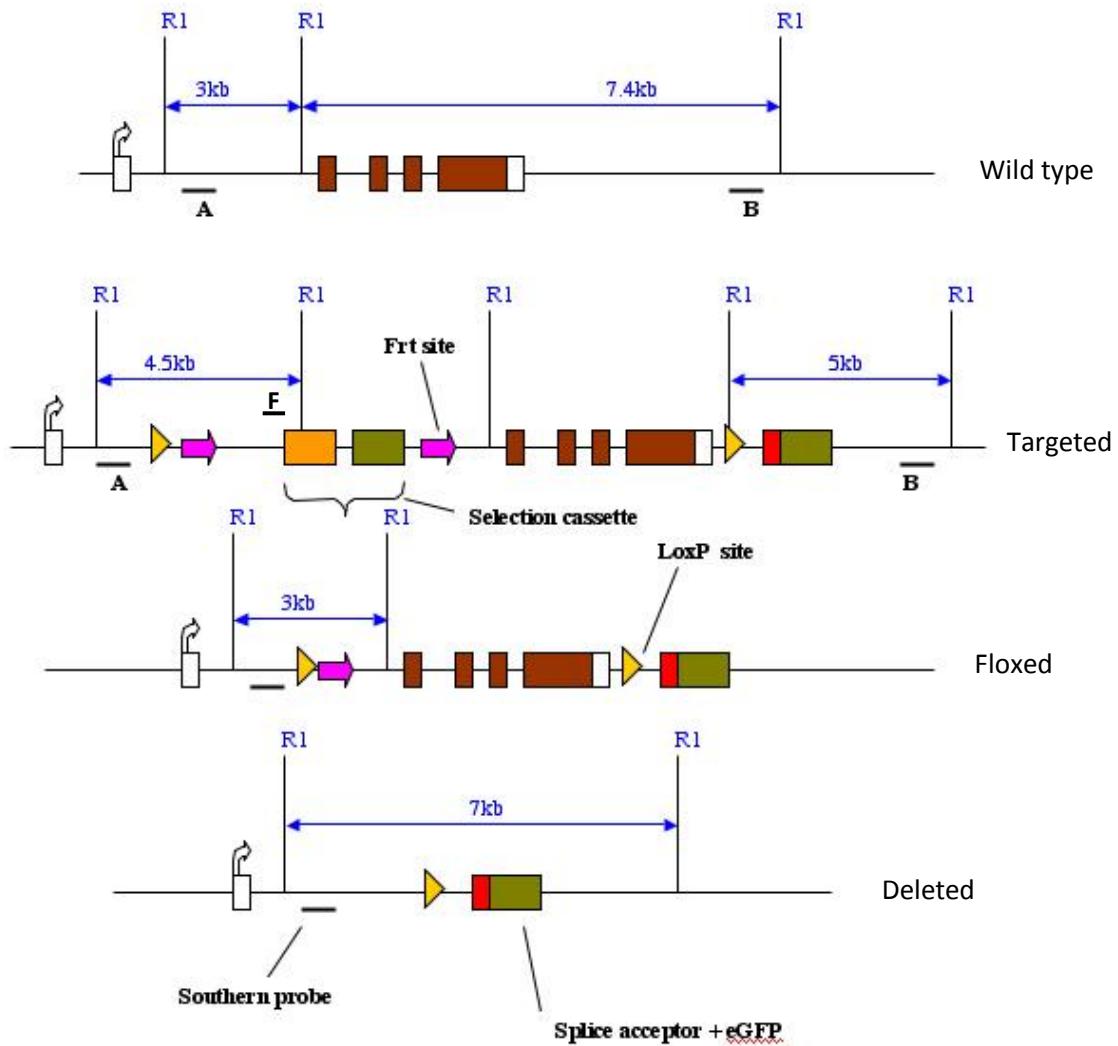
Figure 1. Schematic pictures of the wild type, targeted, floxed and deleted tradd genomic locus are presented indicating EcoR1 restriction sites used for the Southern blot analysis, positions of probes and the expected length of fragments.

Deletion of the LoxP-flanked sequence generates a null TRADD allele and at the same time allows expression of eGFP under control of the endogenous TRADD promoter.

The modified allele (the cloning strategy and the selection strategy are described in detail in Materials and Methods) was introduced into murine embryonic stem (ES) cells via homologous recombination. 288 clones that survived both the positive and the negative selection were picked and processed as described in Materials and Methods. Southern blot

analysis of EcoR1 digested DNA that was prepared from each clone was performed by using external probes A and B (see Figure 1). The initial analysis was performed by using probe A. The strategy was based on the fact that an EcoR1 site was present in the selection cassette of the targeting vector. If the selection cassette together with the adjacent LoxP site were integrated into the genome of cells as expected, probe A would recognize the extra 4.5 kb fragment in addition to the endogenous 3 kb fragment. The analysis revealed 4 clones that correctly integrated the upstream part of the modified allele into their genome (see Figure 2).
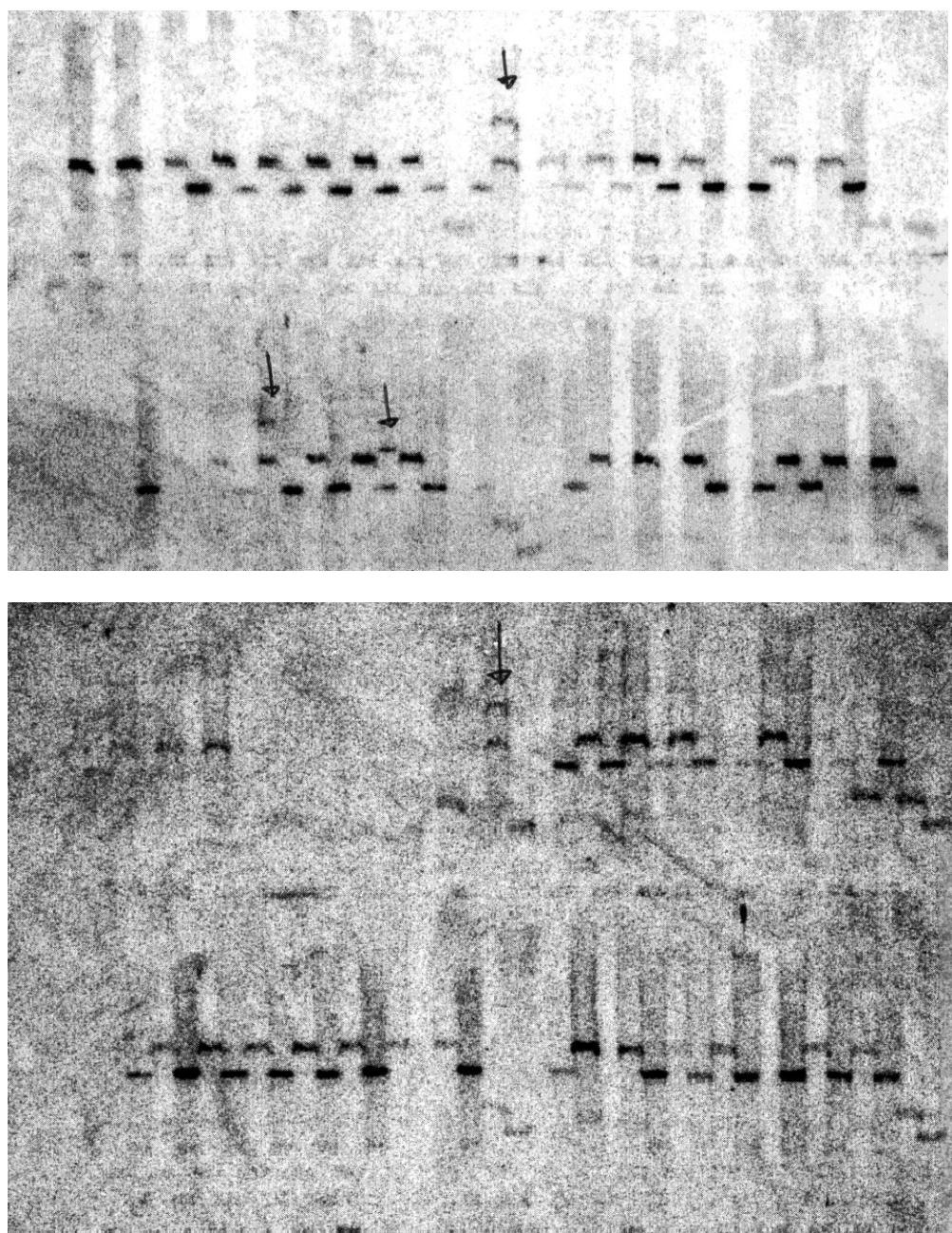
Figure 2: Southern blot analysis of EcoR1 digested genomic DNA isolated from the clones that survived both positive and negative selection is presented showing 4 clones where homologous recombination had occurred (indicated with arrows). Probe A was used for the analysis (see Figure 1 for the position of the probe and the expected length of fragments).

The membranes that contained DNA from putatively positive ES clones were stripped and probed with probe B. The analysis that was performed by using probe B allowed us to determine whether the second (downstream) LoxP site and the cDNA encoding for the eGFP were incorporated into the genome of the clones. The strategy was based on the fact that the recognition sequence for EcoR1 was introduced into the area adjacent to the downstream LoxP site during the generation of the targeting vector. The presence of the additional EcoR1 binding site would indicate that the LoxP site of interest integrated into the genome of the cell. If the splice acceptor-eGFP fragment and the LoxP site were inserted into the genome at the appropriate location probe B would recognize a specific fragment of 5.3 kb in addition to the endogenous 7.4 kb fragment (see Figure 1). The analysis revealed that 2 out of 4 clones that were previously identified were positive for the downstream part of the modified allele (see Figure 3).
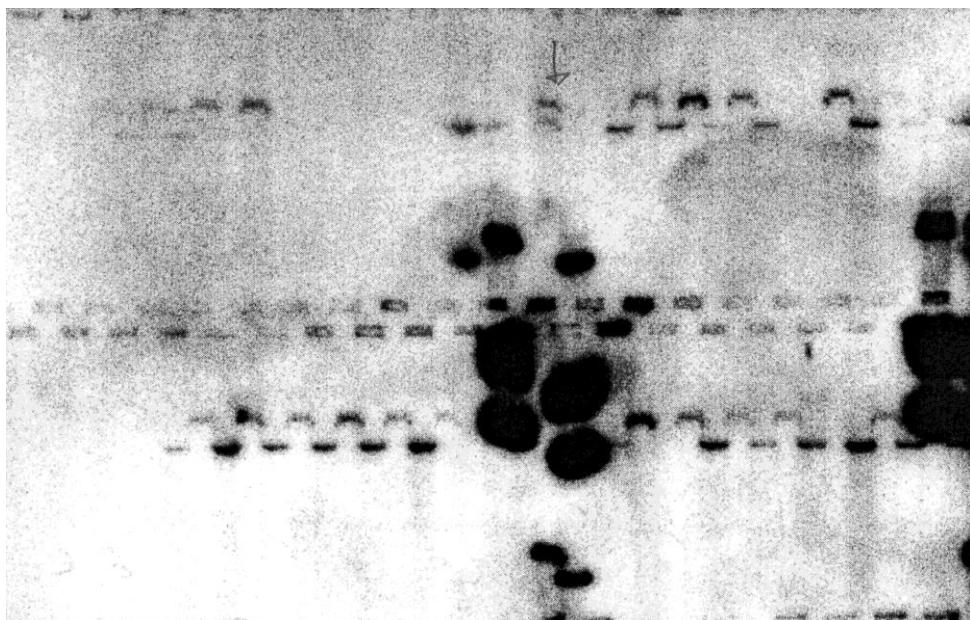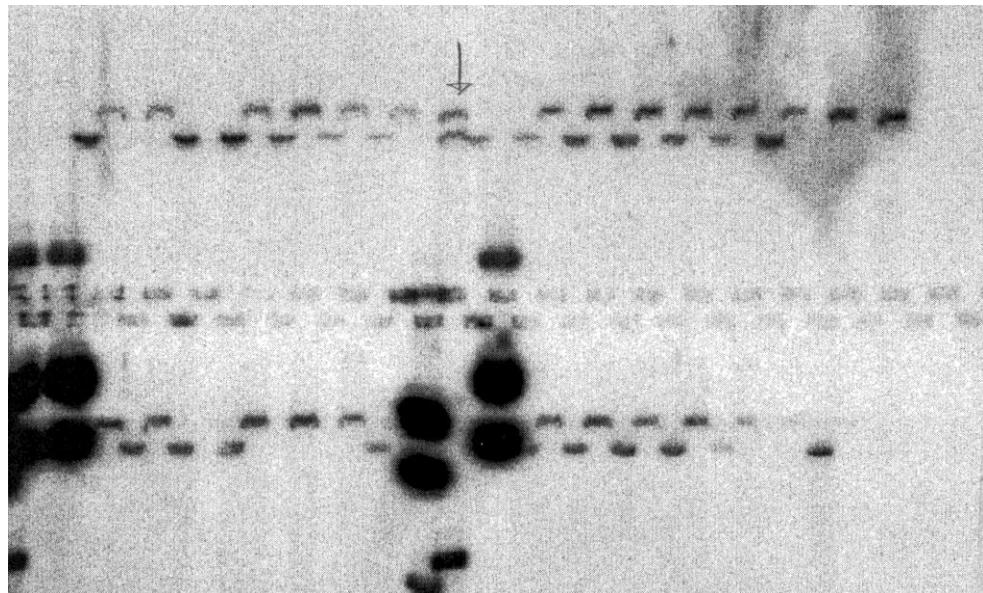
<u>Figure 3:</u> Southern blot analysis is presented showing co-integration of the second LoxP site in 2 out of 4 previously identified positive clones (indicated with arrows). The analysis was performed on the same DNA that was used in <u>Figure 2.</u> Probe B was used for the analysis (see <u>Figure 1</u> for the position of the probe and the expected length of fragments).

Positive clones were isolated from respective wells of 96 well plates, grown as described in Materials and Methods and subjected to analysis by Southern blot in order to confirm their identity. Two negative clones were also isolated and subjected to the same analysis as negative control. The analysis performed by using EcoR1 digested DNA and the external probe A demonstrated the presence of the modified allele in both putatively positive clones (see <u>Figure 4</u>).
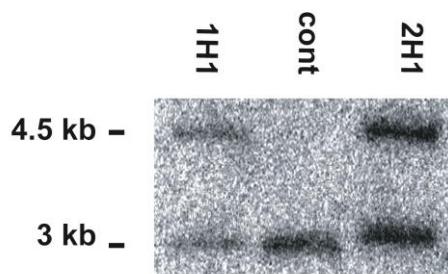
<u>Figure 4.</u> The correct incorporation of the modified *tradd* allele into the genome of two ES clones was evaluated by Southern blot analysis of EcoR1 digested genomic DNA. See Figure 1 for the position of the probe (Probe A) and the expected length of fragments.

After that the EcoR1 digested DNA from positive ES clones was subjected to additional Southern blot analysis in order to eliminate the possibility that an extra copy of the modified allele had randomly integrated into the genome of the clones. Part of the Flp sequence (the Flp sequence was located in the targeting vector in close proximity to the neo gene, see probe F on Figure 1) was used as a probe. A single band of 4.5 kb would be recognized by probe F in case of the lack of non-specific integration of the targeting construct. This was the case for both positive clones (see Figure 5).
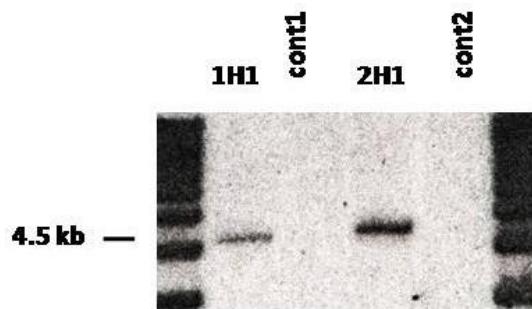
Figure 5. Southern blot analysis of EcoR1 digested genomic DNA by using Probe F is presented. Clones 1H1 and 2H1 show a single 4.5 kb bend consistent with the single correct integration of the modified *tradd* allele into the genome of the clones. *Neo* resistant clones with random integration of the targeting vector were used as control. See Figure 1 for the position of the probe and the expected length of fragments.

Embryonic stem cells from two correctly targeted clones were microinjected into BALB/C blastocysts in order to produce chimeric mice. Blastocysts were transferred into pseudo-pregnant females that had white coat color. Chimeric mice were identified by the presence of spots of black coat color. Male chimaeras were mated to C57BL/6 females. Tail DNA from black progeny was subjected to specific PCR analysis in order to confirm the transmission of the modified allele through the germ line (see Figure 6).
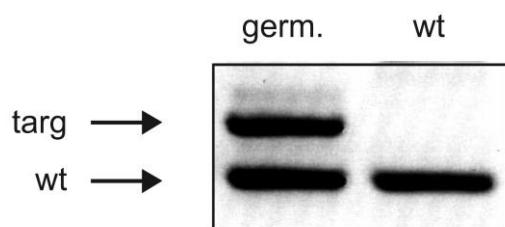
Figure 6. The transmission of the modified tradd allele through the germ line was confirmed by PCR analysis. The targeted allele is marked as targ, the wild type allele is marked as wt.

The mice that were heterozygous for the modified allele were crossed to a ubiquitous Flp-Deleter strain in order to obtain TRADD floxed mice that did not contain the neo/Flp cassette in their genome (see Figure 1). The TRADD floxed allele allows conditional inactivation of the gene in any cell type using Cre mediated recombination. TRADD +/- animals were obtained by crossing the TRADD floxed mice to a ubiquitous Cre-Deleter strain. TRADD knockout animals were generated by crossing parents that were heterozygous for the deleted allele of the gene. The *tradd* deficiency was confirmed at the genomic level by Sothern blot analysis of EcoR1 digested tail DNA obtained from TRADD -/-, TRADD +/- and TRADD +/+ mice. External probe A was used for the analysis (see Figure 7).
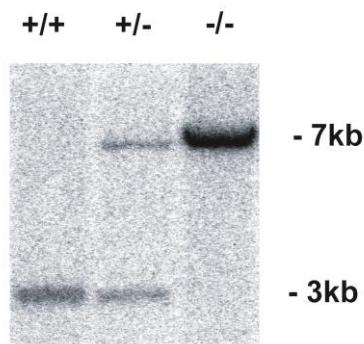
Figure 7: The deletion of the coding region of the tradd gene was confirmed by Southern blot analysis of EcoR1 digested tail DNA. See Figure 1 for the position of the probe (Probe A) and the expected length of fragments.

5.1.2   Initial characterization of the phenotype of TRADD deficient mice.

The animals that were heterozygous for the mutated allele of TRADD were mated in order to produce complete knock out progeny. TRADD deficient pups were born at the normal Mendelian ratio. No obvious specific features that would allow us to define the mutants without genotyping were present. The mutants survived till weaning age (3 weeks) and had no difficulties to start feeding on solid food. The adult TRADD knockout mice did not exhibit apparent physiological abnormalities and were fertile.

In order to confirm that the TRADD deleted allele does not express any TRADD protein we isolated mouse embryonic fibroblasts (MEFs) from TRADD +/+, TRADD +/- and TRADD -/- embryos. We prepared total cell lysates from these MEFs and tested them by immunoblotting for the presence of the TRADD protein. No expression of the TRADD protein could be detected in cell lysates that were prepared from TRADD -/- mouse embryonic fibroblasts while TRADD was expressed in both TRADD +/+ and TRADD +/- cells (see Figure 8).
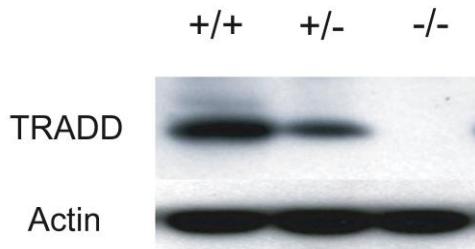
Figure 8. Cell lysates from mouse embryonic fibroblasts with indicated genotypes were analyzed for TRADD expression by immunoblotting with respective specific antibody. Equal loading was accessed by immunoblotting for actin.

We next wanted to determine whether the eGFP cDNA was successfully spliced with the first exon of the TRADD gene upon deletion of exons 2-5 and whether the fluorescent protein was expressed in TRADD deficient cells as a result of that.

Total spleenocytes obtained from wild type, TRADD floxed and TRADD deficient mice were analyzed by FACS for eGFP expression. Some eGFP expression could be detected already in the floxed homozygous state putatively due to a transcriptional read-through. Nevertheless TRADD knockout cells showed markedly enhanced expression of the fluorescent protein compared to TRADD floxed cells (see Figure 9). Therefore the reporter expression could still be used to asses the efficiency of the deletion of the coding region of the *tradd* gene in cases of tissue specific or inducible models.
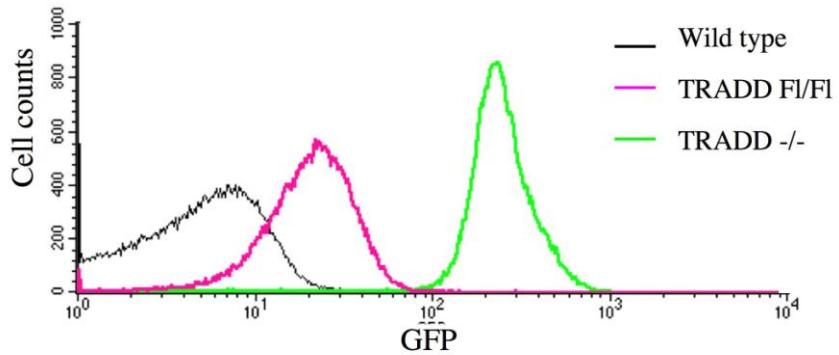
Figure 9. Total spleenocytes from TRADD floxed, TRADD knockout and wild type control mice were analyzed by FACS for eGFP expression.

5.1.3 TNF induced NF-κB and MAPK activation is reduced but not absent in TRADD -/- primary cells.

Since TRADD was proposed to play a major role in signal transduction through TNFR1 we tested the response of TRADD -/- primary cells to TNF. We used primary mouse embryonic fibroblasts (MEFs) obtained from TRADD deficient and control mice as a system to test whether TNF was still able to mediate activation of NF-κB and MAP kinases in the absence of TRADD.

C-jun N-terminal kinase (JNK), extracellular signal regulated kinase (ERK) and p38 are activated by TNF via phosphorylation that can be detected by immuneblotting with specific antibodies. Phosphorylation and degradation of IκBα is commonly used as a marker of NF-κB activation, since it is required for the translocation of the transcription factor into the nucleus. Wild type MEFs showed strong activation of NF-κB upon TNF stimulation, as revealed by the induction of IκBα phosphorylation and degradation at expected times (see Figure 10). At the same time TNF stimulation induced strong MAPK signaling in wild type cells as detected by phosphorylation of JNK, ERK and p38. In contrast the phosphorylation of IκBα, JNK, ERK and p38 was strongly impaired in TRADD deficient MEFs stimulated with TNF. However weak residual activation of indicated cascades could still be detected in

knockout cells showing that TNF-mediated signaling was not completely abolished in MEFs lacking TRADD.
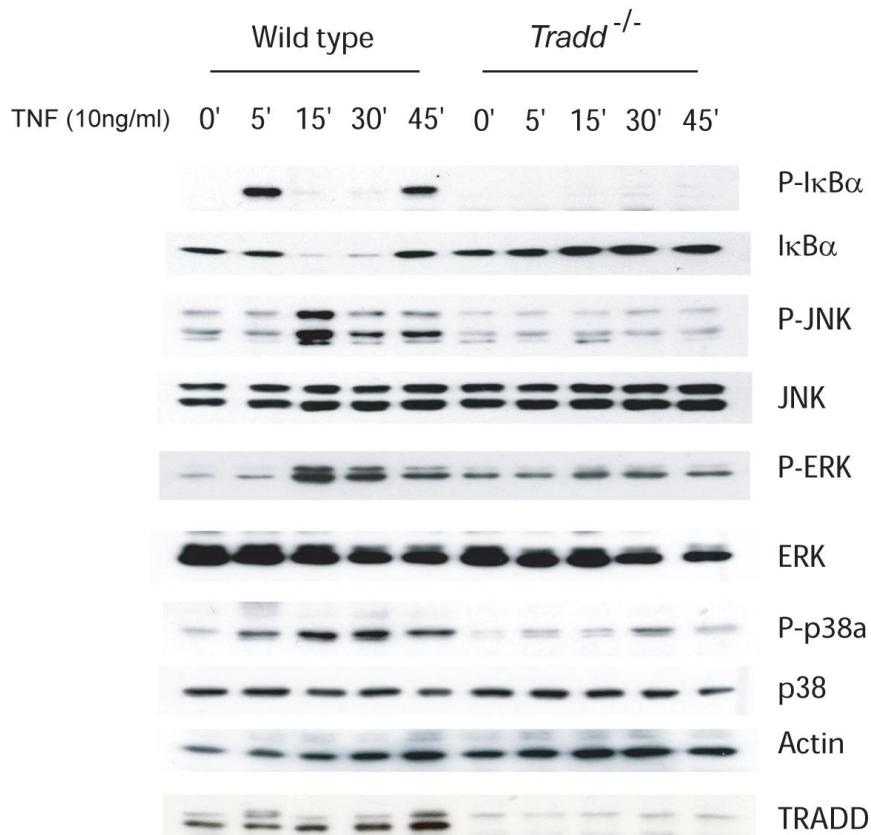
Figure 10. Wild type and TRADD deficient mouse embryonic fibroblasts were stimulated with 10 ng/ml of murine TNF for indicated times. Cell lysates were prepared and analyzed by immunoblotting. NF-kB activation was measured with phospho-specific (P-) antibody for IkB and antibody specific for total IkB. Activation of JNK, ERK and p38 was measured with respective phospho-specific antibodies. Equal expression of MAP kinases was confirmed by immunoblotting with antibodies specific for total JNK, total ERK and total p38.TRADD expression was evaluated by blotting with the specific antibody. Equal loading was accessed by immunoblotting for actin.

We next wanted to investigate whether the residual response to TNF that we observed in TRADD deficient cells was mediated by TNFR1. At the same time we were interested to determine whether the ability to still respond to TNF in the absence of TRADD was specific for MEFs or shared by other cell types. In order to answer both questions we repeated the experiment in a different system – in bone marrow derived macrophages obtained from

TRADD deficient, TNFR1 deficient and wild type mice. TNFR1 knockout cells were added as a control for the dependency of the response on TNFR1. If TNFR1 deficient cells would not show any phosphorylation of IκB, JNK, ERK or p38 upon TNF stimulation it would prove that the effect that we observe under our experimental conditions is mediated by TNFR1.
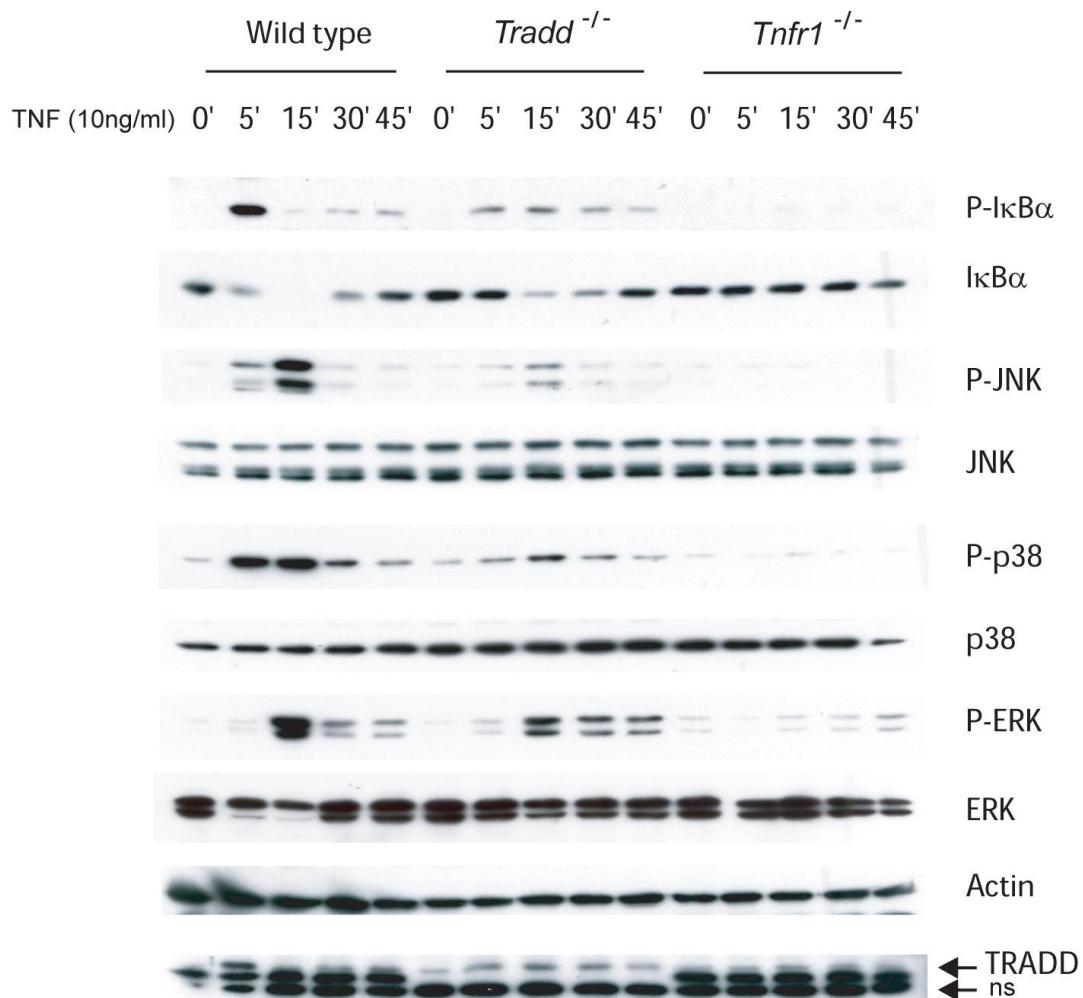
Figure 11. Wild type, TRADD -/- and TNFR1 -/- bone marrow derived macrophages were stimulated with murine TNF(10ng/ml) for indicated times. Cell lysates were prepared and analyzed by immunoblotting as described in Figure 10.

TNF stimulation led to strong activation of NF-κB and MAPK signaling in wild type macrophages which was completely abolished in TNFR1 deficient cells (see Figure 11). At the same time TNF-induced phosphorylation and degradation of IκBα as well as

phosphorylation of p38, JNK and ERK was strongly inhibited but not completely blocked in TRADD-deficient macrophages. Taken together, the results obtained from MEFs and bone marrow derived macrophages demonstrated that genetic ablation of TRADD strongly impaired but did not abolish the activation of proinflammatory signaling downstream of TNFRI.

5.1.4   *TNFR-1 mediated antibacterial responses are severely compromised but still present in TRADD deficient mice.*

As it was previously mentioned, TNF signaling through TNFR1 plays a key role in host defense against pathogens. This is clearly indicated by the high sensitivity of TNF and TNFR1 deficient mice to bacterial and viral infections. Particularly both TNF-/- and TNFR1-/- mice demonstrate reduced survival rates and elevated bacterial titers upon infection with the intracellular pathogen *Listeria monocytogenes*.

To evaluate the physiological impact of TRADD deficiency on TNF-mediated anti-bacterial host defense we compared the susceptibility of TRADD-deficient, TNFRI-deficient and wild type mice to infection with *L. monocytogenes*. Our results demonstrated that when mice were inoculated with high bacteria titers (lethal for 50% of wild type mice) all TRADD -/- and TNFR1 -/- animals died.
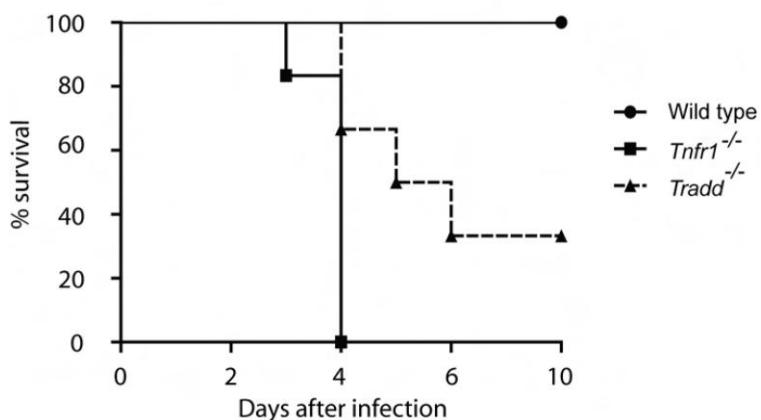
Figure 12: Wild type (n=4), TRADD deficient (n=6) and TNFR1 deficient (n=6) mice were infected i.p. with 500 cfu of *Listeria monocytogenes*. Survival upon infection was monitored for the indicated time. The data is presented as a Kaplan-Meier survival curve.

On the other hand 30% of TRADD knockout mice survived upon infection with low titers of bacteria while all TNFR1 knockout mice succumbed to similar challenge (see Figure 12). Therefore TNFR1 is still able to induce *in vivo* anti-bacterial responses in the absence of TRADD consistent with incomplete blockade of TNFR1-mediated signaling in TRADD deficient primary cells.

5.1.5 *TRADD deficient mice show impaired germinal center formation and T-cell dependant antibody responses upon immunization with sheep red blood cells.*

TNF signaling through TNFR1 is important for the establishment of appropriate architecture of secondary lymphoid organs. TNF knockout and TNFR1 knockout mice show impaired formation of B-cell follicles, follicular dendritic cell (FDC) networks and germinal centers (GC) in the spleen and lymph nodes. In order to investigate whether TRADD is essential for this aspect of TNFR1 function we immunized wild type, TNFR1 deficient, TRADD deficient and respective heterozygous mice with sheep red blood cells (SRBC) to induce the formation of germinal centers, follicular dendritic cell networks and the production of antibodies against the foreign antigen – a process that is also dependant on TNF signaling through TNFR1. We then isolated spleens form these mice and analyzed spleen sections by immunohistochemistry. We used peanut agglutinin (the compound that has high affinity to germinal center B-cells) for detecting germinal center formation. The antibody against complement receptor 1 (CR1) was used for the detection of follicular dendritic cells. Wild type, TNFR1 +/- and TRADD +/- mice formed well defined GC and FDC networks in response to SRBC while TNFR1 knockout and TRADD knockout mice presented similar impairments of these structures (see Figure 13). At the same time both knockouts generated reduced titers of anti-SRBC antibodies compared to heterozygous and wild type control animals (see Figure 14) indicating that TRADD is as essential for this process as TNFR1.

A

PNA/ GC

B

CR1/FDC
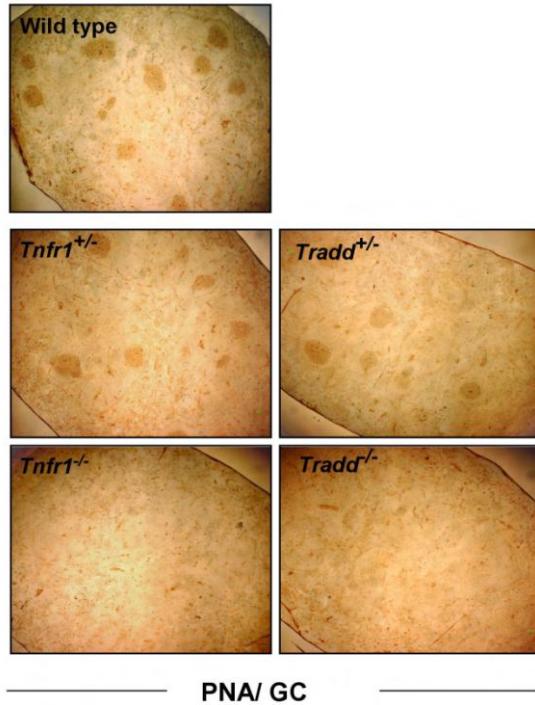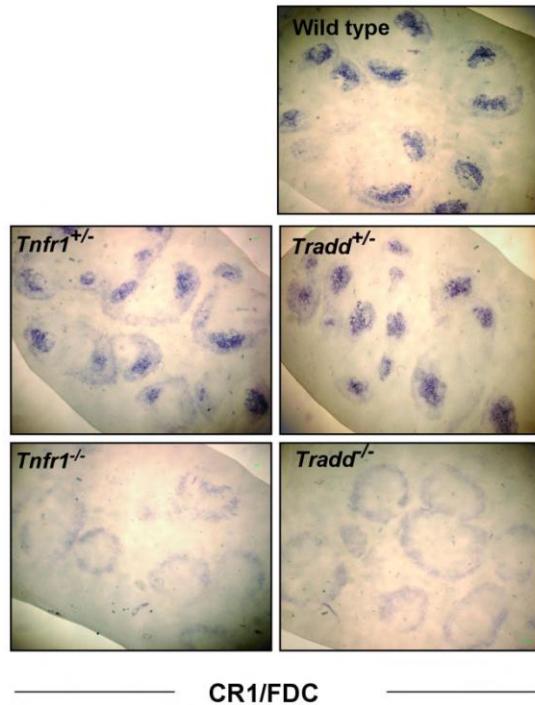
<u>Figure 13:</u> (A) Spleens were dissected from mice with the indicated genotypes 10 days after immunization with SRBC and cryosections were analyzed with immunostaining. Staining with PNA (shown in brown) reveals well formed GC in the spleen of wild type and heterozygous animals, while GC are absent in spleens from both *Tnfrl*^{-/-} and *Tradd*^{-/-} mice. (B) Immunostaining with anti-CR1 antibodies (shown in blue) reveals the formation of organized FDC networks in wild type and heterozygous knockout mice. Both TNFR1-deficient and TRADD-deficient mice lack organized FDC

networks and show only staining with CR1 around the marginal zone area of the white pulp. **-The experiments were performed in collaboration with Dr. Ksanthi Kranidioti, Institute of Immunology, Biomedical Sciences Research Center "Alexander Fleming", Athens, Greece.
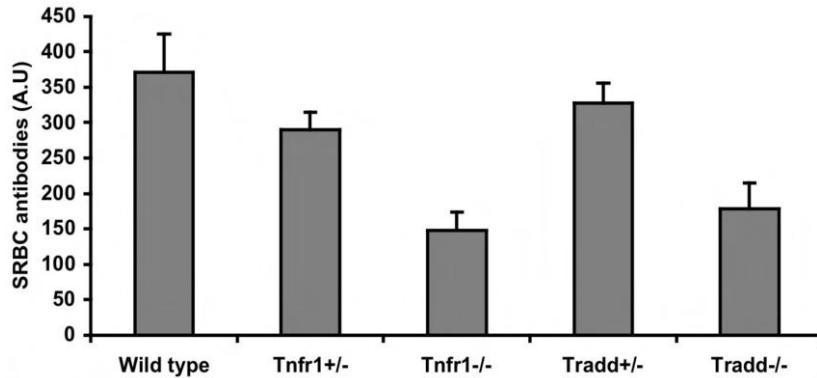
Figure 14: Anti-SRBC IgG antibodies were determined in the serum of mice with the indicated genotypes by a specific ELISA. Wild type $n = 12$, $Tnfrl^{+/-}$ $n = 10$, $Tnfrl^{/-}$ $n = 8$, $Tradd^{+/-}$ $n = 8$ and $Tradd^{/-}$ $n = 6$. Data are presented as arbitrary units. **-The experiment was performed in collaboration with Dr. Ksanthi Kranidioti, Institute of Immunology, Biomedical Sciences Research Center "Alexander Fleming", Athens, Greece.

5.1.6 The TNF-induced formation of TNFR1 proximal signaling complex is altered in TRADD deficient cells: TRAF2 is not recruited to the receptor in the absence of TRADD, RIP1 is still recruited but is no longer modified.

We next wanted to determine the molecular mechanism that could explain the effect of the TRADD deficiency on TNFR1 mediated activation of NF-κB and MAP kinases. The identification of such molecular mechanism would significantly improve our understanding of molecular events that take place in close vicinity to the cytoplasmic part of TNFR1 upon TNF stimulation. As TRADD was proposed to be the key adaptor mediating the recruitment of downstream messengers to the cytosolic death domain of TNFR1; our first choice was to compare the TNF-induced formation of receptor proximal signaling complex in TRADD deficient and control cells. For this experiment we used mouse embryonic fibroblasts as a system. The principle components of the complex important for the activation of NF-κB and MAP kinases are TRAF2 and RIP1. We stimulated wild type and TRADD deficient cells

with Flag-tagged TNF, precipitated the complex from cell lysates with the antibody specific for the tag and analyzed the contents of the precipitate by immunoblotting. We observed that in wild type MEFs both TRAF2 and RIP1 were efficiently recruited to TNFR1 upon ligand binding (see Figure 15) with RIP1 undergoing posttranslational modification within the complex. This modification was most likely ubiquitination as it was previously discussed.
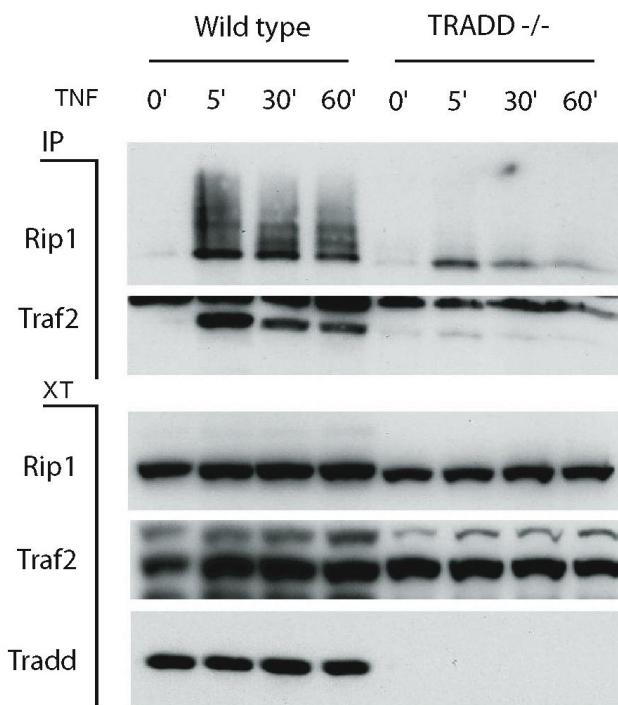
Figure 15. Wild type and TRADD -/- mouse embryonic fibroblasts were stimulated with Flag-tagged TNF (1 μg/ml) for indicated times. Anti-Flag immunoprecipitates and total cell extracts were analyzed for the presence of RIP1 and TRAF2 by immunoblotting with respective specific antibodies. NF-kB activation in response to Flag-tagged TNF was measured with phospho-specific antibody for IkB. TRADD expression was evaluated by blotting with specific antibody. **-The experiment was performed in collaboration with Dr. Marie-Cécile Michallet, Department of Biochemistry, University of Lausanne, Switzerland

By evaluating the composition of the TNFR1 proximal complex in TNF-stimulated TRADD deficient cells we could observe that TRAF2 was no longer part of the complex. Therefore we concluded that TRADD was essential for the recruitment of TRAF2 to TNFR1. We found that residual amounts of RIP1could still associate with TNFR1 in the absence of TRADD but we could not observe slower migrating forms of RIP1 suggesting the lack of TNF-induced

posttranslational modification of the protein. The lack of modified RIP1 correlated with the absence of TRAF2. Since the E3 ligase activity of TRAF2 was shown to be essential for the ubiquitination of RIP1 the absence of TRAF2 from the receptor proximal complex is most likely responsible for impaired RIP1 modification.

As previously described, K63 ubiquitinated RIP1 acts as a platform for the recruitment and/or activation of IKKs (through NEMO) and the complex that contains TAK1. TAK1 is a kinase that activates both the IKK complex and upstream MAP kinases. Therefore the reduced activation of NF-κB and MAP kinases in TNF stimulated TRADD deficient cells is likely to be caused by the inability to recruit or activate the listed mediators due to the lack of RIP1 poly-ubiquitination. The residual activation of indicated cascades that still occurs in mutant cells could be mediated by the kinase activity of RIP1 or by association of RIP1 with some other unidentified factors.

5.1.7 TRADD is indispensable for TNF induced apoptosis in cultured mouse embryonic fibroblasts.

TRADD was proposed to play a role in TNF induced apoptosis via recruiting FADD and pro-caspase-8 to the cytoplasmic death domain of TNFR1 upon TNF stimulation. We next wanted to investigate whether TNF induced apoptosis could still take place in TRADD deficient cells.

We used primary mouse embryonic fibroblast as an experimental system. It is known that MEFs become sensitive to TNF induced death only when TNFR1 mediated expression of protective genes is blocked by chemical agents such as cycloheximide (CHX). We first stimulated TRADD deficient and control cells with TNF/CHX and then evaluated cell viability microscopically after 24 hours (see Figure 16). We observed nearly complete death of wild type cells while the death of TRADD deficient cells stimulated with TNF/CHX was comparable to death of cells stimulated with the cyclohexamide alone. This result suggested that TRADD deficient cells were protected from TNF induced apoptosis.
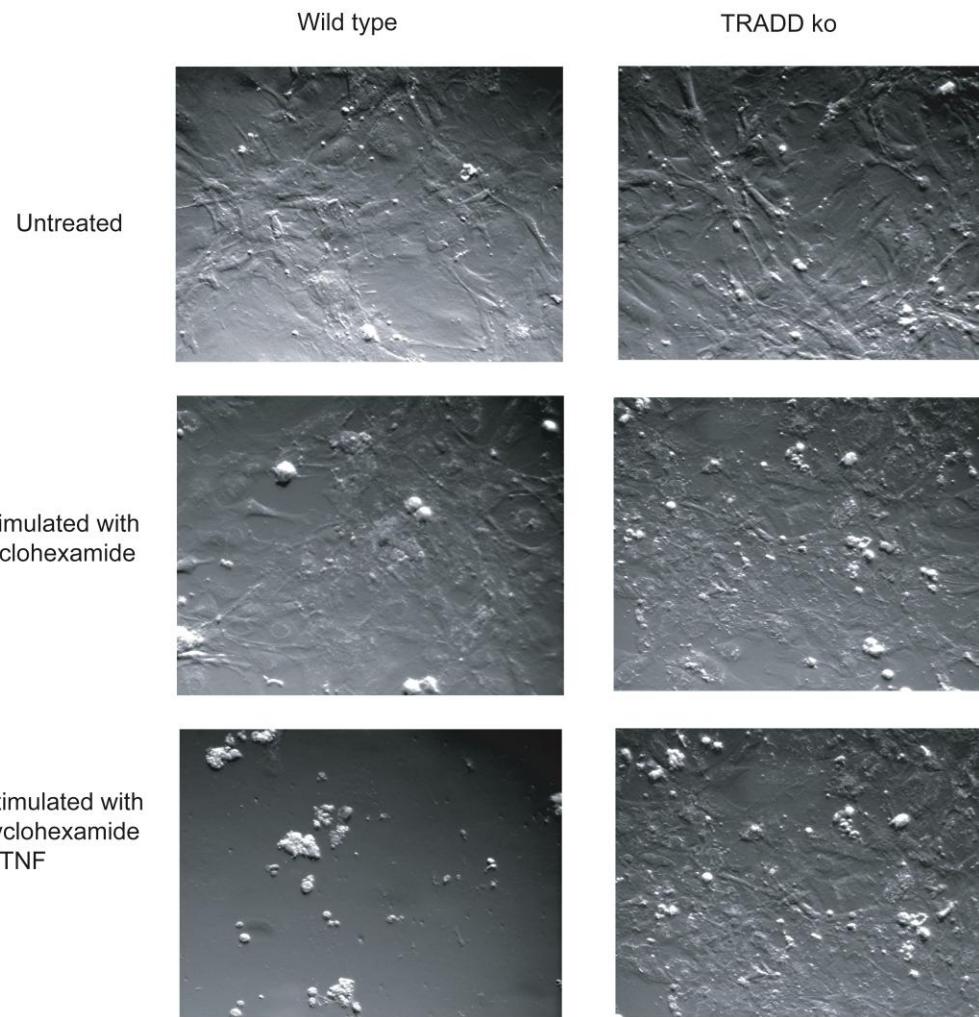
Figure 16. TRADD -/- and wild type mouse embryonic fibroblasts were stimulated with TNF (10 ng/ml) and cyclohexamide (10 µg/ml). Cell death was evaluated microscopically after 24 hours.

In order to confirm the observed effect in a quantitative manner we repeated the stimulation and evaluated the outcome via staining cultures with MTT (3-(4,5-Dimethylthiazol-2-yl)-2,5-diphenyltetrazolium bromide), a compound that gets reduced by the mitochondria of living cells into a blue colored die. The percentage of living cells was then determined by colorimetric analysis. We included TNFR1 deficient mouse embryonic fibroblasts as an additional control in this experiment. TNFR1 deficient cells are not sensitive to TNF-mediated apoptosis that is induced via FADD-caspase 8 signaling axes. We could observe

that the survival of TRADD deficient cells upon treatment with TNF/CHX was comparable to the survival of TNFR1 deficient cell while more wild type cells died (see Figure 17). Therefore we concluded that TRADD was likely to be essential for TNFR1-mediated programmed cell death.
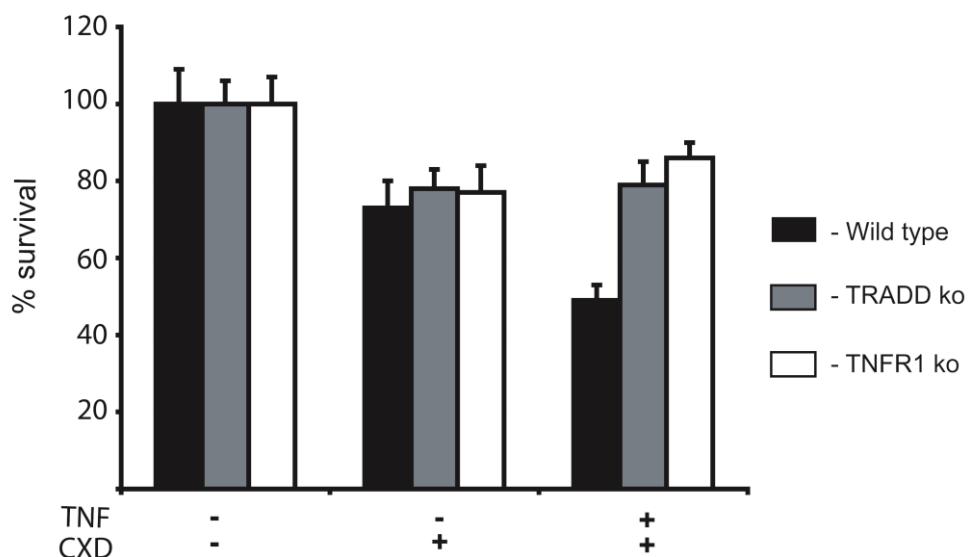
Figure 17. Wild type, TRADD-/- and TNFR1-/- mouse embryonic fibroblasts were stimulated with TNF(10ng/ml) and cyclohexamide (10ug/ml). Cell survival was measured by MTT assay 12 hours after the stimulation.

We next wanted to define whether the increased survival of TRADD deficient cells was due to the blockade of FADD-caspase-8 induced apoptosis. Caspase-8 is activated via auto-processing upon recruitment to death receptors. The processing results in the generation of several products including the 18 kDa catalytically active form of the enzyme. Caspase-8 is an upstream caspase that is activated by initial pro-apoptotic signals and is responsible for the amplification of such signals. One copy of active caspase-8 mediates cleavage of multiple copies of full length effector caspases such as caspase-6, caspase-7 and caspase-3. The specific cleavage of the precursor protein activates effector caspases allowing them to further cleave other protein substrates within the cell resulting in the apoptotic process. The processing of pro-caspase-3 generates the 17 kDa catalytically active form. Active caspases are only present in cells that undergo programmed cell death and therefore can be used as reliable markers of apoptosis. We evaluated the presence of the activated caspase-8 and caspase-3 in cell extracts prepared from wild type and TRADD deficient MEFs 6 hours after

stimulation with TNF/CHX. We could observe efficient activation of both caspases in TNF stimulated wild type cells (see Figure 18) while no caspase activation could be detected in TRADD -/- cells. Therefore we confirmed that TNF-induced apoptosis required TRADD and was blocked by the TRADD deficiency.
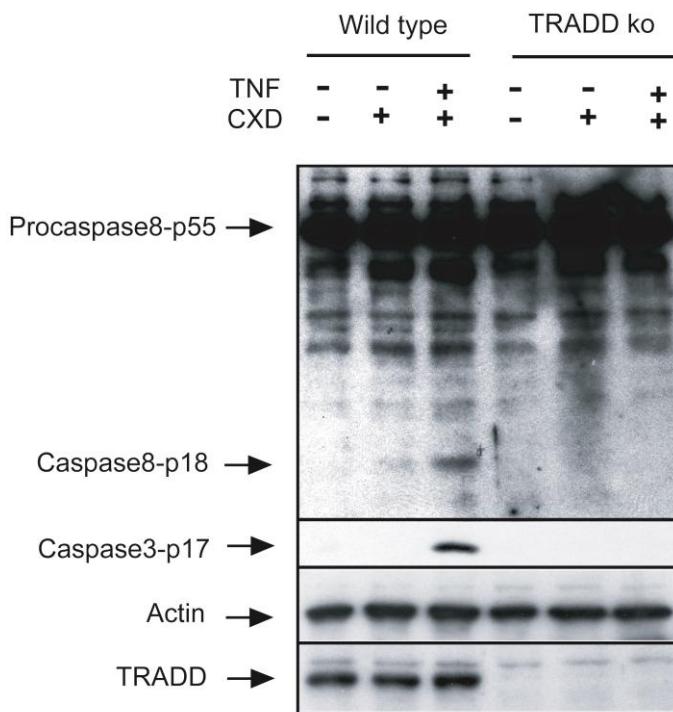
Figure 18. Wild type and TRADD-/- mouse embryonic fibroblasts were stimulated with TNF (20 ng/ml) and cyclohexamide (10 ug/ml). Cell lysates were prepared 6 hours after the stimulation and analyzed by immunoblotting. Caspase-8 activation was measured with the antibody specific for both the full length and the cleaved form of the protein. Caspase-3 activation was measured with the antibody specific for the cleaved form (p17). Equal loading was confirmed by immunoblotting for actin. TRADD expression was evaluated by blotting with the specific antibody.

5.1.8 TRADD deficient mice are protected from liver damage and death in the TNF/Gal-N model of TNF mediated liver toxicity.

We have previously demonstrated that TNF-induced apoptosis was blocked in TRADD knock out primary MEFs. We next wanted to determine whether TRADD deficiency could protect against systemic toxicity of TNF *in vivo*. In order to do that we chose to subject TRADD -/- and control animals to a model of TNF mediated liver failure. In our model of choice mice are challenged with intraperitoneal administration of β-GalN (β-galactosamine)

and intravenous injection of TNF. β-GalN is a chemical that specifically blocks protein synthesis in hepatocytes and sensitizes them to TNF-induced apoptosis. In wild type mice TNF/β-GalN treatment results in lethal liver failure due to massive death of hepatocytes.

TRADD deficient and control mice were treated with β-GalN/TNF and the mortality rate was recorded for a period of 24 hours. 3 out of 5 wild type animals died at 6-8 hours post injection while all TRADD -/- mice survived (see Table 1). Therefore TRADD deficiency protected mice from TNF-induced liver damage.

Doze			Lethality (deaths/total)		
TNF	GalN	FasL-Fc	Wild type	TRADD ko	FADD ^{HEPko}
0,4μg/20g of body weight	20 mg		3/5	0/6	
		10 μg	2/2	2/2	0/2

Table 1. Mice were challenged with TNF/β-GalN or with intravenous administration of FasL-Fc. Non-protected animals were dieing at 6-8 hours post injection in case of TNF/β-GalN stimulation and at around 2 hours post injection in case of stimulation with FasL-Fc.

In order to determine whether the effect of TRADD deficiency was TNF specific we subjected TRADD -/- and control mice to a different model of acute liver failure that was induced by intravenous injection of FasL (Fas ligand). The receptor for FasL − Fas, is expressed on the surface of hepatocytes. Fas belongs to a family of death receptors and mediates programmed cell death via FADD-caspase-8 signaling axes upon ligand binding. We included mice carrying a hepatocyte specific deletion of the FADD gene (FADD^{HEPko} mice) into this experiment as an additional control. FADD^{HEPko} mice are protected from FasL-induced liver failure. Both TRADD -/- and wild type animals died within 2 hours upon injection with the FasL, while FADD^{HEPko} mice survived as expected (see Table 1). Therefore

TRADD deficient mice were protected from the TNF-induced but not FasL-induced hepatocyte death.

We collected blood serum samples from control and TRADD deficient mice before treatment with β-GalN/TNF and after 6-8 hours of treatment (depending on the survival of the animals). We then measured the concentration of alanine aminotransferase (ALT) in the serum. ALT is released into blood upon death of hepatocytes and can be therefore used as a reliable marker of liver damage. We observed elevated levels of ALT in the serum of control mice that were treated with β-GalN/TNF (see Figure 19). In contrast TRADD deficient mice did not show increased levels of ALT upon treatment indicating that the lack of TRADD expression protected them from TNF-induced liver damage.

We also prepared protein extracts from livers of wild type and TRADD -/- mice at 6-8 hours of stimulation with TNF/β-GalN. These extracts were analyzed by immunoblotting for the
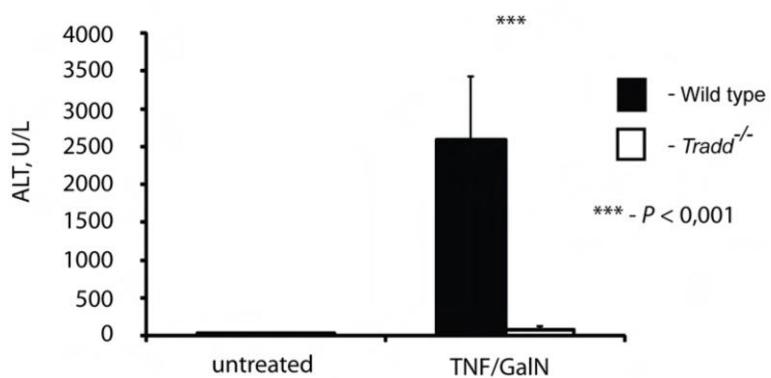
Figure 19. Wild type and TRADD -/- mice were challenged with intraperitoneal administration of beta-GalN (20 mg/mouse) and TNF (0,4µg/20g of body weight). Serum samples were collected from every mouse before injection and 8 hours after injection. The concentration of ALT in the serum was measured by a standard clinical procedure.

presence of activated casepase-8 and caspase-3 as it was described previously. We couldn't detect any caspase activation in extracts that were prepared from livers of TRADD deficient

mice while both caspases were activated in control livers (see Figure 20). Overall our results demonstrated that TRADD deficiency is able to protect cells and organs from the TNF-mediated damage both *in vitro* and *in vivo*.
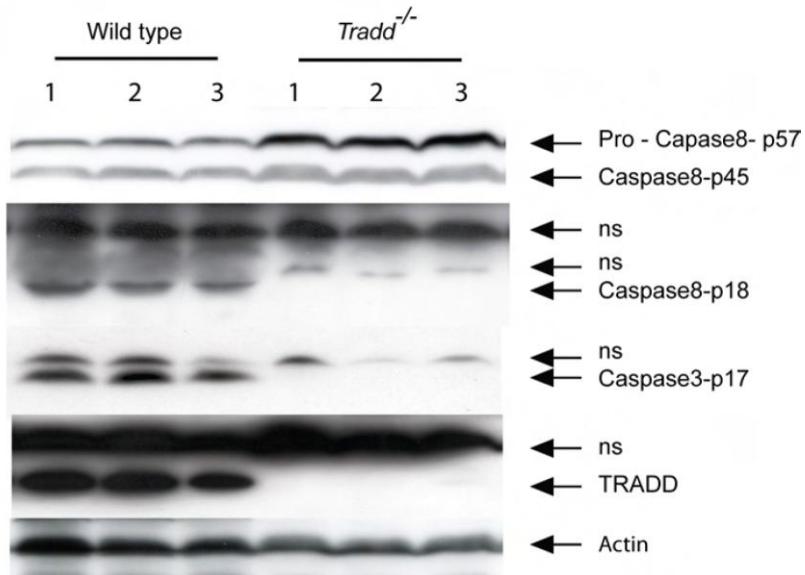
Figure 20. Liver samples were collected from mice used in Figure 19 after 8 hours of stimulation. Protein extracts were prepared and analyzed by immunoblotting as described in Figure 18.

5.1.9 TRADD deficient mice show impairment of TNF production upon in vivo stimulation with polyI:C and LPS but not CpG DNA.

We have previously demonstrated that TRADD plays an important role in pro-inflammatory and immune responses due to the involvement in TNF signaling through TNFR1. We then decided to investigate whether TRADD is implicated in Toll like receptor signaling. As our pilot experiment we treated three groups of TRADD knockout and wild type control mice with ligands for three different TLRs: poly(I:C) (TLR3), LPS (TLR4) and CpG DNA (TLR9). We used TNF expression in the serum of mice as a functional readout of the outcome of the stimulation. As cytokines produced in response to TLR stimulation can act in an autocrine manner leading to expression of more cytokines, we wanted to exclude any effects that could be caused by impairment of autocrine TNF signaling through TNFR1 in TRADD deficient mice. For that reason we included groups of TNFR1 knockout controls into each experiment. To our surprise TRADD knockout mice demonstrated significantly reduced induction of TNF expression upon intravenous injection of poly(I:C) (see Figure 21). This

effect was not present in TNFR1 knockout animals and therefore was unlikely to be caused by the blockade of secondary TNF signaling in TRADD deficient mice.
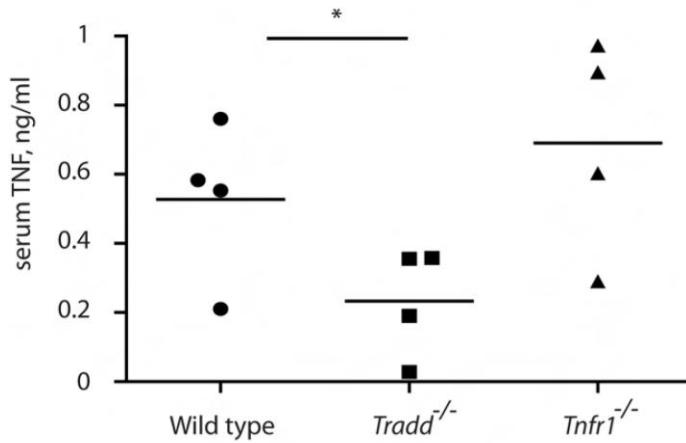
Figure 21: Wild type, *Tradd*^{-/-} and *Tnfr1*^{-/-} mice were injected intravenously with 5μg/20g body weight poly(I:C). Sera were collected at 1 hour of stimulation and analyzed by ELISA for the expression of TNF. The values for individual mice are presented.

We also observed a trend for reduced TNF in response to intraperitoneal injection of LPS in TRADD -/- animals, although it was not statistically significant (see Figure 22). No such trend could be observed in TNFR1 -/- mice, on the contrary these mice showed elevated levels of TNF in the serum upon stimulation with LPS.
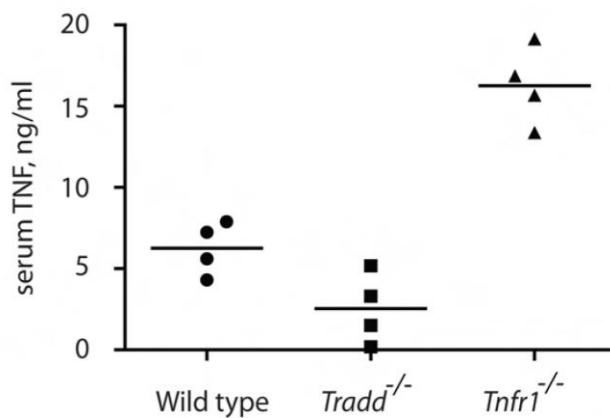
Figure 22: Wild type, *Tradd*^{-/-} and *Tnfr1*^{-/-} mice were injected ip with 5μg/10g body weight LPS. Sera were collected and analyzed as described in Figure 21.

Unlike LPS and poly(I:C), TNF levels induced by intravenous injection of CpG DNA were similar between TRADD deficient and wild type mice (see Figure 23). These data collectively suggested that TRADD may be involved in signal transduction by specific Toll like receptors and dispensable for the signaling via other TLRs.
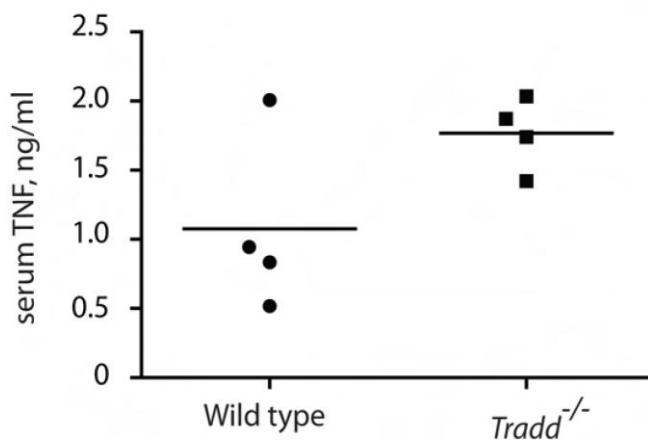
Figure 23: Wild type, and *Tradd*^{-/-} mice were injected i.v. with 50μg of CpG DNA. Sera were collected and analyzed as described in Figure 21.

5.1.10 TRADD is important for NF-κB and MAPK activation by poly(I:C).

In order to follow up on the putative involvement of TRADD in poly(I:C)-induced signaling we decided to perform experiments in isolated primary cells. Since poly(I:C) stimulation is used to mimic responses that are induced by viral infections we first decided to investigate the effect of TRADD deficiency in immune cells on their ability to respond to poly(I:C). Primary splenocytes – a mixed population of different kinds of immune cells, were our cell type of choice. We subjected splenocytes isolated from wild type, TRADD knockout and TNFR1 knockout mice to extracellular stimulation with poly(I:C). We used IL-6 expression in culture supernatants as a functional readout of the stimulation. TNFR1 deficient cells were included to control for the effects caused by the blockade of secondary autocrine TNF signaling. Consistent with our *in vivo* data, TRADD deficient spleenosytes secreted reduced levels of IL-6 compared to wild type and TNFR1 knockout cells upon stimulation with poly(I:C) (see Figure 24).
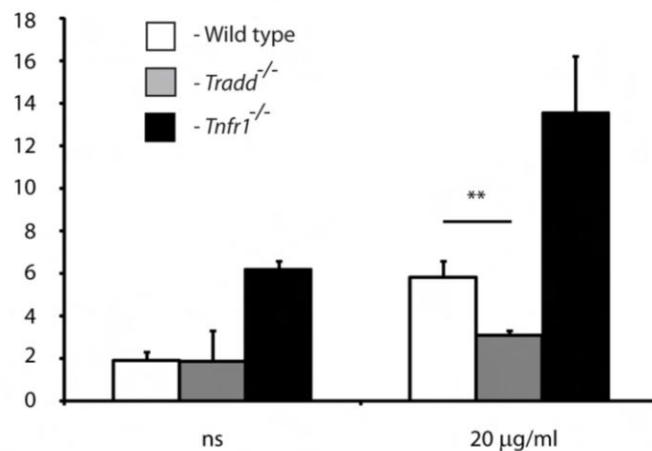
Figure 24: Wild type, *Tradd*^{-/-} and *Tnfr1*^{-/-} splenocytes (10^6 cells/ml) were stimulated with 20 μg/ml poly(I:C) for 24 hours. Culture supernatants were collected and analyzed by ELISA for the expression of IL-6.

On the basis of reduced cytokine production by poly(I:C) stimulated TRADD deficient mice and cells we hypothesized that TRADD may play a direct role in the poly(I:C)-induced signaling cascade. In order to test this hypothesis we stimulated wild type and TRADD knockout mouse embryonic fibroblasts (MEFs) with poly(I:C) by adding it to the cell culture medium and then tested the activation of NF-kB and MAP kinases by detecting phosphorylated forms of IκBα and MAPKs in cell extracts as described previously. Poly(I:C) stimulation induced activation of NF-κB and MAPK pathways in wild type cells, as revealed by the increased phosphorylation of IκBα, JNK, p38 and ERK (see Figure 25). In contrast, TRADD-deficient MEFs showed impaired activation of NF-κB and MAP kinase signaling in response to poly(I:C) stimulation compared to wild type cells suggesting that TRADD is essential for the immediate response of MEFs to poly(I:C) stimulation.
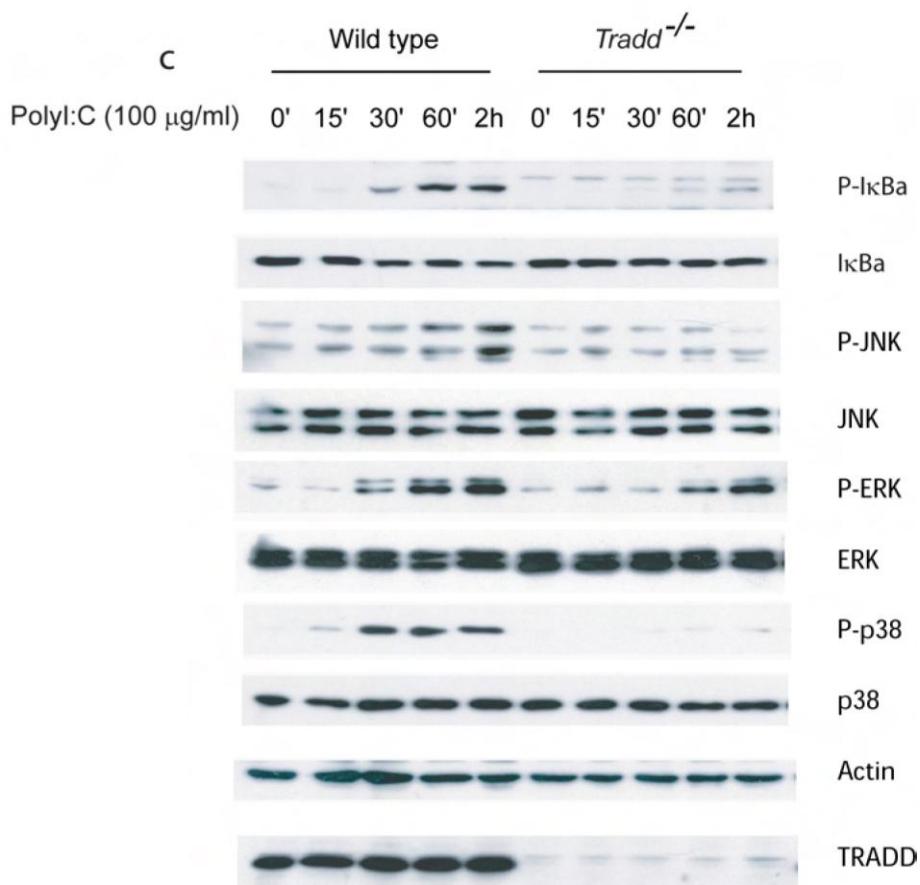
Figure 25: Wild type and *Tradd*^{-/-} mouse embryonic fibroblasts were stimulated with 100 μg/ml poly(I:C) for the indicated time points. Cell lysates were prepared and analyzed by immunoblotting as previously described.

5.1.11 TRADD plays a role in TRIF-dependant TLR4 signaling.

Based on *in vivo* results that were obtained from mice we concluded that TRADD plays a role in signaling via TLR3 and TLR4 but not TLR9. We next attempted to explain the differential involvement of TRADD in TLR signaling.

Toll like receptors activate intracellular signaling events by recruiting two types of adaptor molecules – Myd88 and TRIF. Most TLRs, including TLR9 signal exclusively via Myd88 while TLR3 and TLR4 use TRIF (TLR3 – exclusively, TLR4 – in addition to Myd88). Based

on our results regarding the impact of TRADD deficiency on TLR activation we hypothesized that TRADD may be specifically involved in TRIF-dependant TLR signaling. This hypothesis would explain why TLR3 and 4 were affected by the TRADD deficiency while TLR9 was not.

In our previous experiments we could see that the trend of TRADD knockout mice to express less cytokines in response to LPS stimulation was clear but not statistically significant. If the specific involvement of TRADD in TRIF-dependant TLR signaling was true, the lack of profound impairment of the response to LPS in TRADD deficient mice could be explained by the compensatory effect of Myd88. In order to test this hypothesis we generated mice double deficient for TRADD and Myd88. We then subjected these mice to the *in vivo* stimulation with LPS in parallel with wild type, TRADD deficient and Myd88 deficient animals. In order to improve the sensitivity of the experiment and enhance the putative differences between the genotypes we reduced the amount of LPS that was injected into the mice in comparison to our first experiment. We evaluated the efficiency of the stimulation based on TNF levels in the serum of mice.

By using the modified experimental set up we could observe significant differences in TNF expression between TRADD deficient and wild type mice stimulated with LPS (see Figure 26). This result was consistent with previously published data showing reduced expression of cytokines in TRIF knockout mice that were challenged with LPS. It has to be noted that TRIF-deficient animals demonstrated a very severe impairment of the response to LPS while the impairment we observed in TRADD -/- mice was relatively mild. This difference can be explained by the presence of other mediators such as TRAF6 and TRAF3 that are known to participate in TRIF-mediated signaling and could connect TRIF to the activation of downstream cascades in the absence of TRADD expression.
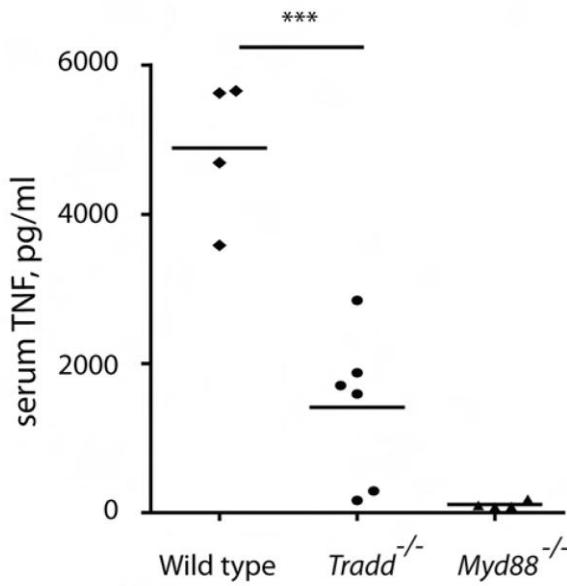
Figure 26: Wild type, TRADD deficient and Myd88 deficient mice were injected i.p. with 50 ng/g body weight LPS. Sera were collected at 1 hour of stimulation and analyzed as described previously.

Myd88 deficient mice demonstrated severe impairment of LPS-induced TNF expression consistent with the previously published data (see Figure 26). Nevertheless these mice still expressed detectable levels of TNF in response to LPS injection. The residual cytokine expression was completely abolished in TRADD/Myd88 double knockout mice (see Figure 27) suggesting that TRADD may be involved in Myd88-independent e.g. TRIF-dependant TLR4 signaling.
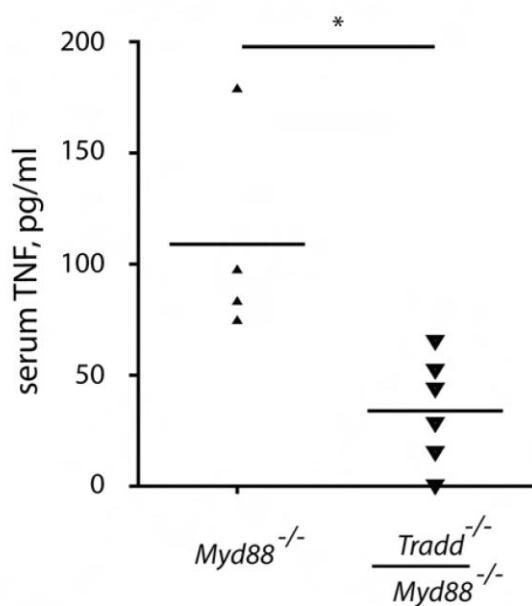
Figure 27: Myd88 deficient and TRADD/Myd88 double deficient mice were injected i.p. with 50 ng/g body weight LPS. Sera were collected at 1 hour of stimulation and analyzed as described previously.

To assess whether TRIF-dependent TLR4 signaling is affected by the absence of TRADD, we analyzed LPS-induced activation of NF-κB and MAPK signaling in MEFs lacking Myd88 or both Myd88 and TRADD. Wild type cells were used as a positive control in this experiment. Consistent with the previously published data, Myd88 deficient MEFs showed impaired activation of NF-κB and MAPK compared to wild type cells as indicated by reduced and delayed phosphorylation of IκBα, JNK, p38 and ERK detected by immunoblotting that was performed on total cell extracts (see Figure 28).
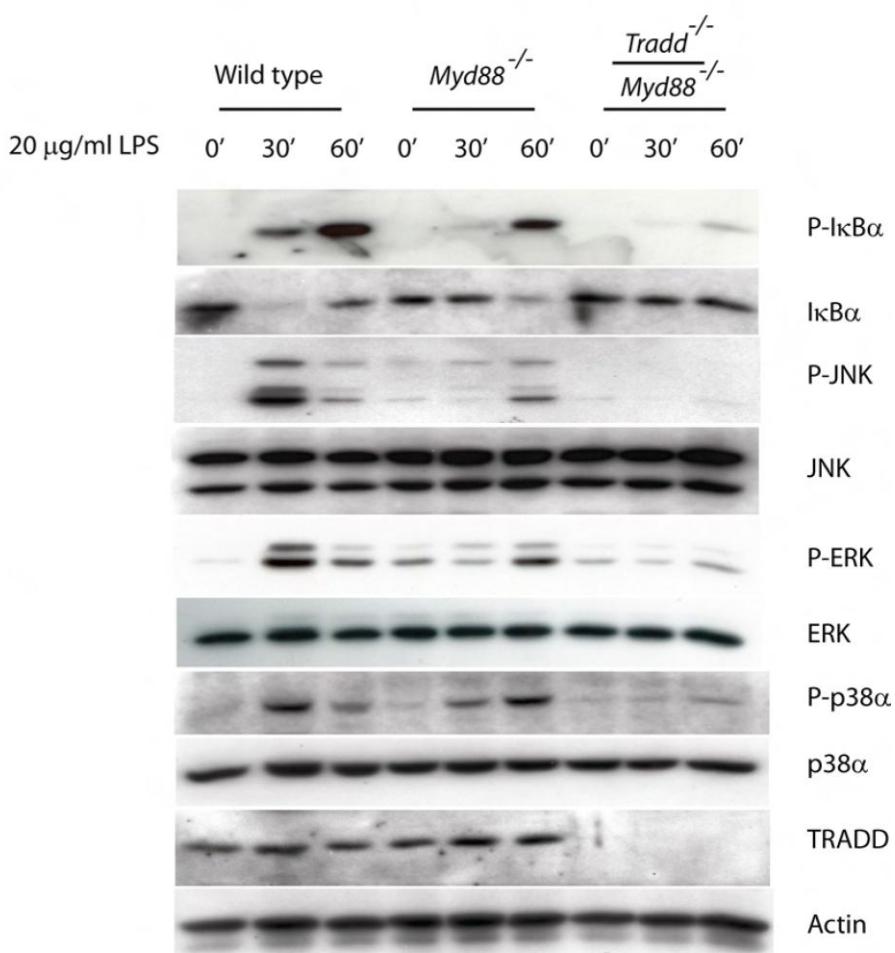
Figure 28: Wild type, Myd88 deficient and TRADD/Myd88 double deficient mouse embryonic fibroblasts were stimulated with 20 μg/ml LPS for indicated time points. Cell lysates were prepared and analyzed by immunoblotting as described previously.

Nevertheless at later time point of LPS stimulation (60 minutes) Myd88 knockout cells demonstrated substantial activation of all cascades of interest in agreement with the previously reported evidence of the late phase of LPS signaling being predominantly dependant on the second adaptor TRIF. In contrast to Myd88 deficient MEFs, Myd88/TRADD double deficient cells did not show significant activation of NF-κB or MAPK at both early and late time points of stimulation. Thereby we were able to demonstrate that the lack of TRADD leads to the blockade of the late phase LPS signaling consistent with the putative role of the molecule in the TRIF-dependant cascade.

5.1.12 TRADD interacts with TRIF via RIP1.

We then tried to find the mechanistic explanation for the role of TRADD in TRIF-mediated signaling. It has been demonstrated previously that RIP-1 is involved in the TRIF cascade. RIP-1 directly interacts with TRIF and is important for the activation of NF-κB and MAPK upon stimulation with poly(I:C).

As we have previously demonstrated, TRADD acts as a partner of RIP-1 in TNFR1 mediated signaling and is essential for the posttranslational modification of RIP-1 upon TNF stimulation. We then hypothesized that the role of TRADD in TRIF mediated signaling may be based on its partnership with RIP-1. In order to test this hypothesis we performed co-immunoprecipitation experiments in HEK293 cells by using plasmid constructs that overexpressed tagged versions of TRIF, RIP-1 and TRADD. In our first experiment we could demonstrate that TRIF interacted with TRADD in the presence of RIP-1 (see Figure 29). When TRADD and TRIF were co-expressed in the absence of RIP-1 overexpression they also interacted weakly presumably due to the presence of the endogenous RIP-1. Therefore in our next experiment we decided to eliminate RIP-1 from the cells by specific RNAi knockdown and then test whether TRADD would still be able to interact with TRIF. We could clearly demonstrate that the interaction between TRADD and TRIF was abolished by the depletion of RIP-1 (see Figure 30).
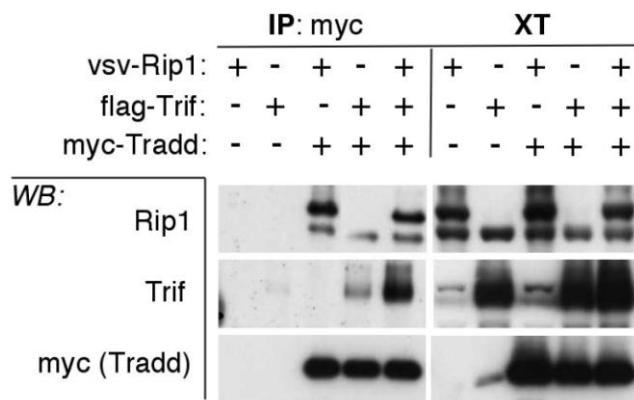
Figure 29: HEK293 cells were transfected with expression vectors encoding vsv-tagged RIP1, flag-tagged TRIF and myc-tagged TRADD as indicated. Anti-myc immunoprecipitates and total cell extracts were analyzed by Western blot for the presence of RIP1, myc (TRADD) and TRIF. [**]-The experiment was performed in collaboration with Dr. Marie-Cécile Michallet, Department of Biochemistry, University of Lausanne, Switzerland
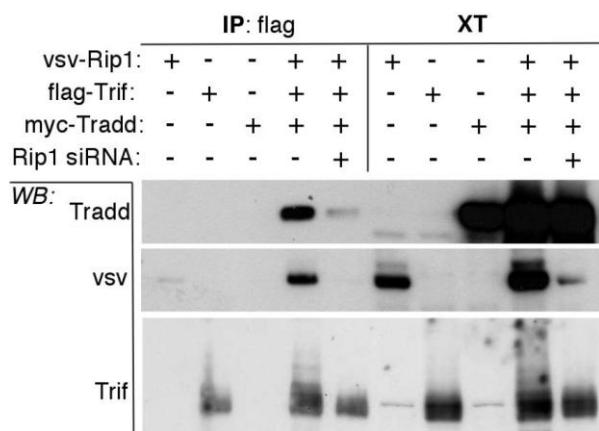
Figure 30: HEK293 cells were transfected as indicated with RIP1 specific siRNA or expression vectors encoding vsv-RIP1, flag-TRIF and myc-TRADD. Anti-Flag immunoprecipitates and total cell extracts were analyzed for the presence of TRIF, TRADD and RIP1 by immunoblotting with antibodies specific for respective tags. [**]-The experiment was performed in collaboration with Dr. Marie-Cécile Michallet, Department of Biochemistry, University of Lausanne, Switzerland

RIP-1 is recruited to TRIF via the RIP Homotypic Interaction Motif (RHIM) while the C-terminal Death Domain is free for binding to other proteins. We hypothesized that TRADD may be recruited to RIP-1 via the interaction of their death domains. In agreement with this hypothesis we could demonstrate that TRADD did not bind efficiently to a mutant RIP1 lacking the death domain (see Figure 31).
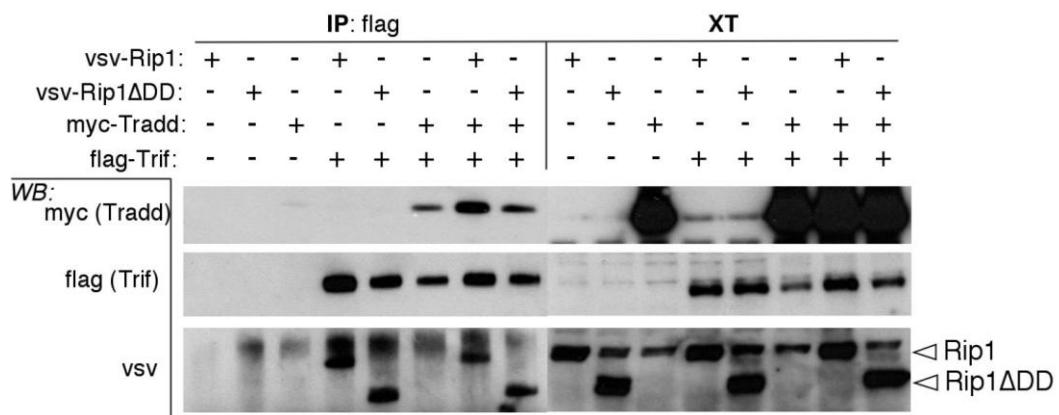
Figure 31: HEK293 cells were transfected with expression vectors encoding vsv-tagged RIP1, vsv-tagged RIP1 lacking its death domain (vsv-RIP1ΔDD), flag-tagged TRIF and myc-tagged TRADD as indicated. Anti-flag immunoprecipitates and total cell extracts were analyzed by Western blot for the presence of vsv (RIP1), myc (TRADD) and flag (TRIF). [**]-The experiment was performed in collaboration with Dr. Marie-Cécile Michallet, Department of Biochemistry, University of Lausanne, Switzerland

5.2 Conditional targeting of CYLD.

5.2.1 Generation of CYLD mutant (CYLD Δ932) mice.

The mouse *cyld* gene is located on chromosome 8. The gene has 17 exons. The region encoding for the respective protein starts in the exon 2 and ends in the beginning of the exon 17; the small 5′ portion of exon 2 and a large 3′ portion of exon 17 are non-coding (see Figure 32).
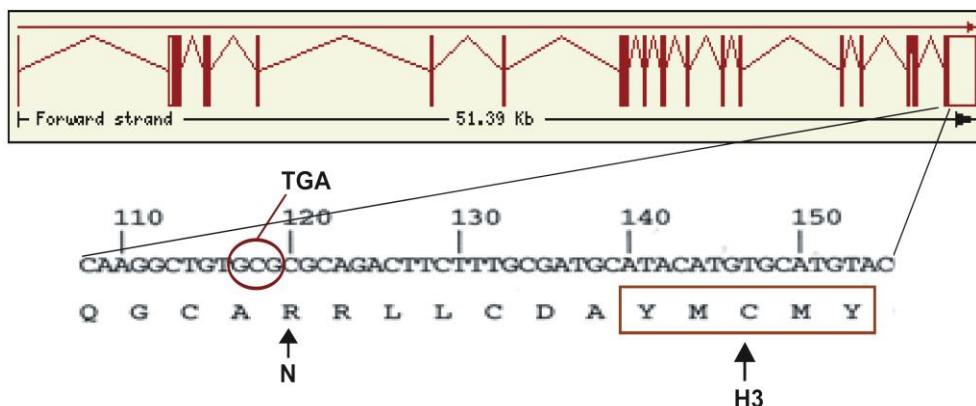
Figure 32: The scheme of the mouse cyld gene (chromosome 8) is presented, indicating the position of the mutation within the exon 17.

The amino acid sequence of the C-terminal part that contains the catalytic domain is identical between human and murine CYLD proteins. Therefore it was possible to introduce the exact mutation that was identified from a case of the human disease (the Δ932 mutation) into a mouse. The mutation leads to the truncation of the last 20 amino acids of the protein that contain the conserved motif essential for the enzymatic function of CYLD. This mutation impairs the catalytic function of CYLD as it was demonstrated previously. At the same time the truncated protein must be still able to interact with its targets and upstream mediators as domains responsible for the protein-protein interaction are preserved. The conserved motif to be removed is encoded by the exon 17 of the mouse *cyld* gene. The truncation occurs due to the insertion of the early stop codon upstream of the motif of interest (see Figure 32).

In our strategy we flanked the exon of interest (exon 17) with LoxP sites (see Figure 33). We inserted a mutant copy of the same exon downstream of the second LoxP site. The mutant copy of the exon will replace the wild type exon 17 upon its Cre mediated excision. A transcriptional STOP cassette was inserted between the predicted polyadenylation signal of the *cyld* gene and the second LoxP site to avoid read-through and generation of the chimeric mutant protein in the absence of the Cre recombinase.

The targeting vector was generated as described in Materials and Methods. It was introduced into C57BL/6 mouse embryonic stem cells via homologous recombination. 384 clones that survived both the negative and the positive selection were isolated and manipulated as described previously. The Spe I digested DNA from these clones was subjected to Southern blot analysis by using external probes A and B (see Figure 33).
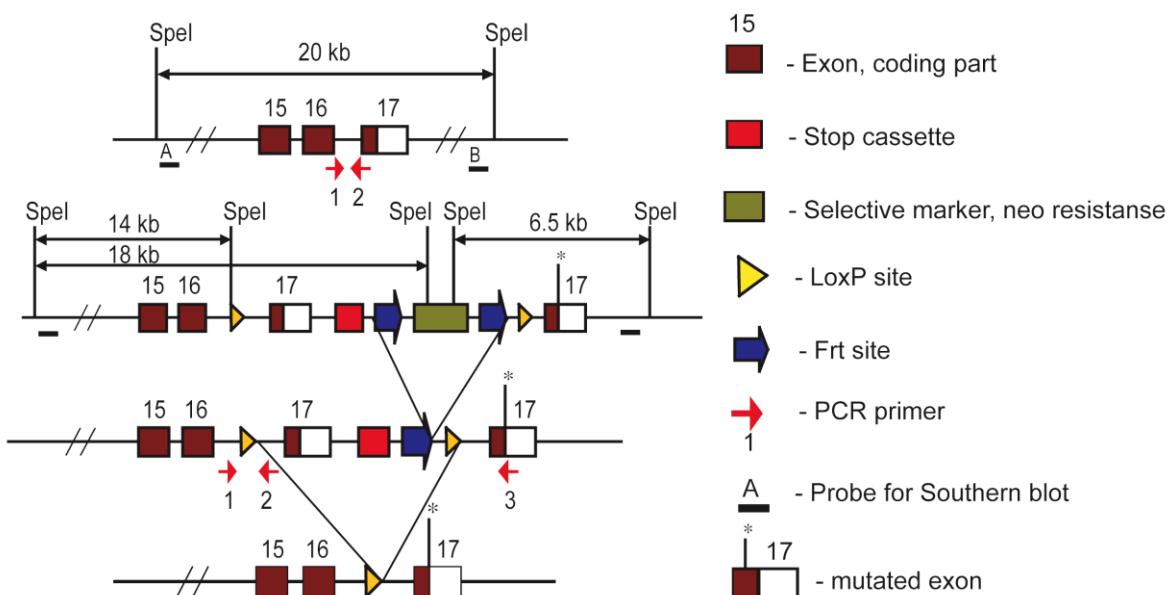
Figure 33: Schematic pictures of the wild type, targeted, floxed and deleted cyld locus are presented, indicating Spe1 restriction sites used for the Southern blot analysis, positions of probes, the expected length of fragments and binding sites for genotyping PCR primers.

The analysis with the probe B would identify clones that incorporated the downstream part of the manipulated allele into the appropriate genomic location. The strategy was based on the

fact that the positive selection cassette of the targeting vector contained the recognition sequence for Spe I. Therefore, in case the cassette and the mutated exon 17 were inserted into the genome as expected, the probe B would recognize a specific fragment of 6.5 kb in addition to the endogenous 20 kb fragment. The subsequent analysis by using probe A would reveal how many of the previously isolated clones also incorporated the second (upstream) LoxP site into their genome. The recognition sequence for Spe I was inserted into the area adjacent to the upstream LoxP site during the generation of the targeting vector. The presence of the extra Spe I binding site would indicate that the upstream LoxP site integrated into the genome. The specific band of 14 kb would be recognized by probe B in case of correct insertion of the LoxP site in question. 11 clones that were positive according to both probes were identified as a result of the analysis. We isolated 4 of them from respective wells of the 96 well plate and processed them as described in Materials and Methods. We then selected two of the 4 clones and prepared genomic DNA from these cells. The DNA was subjected to the analysis by Southern blot in order to confirm the identity of the clones. The initial analysis was performed by using probes A and B. The analysis confirmed that the genomic locus of interest was correctly targeted in both clones (see Figure 34). We then analyzed the same DNA by using part of the Flp sequence as a probe (described previously). This analysis would allow us to eliminate the possibility that another copy of the targeting vector was randomly integrated into the genome of the clones. No such integration was determined (data not shown).
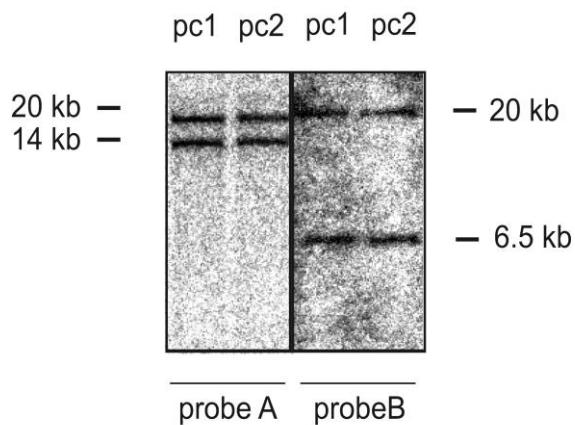
Figure 34: The correct incorporation of the modified cyld allele into the genome of two ES clones (pc1 and pc2) was evaluated by Southern blot analysis of Spe 1 digested genomic DNA. See Figure 33 for the position of the probes and the expected length of fragments.

Upon confirmation of the identity, embryonic stem cells from two correctly targeted clones were microinjected into C57BL/6 blastocysts in order to produce black on black chimaeric mice. This was based on the assumption that the environment of syngenic embryos could have a beneficial effect on the performance of C57Bl/6 ES cells that were used for targeting. We hoped that in this case more ES cells would survive and maintain plurypotency; therefore the cells would contribute more efficiently to the development of various mouse tissues and the probability to obtain germ line transmitting chimeras would increase. Tail biopsies were obtained from every mouse that was born as a result. Genomic DNA was prepared and subjected to the specific PCR analysis (see Figure 33 for primers) in order to identify chimaeras − the mice that would show a specific band consistent with the presence of the modified allele in addition to the wild type band. Male chimeras were mated to C57BL/6 females. Tail biopsies were obtained from the progeny; the genomic DNA was prepared and analyzed for the transmission of the modified allele through the germ line via PCR analysis with previously described primers. The germ-line transmission was successfully obtained and mice heterozygous for the modified *cyld* allele were generated (see Figure 35).

The modified CYLD allele allows conditional introduction of the Δ932 mutation in any cell type using Cre mediated recombination. Mice heterozygous for the modified *cyld* allele were crossed to the ubiquitous Cre-Deleter strain in order to produce animals that would carry a nonsense mutation in the exon 17 of the *cyld* gene in every tissue of the organism (see Figure 35 for the analysis of the progeny). Other heterozygous mice were mated with the ubiquitous Flp-Deleter strain in order to obtain CYLD floxed progeny that would not contain the neo cassette in the targeted locus.
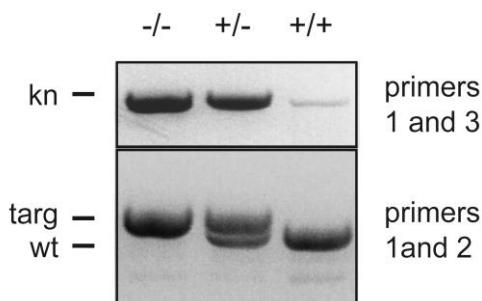
The transmission of the modified cyld allele through the germ line and the removal of the floxed fragment were confirmed by PCR analysis of the mouse tail DNA. Two different combinations of primers were used (see Figure 3 for the position of the primers).The targeted allele is marked as targ, the wild type allele is marked as wt the deleted allele is marked as kn (for knock in of the mutation).

5.2.2 CYLDΔ932 homozygous mouse embryonic fibroblasts express the truncated form of CYLD.

The CYLDΔ932/+ mice obtained as described previously were then mated further in order to produce homozygous mutant progeny. From the first pregnancies embryos were isolated at E13.5 and used for the preparation of mouse embryonic fibroblasts. Wild type, CYLDΔ932/+ and CYLDΔ932 homozygous cells were successfully obtained, cell extracts were prepared and analyzed for the expression of the mutant form of CYLD by immunoblotting with the antibody that specifically binds to the N-terminus of the molecule (not affected by the mutation). In lanes corresponding to mutant MEFs the antibody recognized a faster migrating form of CYLD compared to lanes corresponding to wild type control cells (see Figure 36) consistent with the C-terminal truncation of the protein. In the same experiment we also observed that CYLD protein levels were constitutively lower in mutant cells suggesting that the mutation has an effect on ether the transcription of the gene or on the stability of the respective mRNA/protein.
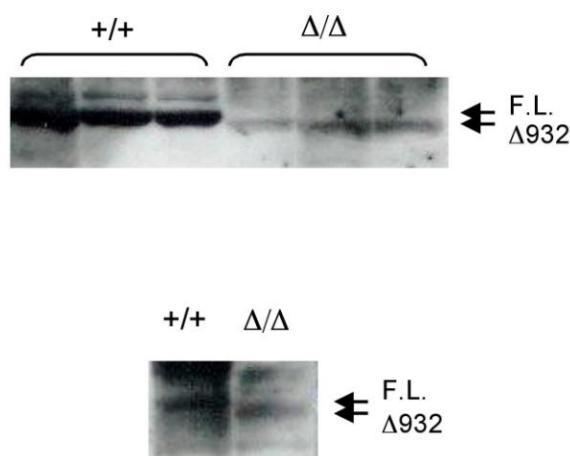
Figure 36: Cell lysates prepared from control and homozygous mutant mouse embryonic fibroblasts were analyzed by immunoblotting with the specific antibody that binds to the N-terminal part of CYLD. Upper panel shows the analysis of 3 different clones of immortalized wild type MEFs (+/+) and 3 different clones of immortalized mutant MEFs (Δ/Δ). Lower panel shows analysis of wild type and

mutant primary MEFs. "F.L." indicated full length CYLD protein; "Δ932" indicates mutant, truncated form of the protein. **-The experiment was performed in collaboration with Dr. Helene Sebban and Dr. Gilles Courtois, INSERM U697, Paris, France.

5.2.3 *CYLDΔ932 homozygous mouse embryonic fibroblasts show elevated NF-κB and JNK activation at steady state and upon stimulation with TNF or IL-1β.*

CYLD deficient cells were demonstrated to show increased activation of NF-κB and MAP kinases in response to pro-inflammatory stimuli. We next wanted to test whether CYLDΔ932 homozygous MEFs would have a similar phenotype. In order to evaluate the activation of NF-κB we first transfected the κB responsive reporter plasmid into control and mutant MEFs and then stimulated these cells with two different pro-inflammatory ligands – TNF and IL-1β. Mutant cells showed elevated expression of the reporter already in non-stimulated state (see Figure 37). The absolute levels of the reporter expression in mutant MEFs were also increased in response to both stimulations while relative induction (compared to the non-stimulated state) was higher in wild type control cells.
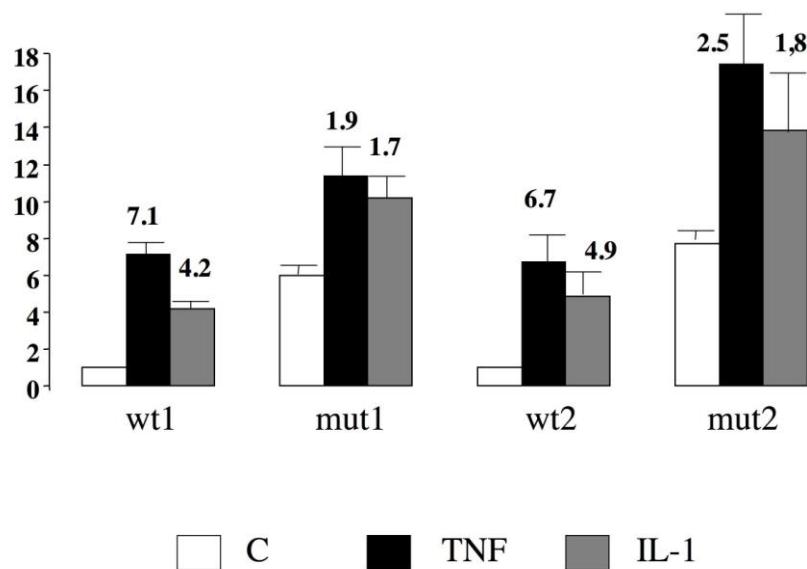
Figure 37: Two different clones of wild type and two different clones of CYLDΔ932 homozygous immortalized mouse embryonic fibroblasts were independently transfected with the plasmid expressing the Igκ luciferase reporter gene. Two days after transfection cells were stimulated with 10 ng/ml TNF and 10 ng/ml IL-1β. Luciferase expression was measured after 4 hours of stimulation. The data is presented as relative luciferase units. The numbers above the bars indicate relative induction

(compared to the non-stimulated state). [**]-The experiment was performed in collaboration with Dr. Helene Sebban and Dr. Gilles Courtois, INSERM U697, Paris, France

In order to evaluate the activation of JNK two clones of wild type and mutant immortalized MEFs were stimulated with TNF. Protein extracts were prepared and analyzed by immunoblotting with the antibody specific for the phosphorylated form of JNK as described previously. We could observe increased phosphorylation of JNK in non-stimulated mutant cells (see Figure 38). The difference between wild type and CYLDΔ932 homozygous MEFs was further enhanced upon stimulation. The experiment was repeated by comparing two other clones of immortalized control MEFs to two other clones of immortalized mutant cells and produced identical results (data not shown). Therefore CYLDΔ932 mutant fibroblasts demonstrated elevated levels of NF-κB and JNK at steady state and upon relevant stimulation consistent with the phenotype of complete knockout cells and the role of CYLD as an inhibitor of TNF signaling through TNFR1 and IL1βR1/TLR signaling.
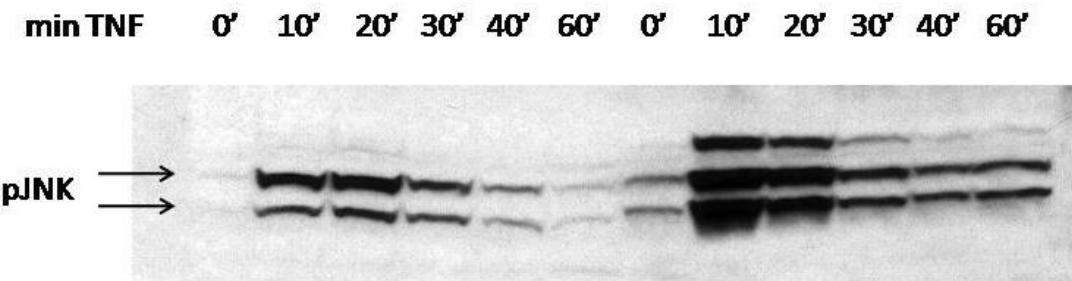
Figure 38: Immortalized wild type and CYLDΔ932 mutant MEFs were stimulated with 10 ng/ml TNF for indicated time points. Total cell extracts were isolated and analyzed by immuniblitting with the antibody specific for the phosphorylated form of JNK as described previously. [**]-The experiment was performed in collaboration with Dr. Helene Sebban and Dr. Gilles Courtois, INSERM U697, Paris, France

5.2.4 CYLDΔ932 homozygous mutant mice die at birth from respiratory distress.

We analyzed a large number of litters coming from *CyldΔ932/+* parents and did not find any homozygous mutant pups surviving until the age of weaning (see Figure 39). At the same time mutant embryos were found at normal mendelian ratio throughout embryogenesis.

Weaning age (8 litters)

	+/+	kn/+	kn/kn
total number	19	37	0
%	33.92	66.07	0
expected %	25	50	25

E12.5 (1 litter)

	+/+	kn/+	kn/kn
total number	4	5	3
%	33.3	41.6	25
expected %	25	50	25

Figure 39. Statistics for the progeny of heterozygous breedings (both parents were heterozygous for the Δ932 mutation) is presented.

Therefore we decided to follow the progeny more closely starting from the very moment of birth. As a result we noticed rapid postnatal death of some pups in almost every litter. The analysis of the genotype revealed that the dying pups were *CyldΔ932* homozygous mutants. In order to identify the precise time and the putative cause of their death we monitored a number of litters obtained by cesarean section at E19.5-E20. We observed that *CyldΔ932* homozygous mutants died within minutes after the operation showing cyanosis and multiple failed attempts to start breathing (data not shown). The control littermates could successfully start breathing under the same conditions. Therefore we hypothesized that the putative cause of the early death of *CyldΔ932* mutants was postnatal respiratory distress.

5.2.5 *CYLDΔ932 homozygous mutant mice show skeletal abnormalities and defects in general body morphology.*

By comparing side by side *CyldΔ932* mutant pups with control littermates we could observe that the mutants were smaller in size and exhibited characteristic deformation of the tail (see Figure 40).
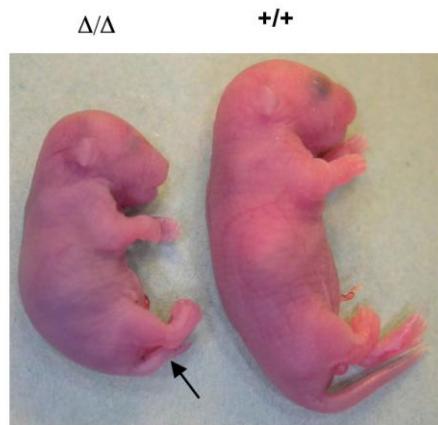
Figure 40: Representative photo of the mutant and the control newborn littermates is presented demonstrating reduced body size of the mutant and the altered shape and length of its tail (indicated with the arrow).

In order to determine whether the altered morphology of mutant mice was caused by skeletal defects we isolated whole skeletons from newborn control and *CyldΔ932* homozygous pups. We then performed specific staining for the bone and the cartilage tissue on isolated skeletons. The staining revealed lack of mineralization of the first three caudal vertebrae of the mutant (see Figure 41). This finding could partly explain the tail phenotype. No other gross alterations of the skeleton could be found in mutant mice.
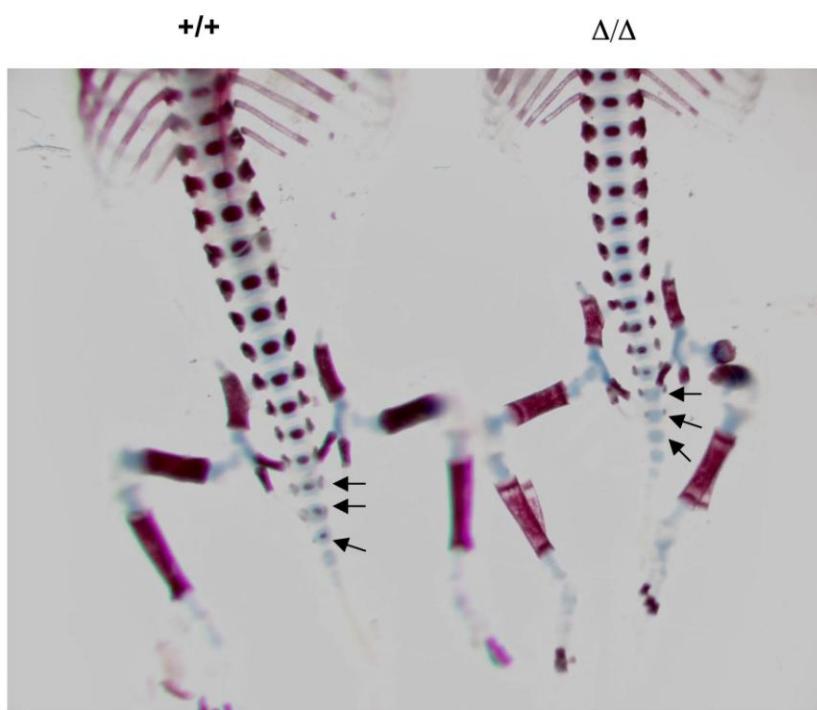
Figure 41: Representative picture of Alcian Blue (cartilage) and Alizarin Red (bone) staining of cleared newborn animals is presented showing the lack of mineralization of caudal vertebrae (indicated with arrows) of CYLDΔ932 homozygous mouse.

6. Discussion.

We successfully generated mice carrying genetic alterations (deletion and point mutation) in genes encoding TNFR1 Associated Death Domain Protein (TRADD) and Familial Cylindromatosis Protein (CYLD). We used our newly generated mouse models to discover the in vivo function of TRADD and CYLD.

6.1 Conditional targeting of TRADD

6.1.1 The role of TRADD in signal transduction through TNFR1.

We generated TRADD deficient mice through inserting LoxP sites on both sides of the coding region of the *tradd* gene via homologous recombination in ES cells, followed by the Cre/LoxP mediated deletion of coding exons in every mouse tissue. TRADD knock out mice were viable, fertile and did not exhibit obvious physiological abnormalities suggesting that the absence of the TRADD protein had no detrimental effect on the development and homeostasis of most mouse tissues.

As TRADD was proposed to be the key adaptor molecule for TNFR1, we studied the response of TRADD deficient primary cells (MEFs and bone marrow derived macrophages) to TNF. We demonstrated that the TNF-mediated activation of NF-κB and MAP kinases could not be blocked by the removal of TRADD, although it was dramatically reduced in mutant cells. The residual response to TNF that was present in TRADD deficient cells was most likely mediated by TNFR1, as TNFR1 -/- cells did not show any activation of indicated cascades in the same experiment. Consistent with the data obtained from primary cells TRADD deficient mice showed increased resistance to the *in vivo* infection with low titers of *Listeria monocytogenes* compared to TNFR1 knockouts demonstrating the ability to induce low levels of TNFR1 mediated anti-bacterial responses. The data lead us to a surprising conclusion that the induction of pro-inflammatory and pro-survival cascades downstream of TNFR1 is still possible in the absence of TRADD. In this respect our results argued against the established model of TNFR1-mediated signaling that puts TRADD in the center of every

response that is initiated by the receptor of interest. It has to be mentioned that some TNFR1 dependant *in vivo* processes do require the presence of TRADD. This was demonstrated by the fact that TRADD deficient mice had altered morphology of secondary lymphoid organs and produced lower titers of antibodies upon immunization with sheep red blood cells similar to TNFR1 deficient animals.

It was previously demonstrated that the activation of NF-κB and MAP kinases by TNFR1 required TNF-dependant recruitment of RIP1 and TRAF2 into a complex associated with the cytoplasmic part of the receptor. TRAF2 catalyzes K63 poly-ubiquitination of RIP1 creating a platform for the recruitment of the IKK complex and the complex containing a potent kinase TAK1. It had been postulated that TRADD could interact with RIP1 via the C-terminal death domain and with TRAF2 via the N-terminal TRAF binding domain. Therefore TRADD could putatively serve as a linker that brings together RIP1 and TRAF2 at the cytoplasmic part of TNFR1 upon ligand binding. In order to understand whether TRAF2 or RIP1 could still be recruited to the receptor in the absence of TRADD we isolated and analyzed complexes that were associated with TNFR1 from TNF stimulated control and TRADD deficient mouse embryonic fibroblasts. While TRAF2 failed to associate with TNFR1 in TRADD deficient cells, residual amounts of RIP1 were still recruited to the receptor in a TNF dependant manner. We also found that receptor-associated RIP1 in control cells was running on a gel as multiple bands consistent with previously reported posttranslational modifications of the molecule within the TNFR1 associated signaling complex. RIP1 was not modified in TRADD deficient cells. As the lack of modification of RIP1 correlated with the absence of TRAF2 from TRADD deficient TNFR1 proximal complexes, it was likely that the missing modification represented TRAF2 mediated poly-ubiquitination of RIP1.

Thus we have demonstrated that TNF stimulation of TRADD deficient cells results in association of a small amount of RIP1 with the cytoplasmic part of TNFR1 while TRAF2 is not recruited to the receptor. The first finding is consistent with previous reports suggesting that RIP1 could directly bind to TNFR1 via the death domain-to-death domain interaction. We also determined that TNFR1-associated RIP1 is not modified in TRADD knockout cells

upon TNF induction. As discussed previously the modification of RIP1 that is missing in TNF-stimulated TRADD deficient cells is likely to be K63-linked polyubiquitination mediated by TRAF2. K63-linked ubiquitination of RIP1 is known to play a key role in TNFR1-mediated signaling by facilitating the recruitment and activation of IKKs as well as the complex containing Transforming growth factor-β-activated kinase 1 (TAK1) – the upstream mediator of NF-κB and MAP kinase induction. It is therefore likely that the impairment of TNF-induced pro-inflammatory and pro-survival signaling observed in TRADD -/- cells is due to the lack of TAK1 activity caused by the putative absence of K63-linked ubiquitination of RIP1. Another factor that may contribute to the observed effect could be the lack of TRAF2-mediated ubiquitination of IKK (IκB Kinase complex) members and upstream MAP kinases. Such ubiquitination has been described as essential for the efficient activation of downstream cascades. Nevertheless TRADD deficient cells show low levels of NF-κB and MAPK induction upon treatment with TNF. Since RIP1 is recruited to TNFR1 in TNF-stimulated TRADD knockout cells we suggest that the residual pro-inflammatory and pro-survival signaling could be mediated by the kinase activity of RIP1 or by putative interaction partners of RIP1 that are currently not known.

In addition to inducing gene expression through the activation of NF-κB and MAP kinases, TNFR1 also mediates death via FADD-caspase-8 signaling axis. We did our first experiments in order to understand whether TRADD was essential for the pro-apoptotic branch of TNFR1 signaling using mouse embryonic fibroblasts (MEFs) as a model system. It is well known that TNF stimulation doesn't lead to death of MEFs because these cells are strongly protected by the expression of pro-survival genes that are activated by TNF in parallel to the induction of apoptosis. Therefore in order to study TNF-induced apoptosis in this cellular system the cytokine has to be given in combination with an inhibitor of gene expression. In our experiments we simultaneously treated cells with TNF and cycloheximide – a blocker of protein biosynthesis. The microscopical analysis of cultures that was performed 24 hours later demonstrated that TRADD deficient MEFs were protected from TNF-induced death. We then assessed the degree of such protection by quantifying the amount of living cells in TRADD-/-, TNFR1-/- and wild type cultures at 12 hours of stimulation with TNF/CHX. The deficiency for TNFR1 is known to block the TNF-induced apoptosis in respective mutant cells. Similar numbers of TRADD -/- and TNFR1 -/- cells survived the treatment. From this

result we concluded that programmed cell death that is mediated by TNFR1 is likely to be impaired in cells lacking TRADD. In order to prove this hypothesis we evaluated the presence of known markers of apoptosis such as activated caspase-8 and activated caspase-3 in lysates that were prepared from TRADD deficient and wild type MEFs after 6 hours of stimulation with TNF/CHX. While both markers were present in extracts that were obtained from wild type cells, no induction of apoptosis could be observed in case of the mutants. It was already suggested by previous reports that FADD and caspase-8 were most likely recruited to TNFR1 through interaction with TRADD. Our data provides the solid genetic proof for this hypothesis.

We next decided to test whether the ability of TRADD to block TNF induced apoptosis had an impact on the systemic toxicity of the cytokine. For that we subjected TRADD deficient and control mice to a TNF/β-GalN model of TNF-induced liver failure. β-GalN (galactosamine) inhibits gene expression in hepatocytes by depleting cellular UTP and therefore sensitizes these cells to TNF-induced killing. Simultaneous treatment with galactosamine and TNF is a well established mouse model of cytokine induced acute hepatitis. We found that wild type animals that were injected with TNF/β-GalN exhibited signs of severe liver damage and died at expected times while TRADD -/- mice survived the treatment. We also could not detect elevated levels of liver enzymes (this parameter was used to asses liver damage) in the serum that was collected from mutant animals. The liver damage in TNF/β-GalN model is caused by massive TNF-induced apoptosis of hepatocytes. We next evaluated the presence of activated caspases in liver extracts that were obtained from wild type and TRADD deficient mice 8 hours after injection with TNF/β-GalN. We could observe clear induction of programmed cell death in wild type livers while no apoptosis could be detected in livers that were collected from mutant mice. Therefore we concluded that the lack of TRADD protein protects cells and tissues from TNF induced death both *in vitro* and at the systemic level.

6.1.1.1 Summary.
With respect to the role of TRADD in TNF mediated signaling we have clearly demonstrated
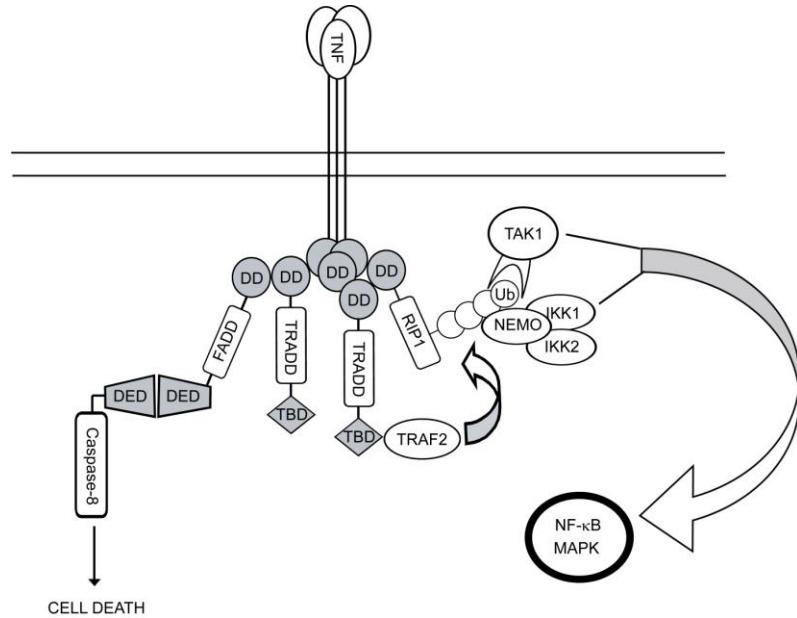
Figure 42: The role of TRADD in signaling via TNFR1. Summary of the model.

that TRADD is indispensable for the induction of apoptosis and is needed for the optimal activation of NF-κB and MAP kinases downstream of TNFR1.

In the absence of TRADD residual NF-κB and MAPK activation in response to TNF can still occur. Such activation is most likely mediated by TNFR1 via RIP1. RIP1 could still be recruited to the cytoplasmic part of the receptor in the absence of TRADD. Although it has been suggested in the past that RIP1 was able to directly bind to the death domain of TNFR1 in a TNF dependant manner, our study is first to provide a possible proof and to give the physiological meaning to this putative interaction.

We demonstrated that TRAF2 couldn't be recruited to TNFR1 in the absence of TRADD. The absence of TRAF2 correlated with the loss of modified forms of the receptor-associated RIP1 and with the reduction in TNF-induced activation of NF-κB and MAP kinases. We suggest that the unmodified RIP1 loses the ability to recruit TAK1, the upstream kinase for MAPKKs and the members of the IKK complex. The absence of TAK1 in combination with the lack of TRAF2-mediated ubiquitination of IKKs and other downstream mediators results

in impaired activation of NF-κB and MAP kinases in TRADD deficient cells (see Figure 42 for the summary of the model).

6.1.1.2 Conclusion and future directions.

The finding that TNFR1 can't induce cell death but still transmits reduced pro-inflammatory and pro-survival signal in the absence of TRADD is new and very interesting. It appears particularly intriguing in light of the important role of the TNF-TNFR1 signaling pair in the pathogenesis of pro-inflammatory and degenerative disorders. In many cases it could be beneficial to specifically block apoptosis mediated by TNFR1 without blocking TNF-induced activation of gene expression that is needed for the proper establishment of immune response against a wide variety of pathogens. In other pathologies the reduction of the excessive pro-inflammatory response mediated by TNF could improve the clinical picture of the disease while a complete block of TNF-induced gene expression could be harmful due to its important role in controlling the destructive behavior of immune cells. In the future we plan to investigate in more detail the effect of TRADD deficiency on the pathogenesis of autoimmune and inflammatory disorders and on the immune response against specific pathogens.

6.1.2   The role of TRADD in signal transduction through TLR3 and TLR4.

We tested the putative involvement of TRADD in pro-inflammatory cascades other then TNF signaling and to our surprise found that TRADD deficient mice had reduced responses to *in vivo* stimulation with ligands for Toll like receptors 3 and 4 but not Toll like receptor 9. These findings lead us to think that TRADD may play a role in TRIF-dependant TLR signaling (the adaptor TRIF is involved specifically in signal transduction via TLR3 and TLR4). In order to test this hypothesis we performed experiments in primary mouse embryonic fibroblasts and splenocytes isolated from control and mutant mice. We could show reduced cytokine production and impaired activation of NF-κB and MAP kinases in TRADD deficient cells stimulated with the TLR3 ligand poly(I:C). This result favored our hypothesis but we first had to evaluate whether the effect of TRADD was direct or whether it was due to inhibition of the secondary stimulation of cells by TNF. TNF is rapidly produced by cells in response to TLR stimulation. It is secreted into the culture medium and is able to

act on cells in the autocrine manner. To rule out the TNF-dependency of the phenotype of poly(I:C) stimulated TRADD knockout animals and cells we compared the response of TRADD deficient and TNFR1 deficient mice to the *in vivo* stimulation with poly(I:C). TNFR1 deficient mice did not show reduction of serum TNF levels upon poly(I:C) injection, moreover they produced more cytokine compared to wild type control mice that were stimulated in parallel. Therefore it was likely that the deficiency of TRADD directly impaired initial steps of polyI:C mediated signaling.

From our in vivo data we could see that the impact of TRADD deficiency on TLR4 signaling was milder then the impact on TLR3 signaling. Unlike TLR3 that entirely relies on TRIF, TLR4 signals via two adaptors – TRIF and Myd88. Therefore we speculated that the impact of TRADD on TLR4/TRIF cascade could not be clearly seen due to compensatory effect of TLR4/Myd88 cascade. In order to test this hypothesis we generated mice that were double deficient for TRADD and Myd88. Myd88 knockout mice show severe impairment of cytokine production in response to *in vivo* stimulation with LPS. Nevertheless they still produce measurable amounts of cytokines including TNF. We could show that unlike Myd88 deficient TRADD/Myd88 double deficient mice did not produce TNF upon intraperitoneal injection of LPS. Consistent with this result LPS-stimulated TRADD/Myd88 double knockout MEFs presented a more severe phenotype in terms of reduction in NF-κB and MAPK activation compared to Myd88 knockout cells. Therefore TRADD was likely to play a role in TRIF dependant TLR signaling via a yet unknown mechanism.

It was previously reported that RIP1 was essential for the activation of NF-κB by Toll like receptors 3 and 4 in mouse embryonic fibroblasts. In both cases RIP1 was recruited to the receptor via the TLR adaptor TRIF. It was demonstrated that RIP1 was poly-ubiquitinated in response to TLR3 ligand polyI:C. However, the molecular mechanism that linked RIP1 to NF-κB activation in case of TLR signaling was never clarified.

It was demonstrated that the activation of NF-κB by RIP1-independent branch of TLR3 and TLR4 signaling relied on the K63 self-ubiquitination of TRAF6 and subsequent recruitment of TAK1. Poly-ubiquitinated RIP1 is also capable of recruiting TAK1 as it was demonstrated for TNFR1 mediated signaling. It is known that in response to TNF RIP1 undergoes K63

poly-ubiquitination that is mediated by TRAF2. Our previous data indicated that TRADD acts as a bridge linking TRAF2 and RIP1 at the cytoplasmic part of TNFR1 upon ligand binding. The death domain of RIP1 is not involved in binding to TRIF. Therefore it can be used for interaction with other death domain containing molecules. TRADD is one of such molecules. As it was previously demonstrated that RIP1 is able to interact with TRADD we speculated that TRADD could be recruited to RIP1 upon TLR stimulation. TRADD could then recruit TRAF2, a known ubiquitn ligase for RIP1, via the N-terminal TRAF binding domain. This putative mechanism could explain how RIP1 gets poly-ubiquitinated in response to polyI:C or LPS.

We next did experiments in order to evaluate whether TRADD could interact with TRIF and whether RIP1 was a linker between the two of them as we hypothesized previously. We co-expressed tagged RIP1, TRADD and TRIF in HEK293 cells. We then prepared extracts from these cells and used them for precipitation with the antibody specific for the tagged TRADD. We analyzed precipitates by Western blot and could determine that RIP1 and TRIF interacted with TRADD. Moreover TRADD and TRIF also interacted with one another in the absence of RIP1 over-expression putatively due to the presence of the endogenous RIP1 in the cells. In order to prove that RIP1 was a necessary link between TRIF and TRADD we generated a knock down of RIP1 by transfecting HEK293 cells with the vector that expressed siRNA that was specific for RIP1. Consistent with our hypothesis, the interaction between TRIF and TRADD was dramatically reduced in RIP1 knock down cells. TRIF and TRADD could not interact in cells overexpressing the mutated form of RIP1 that was lacking the death domain in agreement with our hypothesis about the key role of the death domain of RIP1 in recruiting TRADD to TLR3 and 4 upon stimulation with respective ligands.

6.1.2.1 Summary.
We observed impaired production of TNF by TRADD deficient mice upon *in vivo* stimulation with the TLR3 ligand poly(I:C). Consistent with this observation TRADD knockout primary cells showed impaired activation of NF-κB and MAP kinases along with reduced cytokine production in response to poly(I:C). TRADD/Myd88 double knockout mice and primary cells exhibited more severe impairment of TLR4 signaling compared to Myd88 single knockout cells and animals. In summary these results were indicative of the

involvement of TRADD in TRIF-dependant TLR signaling. We hypothesized that the RIP1-dependant activation of NF-κB and MAP kinases downstream of TLR3 and TLR4 involves the association between RIP1, TRADD and TRAF2 and thereby depends on the presence of TRADD. We demonstrated that TRADD was recruited to the TLR3/4 adaptor TRIF via interaction with the death domain of RIP1 (see Figure 43 for the summary of the model).
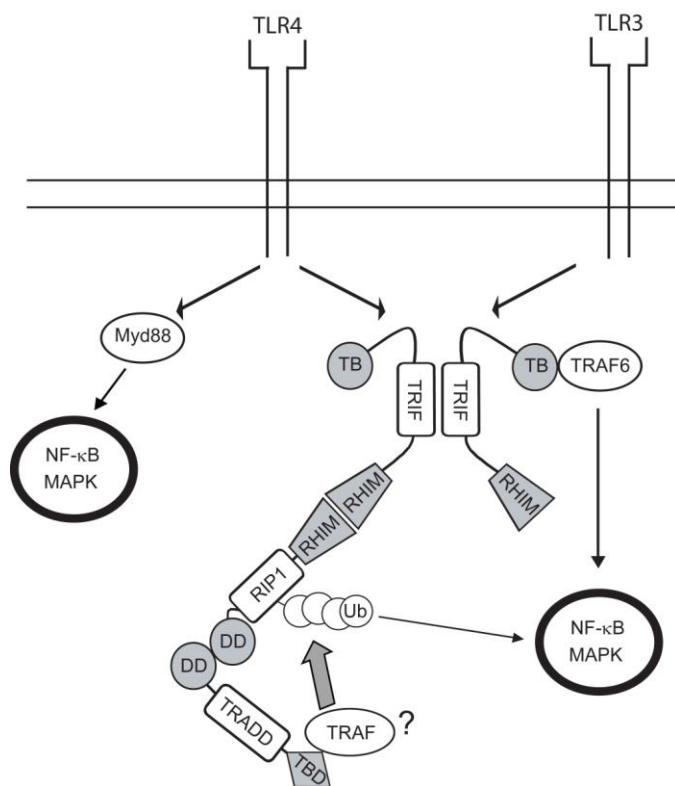
Figure 43: The role of TRADD in signaling via TLR3. Summary of the model.

6.1.2.2 Conclusion and future directions.

We demonstrated that the role of TRADD in immune and inflammatory processes is not restricted to events that are related to TNF-TNFR1 mediated signaling. We showed that TRADD participates in signal transduction through Toll like receptors 3 and 4. TRADD is recruited to the TLR3/4 adaptor TRIF via RIP1. Based on the fact that RIP1 gets poly-ubiquitinated in response to TLR stimulation and on the fact that TRADD links RIP1 and the ubiquitin ligase TRAF2 at the cytoplasmic part of TNFR1, we suggest that the TRADD/RIP1/TRAF2 interaction may be mediating the RIP1 dependant branch of TLR signaling.

In the future we plan to subject TRADD -/- mice to *in vivo* models that depend on TLR3 and TLR4 signaling in order to investigate whether the deficiency for TRADD will have a relevant effect at the systemic level. We finally plan to test whether TRADD will have an effect on the NF-κB activation via other signaling cascades that are known to involve RIP-1 or may involve RIP-1 such as induction of gene expression through the PIDDosome in response to the DNA damage or RIG-I/MDA-5 mediated gene expression.

6.2   Conditional targeting of CYLD

CYLD is a deubiquitinating enzyme that was originally identified as a tumor supressor mutated in Brooke-Spiegler syndrome (BSS), an autosomal dominant disorder predisposing to multiple tumors that express features of different skin appendages. It was proposed that in BSS the mutation of the *CYLD* gene targets processes that are involved in proliferation and differentiation of epidermal stem cells.

In vitro studies demonstrated that CYLD inhibits NF-kB activation downstream of TNFR superfamily members (and potentially members of other families of receptors) by acting on targets such as TRAF2, TRAF6 and NEMO. Other studies suggested that CYLD acts as a negative regulator of mitogen-activated protein (MAP) kinase activation.

The generation of CYLD deficient mice confirmed the *in vitro* data and revealed additional functions of the molecule. It was demonstrated that CYLD is required for the T-cell receptor signaling and timely entry of cells into mitosis. CYLD deficient mice were viable and fertile despite the putative defect in spermatogenesis. Although none of the reported CYLD knock out mouse lines demonstrated an overt phenotype careful examination revealed putative alterations of T and B lymphocyte development as well as susceptibility to pro-inflammatory stimuli and induced tumorogenesis.

At the time our project started no CYLD deficient mouse was generated yet and therefore the *in vivo* role of the molecule was still enigmatic. It was not clear whether the mammalian

organism could develop and function in the absence of CYLD, as individuals affected by the Brooke-Spiegler syndrome were missing CYLD activity only in tumors while in the rest of the body it was still present.

We kept in mind that none of different CYLD mutations isolated from BSS patients led to the complete absence of the molecule. Instead such mutations led to the expression of C-terminal truncations of CYLD that still contained domains involved in protein-protein interactions but missed the catalytic function. After carefully evaluating a number of options we decided to make use of the Cre / LoxP system in order to introduce a mutation that was isolated from human BSS patients into a mouse genome in a conditional manner. The mutation of choice signals termination of CYLD mRNA translation at amino acid 932 (out of 953) and therefore leads to the truncation of last 20 C-terminal amino acids of the protein containing a conserved motif essential for the enzymatic function of CYLD (see Figure 44). We then planned to evaluate the effect of the mutation at the level of the whole organism and to study cell-specific effects by taking advantage of the conditional approach.
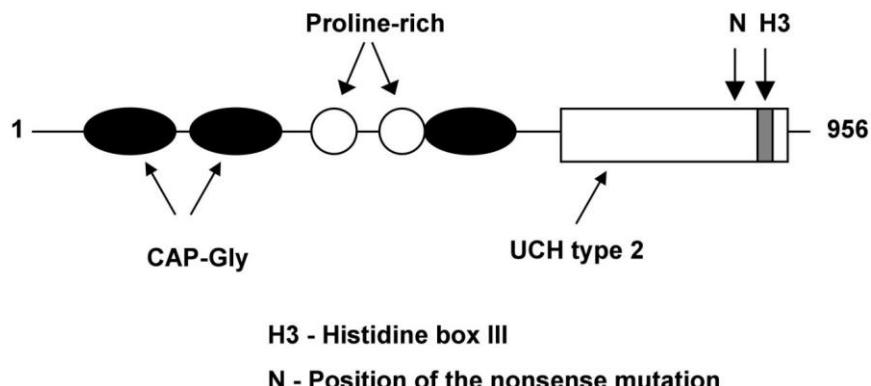
Figure 44: The schematic of the human CYLD, showing the domain structure of the protein and the position of the mutation of interest.

We utilized homologous recombination in murine embryonic stem cells to introduce a modified *cyld* allele into the mouse genome and generated *CYLDΔ932* heterozygous animals by crossing mice that carried the targeted *cyld* allele in the germline to a Cre-deleter mouse strain. *CYLDΔ932* heterozygous mice did not exhibit obvious defects.

We then tried to obtain *CYLDΔ932* homozygous mice by crossing heterozygous parents and discovered that homozygous mutants died within minutes after birth showing features of respiratory distress. *CYLDΔ932* homozygous pups were smaller then heterozygous or wild type littermates and exhibited a characteristic tail deformation. We confirmed the expression of the truncated form of CYLD in *CYLDΔ932* mutant cells by Western blot analysis.

The size and the shape of the tail along with the lack of mineralization of the first three caudal vertebrae were the only visible alterations we could report in homozygous mutant mice as a result of the preliminary analysis. The finding that the phenotype of the *CYLDΔ932* mutant was early postnatal lethal surprised us since it was previously demonstrated by a number of independent research groups that CYLD deficient mice had a very minor phenotype.

The absence of the CYLD enzymatic activity in a limited population of cells leads to dramatic consequences in human BSS patients. In this context the lack of an overt phenotype in all previously reported CYLD deficient mice appeared surprising and somewhat disappointing. It did lead us to think that despite the fair amount of potential targets identified *in vitro* and *in vivo* CYLD rather controls a restricted number of specific processes then being essential for the overall homeostasis. Another phenomenon explaining the relatively mild phenotype of knock out mice would be the existence of an enzyme with similar properties that could take over certain functions in CYLD deficient cells. If that were true one would imagine that CYLD has higher affinity to its specific targets compared to the unknown substituting enzyme. Therefore one could speculate that the expression of the catalytically inactive form of CYLD would produce a more dramatic phenotype in comparison to the complete absence of the protein. The product of the *CYLDΔ932* allele is lacking enzymatic function; at the same time its large N-terminal portion responsible for the interaction with target proteins is not affected by the mutation. Unlike CYLD deficiency, homozygousity for the *CYLDΔ932* allele results in growth retardation, skeletal abnormalities and early postnatal lethality in mice. At the same time we have demonstrated that certain phenomena such as enhanced activation of NF-κB and JNK are shared by knock out and mutant cells. Overall the

CYLDΔ932 mutation appears to produce a stronger phenotype compared to the complete lack of the CYLD protein putatively due to its potential dominant negative nature.

The surprisingly strong phenotype of *CYLDΔ932* mutant suggests that the *in vivo* role of CYLD must go beyond the previously suggested involvement in immune and inflammatory processes. We plan to cross the *CYLDΔ932* floxed mice to transgenic mice expressing Cre recombinase under control of tissue specific promoters in order to learn about the physiological role of CYLD in particular organs and cell types.

7. **Bibliography.**

1.   Carswell, E.A., et al., *An end toxin-induced serum factor that causes necrosis of tumors.* Proc Natl Acad Sci U S A, 1975. **72**(9): p. 3666-70.

2.   Takeda, K., et al., *Identity of differentiation inducing factor and tumour necrosis factor.* Nature, 1986. **323**(6086): p. 338-40.

3.   Beutler, B., et al., *Identity of tumour necrosis factor and the macrophage-secreted factor cachectin.* Nature, 1985. **316**(6028): p. 552-4.

4.   Fried, S.K. and R. Zechner, *Cachectin/tumor necrosis factor decreases human adipose tissue lipoprotein lipase mRNA levels, synthesis, and activity.* J Lipid Res, 1989. **30**(12): p. 1917-23.

5.   Beutler, B. and A. Cerami, *The biology of cachectin/TNF--a primary mediator of the host response.* Annu Rev Immunol, 1989. **7**: p. 625-55.

6.   Beutler, B.A., *Orchestration of septic shock by cytokines: the role of cachectin (tumor necrosis factor).* Prog Clin Biol Res, 1989. **286**: p. 219-35.

7.   Hotamisligil, G.S. and B.M. Spiegelman, *Tumor necrosis factor alpha: a key component of the obesity-diabetes link.* Diabetes, 1994. **43**(11): p. 1271-8.

8.   Holtmann, M.H. and M.F. Neurath, *Differential TNF-signaling in chronic inflammatory disorders.* Curr Mol Med, 2004. **4**(4): p. 439-44.

9.   MacEwan, D.J., *TNF ligands and receptors--a matter of life and death.* Br J Pharmacol, 2002. **135**(4): p. 855-75.

10.   Collart, M.A., P. Baeuerle, and P. Vassalli, *Regulation of tumor necrosis factor alpha transcription in macrophages: involvement of four kappa B-like motifs and of constitutive and inducible forms of NF-kappa B.* Mol Cell Biol, 1990. **10**(4): p. 1498-506.

11.   Preischl, E.E., et al., *Induction of the TNF-alpha promoter in the murine dendritic cell line 18 and the murine mast cell line CPII is differently regulated.* J Immunol, 1996. **157**(6): p. 2645-53.

12.   Jue, D.M., et al., *Processing of newly synthesized cachectin/tumor necrosis factor in endotoxin-stimulated macrophages.* Biochemistry, 1990. **29**(36): p. 8371-7.

13.   Black, R.A., et al., *A metalloproteinase disintegrin that releases tumour-necrosis factor-alpha from cells.* Nature, 1997. **385**(6618): p. 729-33.

14.   Moss, M.L., et al., *Cloning of a disintegrin metalloproteinase that processes precursor tumour-necrosis factor-alpha.* Nature, 1997. **385**(6618): p. 733-6.

15.   Kriegler, M., et al., *A novel form of TNF/cachectin is a cell surface cytotoxic transmembrane protein: ramifications for the complex physiology of TNF.* Cell, 1988. **53**(1): p. 45-53.

16.   Mohler, K.M., et al., *Protection against a lethal dose of endotoxin by an inhibitor of tumour necrosis factor processing.* Nature, 1994. **370**(6486): p. 218-20.

17.   Solorzano, C.C., et al., *Involvement of 26-kDa cell-associated TNF-alpha in experimental hepatitis and exacerbation of liver injury with a matrix metalloproteinase inhibitor.* J Immunol, 1997. **158**(1): p. 414-9.

18.   Brockhaus, M., et al., *Identification of two types of tumor necrosis factor receptors on human cell lines by monoclonal antibodies.* Proc Natl Acad Sci U S A, 1990. **87**(8): p. 3127-31.

19.   Loetscher, H., et al., *Molecular cloning and expression of the human 55 kd tumor necrosis factor receptor.* Cell, 1990. **61**(2): p. 351-9.

20.   Schall, T.J., et al., *Molecular cloning and expression of a receptor for human tumor necrosis factor.* Cell, 1990. **61**(2): p. 361-70.

21.   Dembic, Z., et al., *Two human TNF receptors have similar extracellular, but distinct intracellular, domain sequences.* Cytokine, 1990. **2**(4): p. 231-7.

22.   Tartaglia, L.A., et al., *A novel domain within the 55 kd TNF receptor signals cell death.* Cell, 1993. **74**(5): p. 845-53.

23.   Hsu, H., J. Xiong, and D.V. Goeddel, *The TNF receptor 1-associated protein TRADD signals cell death and NF-kappa B activation.* Cell, 1995. **81**(4): p. 495-504.

24.   Hsu, H., et al., *TRADD-TRAF2 and TRADD-FADD interactions define two distinct TNF receptor 1 signal transduction pathways.* Cell, 1996. **84**(2): p. 299-308.

25.   Hsu, H., et al., *TNF-dependent recruitment of the protein kinase RIP to the TNF receptor-1 signaling complex.* Immunity, 1996. **4**(4): p. 387-96.

26.   Rothe, M., et al., *A novel family of putative signal transducers associated with the cytoplasmic domain of the 75 kDa tumor necrosis factor receptor.* Cell, 1994. **78**(4): p. 681-92.

27.   Rothe, M., et al., *TRAF2-mediated activation of NF-kappa B by TNF receptor 2 and CD40.* Science, 1995. **269**(5229): p. 1424-7.

28.   Liu, Z.G., et al., *Dissection of TNF receptor 1 effector functions: JNK activation is not linked to apoptosis while NF-kappaB activation prevents cell death.* Cell, 1996. **87**(3): p. 565-76.

29.   Boone, E., et al., *Activation of p42/p44 mitogen-activated protein kinases (MAPK) and p38 MAPK by tumor necrosis factor (TNF) is mediated through the death domain of the 55-kDa TNF receptor.* FEBS Lett, 1998. **441**(2): p. 275-80.

30.   Jupp, O.J., et al., *Type II tumour necrosis factor-alpha receptor (TNFR2) activates c-Jun N-terminal kinase (JNK) but not mitogen-activated protein kinase (MAPK) or p38 MAPK pathways.* Biochem J, 2001. **359**(Pt 3): p. 525-35.

31.   Pan, S., et al., *Etk/Bmx as a tumor necrosis factor receptor type 2-specific kinase: role in endothelial cell migration and angiogenesis.* Mol Cell Biol, 2002. **22**(21): p. 7512-23.

32.   Bigda, J., et al., *Dual role of the p75 tumor necrosis factor (TNF) receptor in TNF cytotoxicity.* J Exp Med, 1994. **180**(2): p. 445-60.

33.   Shalaby, M.R., et al., *Binding and regulation of cellular functions by monoclonal antibodies against human tumor necrosis factor receptors.* J Exp Med, 1990. **172**(5): p. 1517-20.

34.   Erickson, S.L., et al., *Decreased sensitivity to tumour-necrosis factor but normal T-cell development in TNF receptor-2-deficient mice.* Nature, 1994. **372**(6506): p. 560-3.

35.   Medvedev, A.E., A. Sundan, and T. Espevik, *Involvement of the tumor necrosis factor receptor p75 in mediating cytotoxicity and gene regulating activities.* Eur J Immunol, 1994. **24**(11): p. 2842-9.

36.   Li, X., Y. Yang, and J.D. Ashwell, *TNF-RII and c-IAP1 mediate ubiquitination and degradation of TRAF2.* Nature, 2002. **416**(6878): p. 345-7.

37.   Cho, S.G. and E.J. Choi, *Apoptotic signaling pathways: caspases and stress-activated protein kinases.* J Biochem Mol Biol, 2002. **35**(1): p. 24-7.

38.   Pfeffer, K., et al., *Mice deficient for the 55 kd tumor necrosis factor receptor are resistant to endotoxic shock, yet succumb to L. monocytogenes infection.* Cell, 1993. **73**(3): p. 457-67.

39.   Mukhopadhyay, A., et al., *Genetic deletion of the tumor necrosis factor receptor p60 or p80 abrogates ligand-mediated activation of nuclear factor-kappa B and of mitogen-activated protein kinases in macrophages.* J Biol Chem, 2001. **276**(34): p. 31906-12.

40.   Vandenabeele, P., et al., *Two tumour necrosis factor receptors: structure and function.* Trends Cell Biol, 1995. **5**(10): p. 392-9.

41.   Grell, M., et al., *The transmembrane form of tumor necrosis factor is the prime activating ligand of the 80 kDa tumor necrosis factor receptor.* Cell, 1995. **83**(5): p. 793-802.

42.   Pasparakis, M., et al., *Immune and inflammatory responses in TNF alpha-deficient mice: a critical requirement for TNF alpha in the formation of primary B cell follicles, follicular dendritic cell networks and germinal centers, and in the maturation of the humoral immune response.* J Exp Med, 1996. **184**(4): p. 1397-411.

43.   Pasparakis, M., et al., *Peyer's patch organogenesis is intact yet formation of B lymphocyte follicles is defective in peripheral lymphoid organs of mice deficient for tumor necrosis factor and its 55-kDa receptor.* Proc Natl Acad Sci U S A, 1997. **94**(12): p. 6319-23.

44.   Malaviya, R., et al., *Mast cell modulation of neutrophil influx and bacterial clearance at sites of infection through TNF-alpha.* Nature, 1996. **381**(6577): p. 77-80.

45.   Matsushima, H., et al., *TLR3-, TLR7-, and TLR9-mediated production of proinflammatory cytokines and chemokines from murine connective tissue type skin-derived mast cells but not from bone marrow-derived mast cells.* J Immunol, 2004. **173**(1): p. 531-41.

46.   Paleolog, E.M., et al., *Functional activities of receptors for tumor necrosis factor-alpha on human vascular endothelial cells.* Blood, 1994. **84**(8): p. 2578-90.

47.   Smart, S.J. and T.B. Casale, *TNF-alpha-induced transendothelial neutrophil migration is IL-8 dependent.* Am J Physiol, 1994. **266**(3 Pt 1): p. L238-45.

48.   Moll, H., *Dendritic cells and host resistance to infection.* Cell Microbiol, 2003. **5**(8): p. 493-500.

49.   Rahman, M.M. and G. McFadden, *Modulation of tumor necrosis factor by microbial pathogens.* PLoS Pathog, 2006. **2**(2): p. e4.

50.   Bean, A.G., et al., *Structural deficiencies in granuloma formation in TNF gene-targeted mice underlie the heightened susceptibility to aerosol Mycobacterium tuberculosis infection, which is not compensated for by lymphotoxin.* J Immunol, 1999. **162**(6): p. 3504-11.

51.   Ehlers, S., et al., *Lethal granuloma disintegration in mycobacteria-infected TNFRp55-/- mice is dependent on T cells and IL-12.* J Immunol, 2000. **165**(1): p. 483-92.

52.   Zakharova, M. and H.K. Ziegler, *Paradoxical anti-inflammatory actions of TNF-alpha: inhibition of IL-12 and IL-23 via TNF receptor 1 in macrophages and dendritic cells.* J Immunol, 2005. **175**(8): p. 5024-33.

53.   Van Deventer, S.J., *Tumour necrosis factor and Crohn's disease.* Gut, 1997. **40**(4): p. 443-8.

54.   Feldmann, M. and R.N. Maini, *Anti-TNF alpha therapy of rheumatoid arthritis: what have we learned?* Annu Rev Immunol, 2001. **19**: p. 163-96.

55.   Lee, D.M., et al., *Mast cells: a cellular link between autoantibodies and inflammatory arthritis.* Science, 2002. **297**(5587): p. 1689-92.

56.   Wang, J.Y. and M.H. Roehrl, *Glycosaminoglycans are a potential cause of rheumatoid arthritis.* Proc Natl Acad Sci U S A, 2002. **99**(22): p. 14362-7.

57.   Bischoff, S.C., et al., *Mast cells are an important cellular source of tumour necrosis factor alpha in human intestinal tissue.* Gut, 1999. **44**(5): p. 643-52.

58.   Kontoyiannis, D., et al., *Impaired on/off regulation of TNF biosynthesis in mice lacking TNF AU-rich elements: implications for joint and gut-associated immunopathologies.* Immunity, 1999. **10**(3): p. 387-98.

59.   Ji, H., et al., *Critical roles for interleukin 1 and tumor necrosis factor alpha in antibody-induced arthritis.* J Exp Med, 2002. **196**(1): p. 77-85.

60.   Gordon, C. and D. Wofsy, *Effects of recombinant murine tumor necrosis factor-alpha on immune function.* J Immunol, 1990. **144**(5): p. 1753-8.

61.   Wu, A.J., et al., *Tumor necrosis factor-alpha regulation of CD4+CD25+ T cell levels in NOD mice.* Proc Natl Acad Sci U S A, 2002. **99**(19): p. 12287-92.

62.   Jacob, C.O. and H.O. McDevitt, *Tumour necrosis factor-alpha in murine autoimmune 'lupus' nephritis.* Nature, 1988. **331**(6154): p. 356-8.

63.   Gordon, C., et al., *Chronic therapy with recombinant tumor necrosis factor-alpha in autoimmune NZB/NZW F1 mice.* Clin Immunol Immunopathol, 1989. **52**(3): p. 421-34.

64.   Kassiotis, G., et al., *A tumor necrosis factor-induced model of human primary demyelinating diseases develops in immunodeficient mice.* Eur J Immunol, 1999. **29**(3): p. 912-7.

65.   Kassiotis, G., et al., *TNF accelerates the onset but does not alter the incidence and severity of myelin basic protein-induced experimental autoimmune encephalomyelitis.* Eur J Immunol, 1999. **29**(3): p. 774-80.

66.   *TNF neutralization in MS: results of a randomized, placebo-controlled multicenter study. The Lenercept Multiple Sclerosis Study Group and The University of British Columbia MS/MRI Analysis Group.* Neurology, 1999. **53**(3): p. 457-65.

67.   Kassiotis, G. and G. Kollias, *Uncoupling the proinflammatory from the immunosuppressive properties of tumor necrosis factor (TNF) at the p55 TNF receptor level: implications for pathogenesis and therapy of autoimmune demyelination.* J Exp Med, 2001. **193**(4): p. 427-34.

68.   Azuma, Y., et al., *Tumor necrosis factor-alpha induces differentiation of and bone resorption by osteoclasts.* J Biol Chem, 2000. **275**(7): p. 4858-64.

69.   Leibovich, S.J., et al., *Macrophage-induced angiogenesis is mediated by tumour necrosis factor-alpha.* Nature, 1987. **329**(6140): p. 630-2.

70.   Yoshida, S., et al., *Involvement of interleukin-8, vascular endothelial growth factor, and basic fibroblast growth factor in tumor necrosis factor alpha-dependent angiogenesis.* Mol Cell Biol, 1997. **17**(7): p. 4015-23.

71.   Stellwagen, D. and R.C. Malenka, *Synaptic scaling mediated by glial TNF-alpha.* Nature, 2006. **440**(7087): p. 1054-9.

72.   Beattie, E.C., et al., *Control of synaptic strength by glial TNFalpha.* Science, 2002. **295**(5563): p. 2282-5.

73.   Hube, F. and H. Hauner, *The two tumor necrosis factor receptors mediate opposite effects on differentiation and glucose metabolism in human adipocytes in primary culture.* Endocrinology, 2000. **141**(7): p. 2582-8.

74.   Liu, L.S., et al., *Tumor necrosis factor-alpha acutely inhibits insulin signaling in human adipocytes: implication of the p80 tumor necrosis factor receptor.* Diabetes, 1998. **47**(4): p. 515-22.

75.   Argiles, J.M., et al., *Journey from cachexia to obesity by TNF.* Faseb J, 1997. **11**(10): p. 743-51.

76.   Marsters, S.A., et al., *Identification of cysteine-rich domains of the type 1 tumor necrosis factor receptor involved in ligand binding.* J Biol Chem, 1992. **267**(9): p. 5747-50.

77.   Segui, B., et al., *Involvement of FAN in TNF-induced apoptosis.* J Clin Invest, 2001. **108**(1): p. 143-51.

78.	Takada, H., et al., *Role of SODD in regulation of tumor necrosis factor responses.* Mol Cell Biol, 2003. **23**(11): p. 4026-33.

79.	Micheau, O. and J. Tschopp, *Induction of TNF receptor I-mediated apoptosis via two sequential signaling complexes.* Cell, 2003. **114**(2): p. 181-90.

80.	Schneider-Brachert, W., et al., *Compartmentalization of TNF receptor 1 signaling: internalized TNF receptosomes as death signaling vesicles.* Immunity, 2004. **21**(3): p. 415-28.

81.	Lee, T.H., et al., *The kinase activity of Rip1 is not required for tumor necrosis factor-alpha-induced IkappaB kinase or p38 MAP kinase activation or for the ubiquitination of Rip1 by Traf2.* J Biol Chem, 2004. **279**(32): p. 33185-91.

82.	Ea, C.K., et al., *Activation of IKK by TNFalpha requires site-specific ubiquitination of RIP1 and polyubiquitin binding by NEMO.* Mol Cell, 2006. **22**(2): p. 245-57.

83.	Wang, C., et al., *TAK1 is a ubiquitin-dependent kinase of MKK and IKK.* Nature, 2001. **412**(6844): p. 346-51.

84.	Tang, E.D., et al., *A role for NF-kappaB essential modifier/IkappaB kinase-gamma (NEMO/IKKgamma) ubiquitination in the activation of the IkappaB kinase complex by tumor necrosis factor-alpha.* J Biol Chem, 2003. **278**(39): p. 37297-305.

85.	Kovalenko, A. and D. Wallach, *If the prophet does not come to the mountain: dynamics of signaling complexes in NF-kappaB activation.* Mol Cell, 2006. **22**(4): p. 433-6.

86.	Irmler, M., et al., *Inhibition of death receptor signals by cellular FLIP.* Nature, 1997. **388**(6638): p. 190-5.

87.	Fang, D., et al., *Dysregulation of T lymphocyte function in itchy mice: a role for Itch in TH2 differentiation.* Nat Immunol, 2002. **3**(3): p. 281-7.

88.	Kamata, H., et al., *Reactive oxygen species promote TNFalpha-induced death and sustained JNK activation by inhibiting MAP kinase phosphatases.* Cell, 2005. **120**(5): p. 649-61.

89.   Chang, L., et al., *The E3 ubiquitin ligase itch couples JNK activation to TNFalpha-induced cell death by inducing c-FLIP(L) turnover.* Cell, 2006. **124**(3): p. 601-13.

90.   Kim, R., *Unknotting the roles of Bcl-2 and Bcl-xL in cell death.* Biochem Biophys Res Commun, 2005. **333**(2): p. 336-43.

91.   Gupta, S., *Molecular steps of tumor necrosis factor receptor-mediated apoptosis.* Curr Mol Med, 2001. **1**(3): p. 317-24.

92.   Heinrich, M., et al., *Cathepsin D links TNF-induced acid sphingomyelinase to Bid-mediated caspase-9 and -3 activation.* Cell Death Differ, 2004. **11**(5): p. 550-63.

93.   Krikos, A., C.D. Laherty, and V.M. Dixit, *Transcriptional activation of the tumor necrosis factor alpha-inducible zinc finger protein, A20, is mediated by kappa B elements.* J Biol Chem, 1992. **267**(25): p. 17971-6.

94.   Jono, H., et al., *NF-kappaB is essential for induction of CYLD, the negative regulator of NF-kappaB: evidence for a novel inducible autoregulatory feedback pathway.* J Biol Chem, 2004. **279**(35): p. 36171-4.

95.   Kovalenko, A., et al., *The tumour suppressor CYLD negatively regulates NF-kappaB signalling by deubiquitination.* Nature, 2003. **424**(6950): p. 801-5.

96.   Heyninck, K. and R. Beyaert, *A20 inhibits NF-kappaB activation by dual ubiquitin-editing functions.* Trends Biochem Sci, 2005. **30**(1): p. 1-4.

97.   Wertz, I.E., et al., *De-ubiquitination and ubiquitin ligase domains of A20 downregulate NF-kappaB signalling.* Nature, 2004. **430**(7000): p. 694-9.

98.   Reiley, W., M. Zhang, and S.C. Sun, *Negative regulation of JNK signaling by the tumor suppressor CYLD.* J Biol Chem, 2004. **279**(53): p. 55161-7.

99.   Jin, Z. and W.S. El-Deiry, *Distinct signaling pathways in TRAIL- versus tumor necrosis factor-induced apoptosis.* Mol Cell Biol, 2006. **26**(21): p. 8136-48.

100.   Zheng, L., et al., *Competitive control of independent programs of tumor necrosis factor receptor-induced cell death by TRADD and RIP1.* Mol Cell Biol, 2006. **26**(9): p. 3505-13.

101.   Guo, D., et al., *Induction of Jak/STAT signaling by activation of the type 1 TNF receptor.* J Immunol, 1998. **160**(6): p. 2742-50.

102.   Wang, Y., et al., *Stat1 as a component of tumor necrosis factor alpha receptor 1-TRADD signaling complex to inhibit NF-kappaB activation.* Mol Cell Biol, 2000. **20**(13): p. 4505-12.

103.   Wesemann, D.R., et al., *TRADD interacts with STAT1-alpha and influences interferon-gamma signaling.* Nat Immunol, 2004. **5**(2): p. 199-207.

104.   Morgan, M., et al., *Nuclear and cytoplasmic shuttling of TRADD induces apoptosis via different mechanisms.* J Cell Biol, 2002. **157**(6): p. 975-84.

105.   Bender, L.M., et al., *The adaptor protein TRADD activates distinct mechanisms of apoptosis from the nucleus and the cytoplasm.* Cell Death Differ, 2005. **12**(5): p. 473-81.

106.   Johnson, D.E., *Noncaspase proteases in apoptosis.* Leukemia, 2000. **14**(9): p. 1695-703.

107.   Caulin, C., et al., *Keratin-dependent, epithelial resistance to tumor necrosis factor-induced apoptosis.* J Cell Biol, 2000. **149**(1): p. 17-22.

108.   Inada, H., et al., *Keratin attenuates tumor necrosis factor-induced cytotoxicity through association with TRADD.* J Cell Biol, 2001. **155**(3): p. 415-26.

109.   Tong, X. and P.A. Coulombe, *Keratin 17 modulates hair follicle cycling in a TNFalpha-dependent fashion.* Genes Dev, 2006. **20**(10): p. 1353-64.

110.   Izumi, K.M. and E.D. Kieff, *The Epstein-Barr virus oncogene product latent membrane protein 1 engages the tumor necrosis factor receptor-associated death domain protein to mediate B lymphocyte growth transformation and activate NF-kappaB.* Proc Natl Acad Sci U S A, 1997. **94**(23): p. 12592-7.

111.   Izumi, K.M., et al., *The Epstein-Barr virus oncoprotein latent membrane protein 1 engages the tumor necrosis factor receptor-associated proteins TRADD and receptor-interacting protein (RIP) but does not induce apoptosis or require RIP for NF-kappaB activation.* Mol Cell Biol, 1999. **19**(8): p. 5759-67.

112. Kieser, A., C. Kaiser, and W. Hammerschmidt, *LMP1 signal transduction differs substantially from TNF receptor 1 signaling in the molecular functions of TRADD and TRAF2.* Embo J, 1999. **18**(9): p. 2511-21.

113. Medzhitov, R. and C.A. Janeway, Jr., *Innate immunity: impact on the adaptive immune response.* Curr Opin Immunol, 1997. **9**(1): p. 4-9.

114. Asea, A., et al., *Novel signal transduction pathway utilized by extracellular HSP70: role of toll-like receptor (TLR) 2 and TLR4.* J Biol Chem, 2002. **277**(17): p. 15028-34.

115. Hashimoto, C., K.L. Hudson, and K.V. Anderson, *The Toll gene of Drosophila, required for dorsal-ventral embryonic polarity, appears to encode a transmembrane protein.* Cell, 1988. **52**(2): p. 269-79.

116. Belvin, M.P. and K.V. Anderson, *A conserved signaling pathway: the Drosophila toll-dorsal pathway.* Annu Rev Cell Dev Biol, 1996. **12**: p. 393-416.

117. Lemaitre, B., et al., *The dorsoventral regulatory gene cassette spatzle/Toll/cactus controls the potent antifungal response in Drosophila adults.* Cell, 1996. **86**(6): p. 973-83.

118. Kaisho, T. and S. Akira, *Toll-like receptor function and signaling.* J Allergy Clin Immunol, 2006. **117**(5): p. 979-87; quiz 988.

119. Kagan, J.C. and R. Medzhitov, *Phosphoinositide-mediated adaptor recruitment controls Toll-like receptor signaling.* Cell, 2006. **125**(5): p. 943-55.

120. O'Neill, L.A., *How Toll-like receptors signal: what we know and what we don't know.* Curr Opin Immunol, 2006. **18**(1): p. 3-9.

121. Medzhitov, R., et al., *MyD88 is an adaptor protein in the hToll/IL-1 receptor family signaling pathways.* Mol Cell, 1998. **2**(2): p. 253-8.

122. Adachi, O., et al., *Targeted disruption of the MyD88 gene results in loss of IL-1- and IL-18-mediated function.* Immunity, 1998. **9**(1): p. 143-50.

123. Kawai, T., et al., *Unresponsiveness of MyD88-deficient mice to endotoxin.* Immunity, 1999. **11**(1): p. 115-22.

124. Takeuchi, O., et al., *Cellular responses to bacterial cell wall components are mediated through MyD88-dependent signaling cascades.* Int Immunol, 2000. **12**(1): p. 113-7.

125. Hacker, H., et al., *Specificity in Toll-like receptor signalling through distinct effector functions of TRAF3 and TRAF6.* Nature, 2006. **439**(7073): p. 204-7.

126. Suzuki, N., et al., *Severe impairment of interleukin-1 and Toll-like receptor signalling in mice lacking IRAK-4.* Nature, 2002. **416**(6882): p. 750-6.

127. Li, S., et al., *IRAK-4: a novel member of the IRAK family with the properties of an IRAK-kinase.* Proc Natl Acad Sci U S A, 2002. **99**(8): p. 5567-72.

128. Cao, Z., W.J. Henzel, and X. Gao, *IRAK: a kinase associated with the interleukin-1 receptor.* Science, 1996. **271**(5252): p. 1128-31.

129. Muzio, M., et al., *IRAK (Pelle) family member IRAK-2 and MyD88 as proximal mediators of IL-1 signaling.* Science, 1997. **278**(5343): p. 1612-5.

130. Deng, L., et al., *Activation of the IkappaB kinase complex by TRAF6 requires a dimeric ubiquitin-conjugating enzyme complex and a unique polyubiquitin chain.* Cell, 2000. **103**(2): p. 351-61.

131. Takaesu, G., et al., *TAB2, a novel adaptor protein, mediates activation of TAK1 MAPKKK by linking TAK1 to TRAF6 in the IL-1 signal transduction pathway.* Mol Cell, 2000. **5**(4): p. 649-58.

132. Saha, S.K. and G. Cheng, *TRAF3: a new regulator of type I interferons.* Cell Cycle, 2006. **5**(8): p. 804-7.

133. Yamamoto, M., et al., *Cutting edge: a novel Toll/IL-1 receptor domain-containing adapter that preferentially activates the IFN-beta promoter in the Toll-like receptor signaling.* J Immunol, 2002. **169**(12): p. 6668-72.

134. Oshiumi, H., et al., *TICAM-1, an adaptor molecule that participates in Toll-like receptor 3-mediated interferon-beta induction.* Nat Immunol, 2003. **4**(2): p. 161-7.

135. Sato, S., et al., *Toll/IL-1 receptor domain-containing adaptor inducing IFN-beta (TRIF) associates with TNF receptor-associated factor 6 and TANK-binding kinase 1, and*

activates two distinct transcription factors, NF-kappa B and IFN-regulatory factor-3, in the Toll-like receptor signaling. J Immunol, 2003. **171**(8): p. 4304-10.

136. Hoebe, K. and B. Beutler, *TRAF3: a new component of the TLR-signaling apparatus.* Trends Mol Med, 2006. **12**(5): p. 187-9.

137. Meylan, E., et al., *RIP1 is an essential mediator of Toll-like receptor 3-induced NF-kappa B activation.* Nat Immunol, 2004. **5**(5): p. 503-7.

138. Cusson-Hermance, N., et al., *Rip1 mediates the Trif-dependent toll-like receptor 3- and 4-induced NF-{kappa}B activation but does not contribute to interferon regulatory factor 3 activation.* J Biol Chem, 2005. **280**(44): p. 36560-6.

139. Hoebe, K., et al., *Identification of Lps2 as a key transducer of MyD88-independent TIR signalling.* Nature, 2003. **424**(6950): p. 743-8.

140. Gohda, J., T. Matsumura, and J. Inoue, *Cutting edge: TNFR-associated factor (TRAF) 6 is essential for MyD88-dependent pathway but not toll/IL-1 receptor domain-containing adaptor-inducing IFN-beta (TRIF)-dependent pathway in TLR signaling.* J Immunol, 2004. **173**(5): p. 2913-7.

141. Bignell, G.R., et al., *Identification of the familial cylindromatosis tumour-suppressor gene.* Nat Genet, 2000. **25**(2): p. 160-5.

142. Li, S., et al., *Crystal structure of the cytoskeleton-associated protein glycine-rich (CAP-Gly) domain.* J Biol Chem, 2002. **277**(50): p. 48596-601.

143. Baek, K.H., *Conjugation and deconjugation of ubiquitin regulating the destiny of proteins.* Exp Mol Med, 2003. **35**(1): p. 1-7.

144. Trompouki, E., et al., *CYLD is a deubiquitinating enzyme that negatively regulates NF-kappaB activation by TNFR family members.* Nature, 2003. **424**(6950): p. 793-6.

145. Brummelkamp, T.R., et al., *Loss of the cylindromatosis tumour suppressor inhibits apoptosis by activating NF-kappaB.* Nature, 2003. **424**(6950): p. 797-801.

146. Reiley, W., et al., *Regulation of the deubiquitinating enzyme CYLD by IkappaB kinase gamma-dependent phosphorylation.* Mol Cell Biol, 2005. **25**(10): p. 3886-95.

147. Reiley, W.W., et al., *Regulation of T cell development by the deubiquitinating enzyme CYLD.* Nat Immunol, 2006. **7**(4): p. 411-7.

148. Massoumi, R., et al., *Cyld inhibits tumor cell proliferation by blocking Bcl-3-dependent NF-kappaB signaling.* Cell, 2006. **125**(4): p. 665-77.

149. Zhang, J., et al., *Impaired regulation of NF-kappaB and increased susceptibility to colitis-associated tumorigenesis in CYLD-deficient mice.* J Clin Invest, 2006. **116**(11): p. 3042-9.

150. Jin, W., et al., *Deubiquitinating enzyme CYLD regulates the peripheral development and naive phenotype maintenance of B cells.* J Biol Chem, 2007.

151. Kontoyiannis, D et al., Impaired on/off regulation of TNF biosynthesis in mice lacking TNF AU-rich elements: implications for joint and gut-associated immunopathologies. *Immunity, 1999. 10(3): p. 387-98*

152. Carballo, E et al., Feedback inhibition of macrophage tumor necrosis factor-alpha production by tristetraprolin. *Science, 1998. 281(5379): p. 1001-5*

153. Lee, E.G., et al., Failure to regulate TNF-induced NF-kappaB and cell death responses in A20-deficient mice. *Science, 2000. 289(5488): p. 2350-4*

154. Turer, E., et al., Homeostatic MyD88-dependent signals cause lethal inflammation in the absence of A20. *J Exp Med, 2008. 205(2): p. 451-464*

155. Welch, J.P., R.S. Wells, and C.B. Kerr, Ancell-Spiegler cylindromas (turban tumours) and Brooke-Fordyce Trichoepitheliomas: evidence for a single genetic entity. *J Med Genet, 1968. 5(1): p. 29-35.*

156. Gottschalk, H.R., Proceedings: Dermal eccrine cylindroma, epithelioma adenoides cysticum of Brooke, and ecrine spiradenoma. *Arch Dermatol, 1974. 110(3): p. 473-4.*

157. Fenske, C., et al., Brooke-Spiegler syndrome locus assigned to 16q12-q13. J Invest Dermatol, 2000. 114(5): p. 1057-8.

158. Poblete Gutierrez, P., et al., Phenotype diversity in familial cylindromatosis: a frameshift mutation in the tumor suppressor gene CYLD underlies different tumors of skin appendages. *J Invest Dermatol, 2002. 119(2): p. 527-31.*

159. Stegmeier, F., et al., The tumor suppressor CYLD regulates entry into mitosis. Proc Natl Acad Sci U S A, *2007. 104(21): p. 8869-74.*

160.   Wright, A., et al., Regulation of early wave of germ cell apoptosis and spermatogenesis by deubiquitinating enzyme CYLD. *Dev Cell, 2007. 13(5): p. 705-16.*

161. Kim, Y et al. TLRs bent into shape. Nat. Immunol, 2007. *8*: p. 675 - 677